Measurement of ZZ production in pp collisions at $\sqrt{s} = 7$ TeV and limits on anomalous ZZZ and $ZZ\gamma$ couplings with the ATLAS detector

The ATLAS collaboration

E-mail: atlas.publications@cern.ch

ABSTRACT: A measurement of the ZZ production cross section in proton-proton collisions at $\sqrt{s} = 7$ TeV using data recorded by the ATLAS experiment at the Large Hadron Collider is presented. In a data sample corresponding to an integrated luminosity of 4.6 fb^{-1} collected in 2011, events are selected that are consistent either with two Z bosons decaying to electrons or muons or with one Z boson decaying to electrons or muons and a second Z boson decaying to neutrinos. The $ZZ^{(*)} \to \ell^+\ell^-\ell'^+\ell'^-$ and $ZZ \to \ell^+\ell^-\nu\bar{\nu}$ cross sections are measured in restricted phase-space regions. These results are then used to derive the total cross section for ZZ events produced with both Z bosons in the mass range 66 to 116 GeV, $\sigma_{ZZ}^{\text{tot}} = 6.7 \pm 0.7$ (stat.) $^{+0.4}_{-0.3}$ (syst.) ± 0.3 (lumi.) pb, which is consistent with the Standard Model prediction of $5.89^{+0.22}_{-0.18}$ pb calculated at next-to-leading order in QCD. The normalized differential cross sections in bins of various kinematic variables are presented. Finally, the differential event yield as a function of the transverse momentum of the leading Z boson is used to set limits on anomalous neutral triple gauge boson couplings in ZZ production.

KEYWORDS: Hadron-Hadron Scattering

Contents

1 Introduction

The production of pairs of Z bosons at the Large Hadron Collider (LHC) provides an excellent opportunity to test the predictions of the electroweak sector of the Standard Model (SM) at the TeV energy scale. In the SM, Z boson pairs can be produced via non-resonant processes or in the decay of Higgs bosons. Deviations from SM expectations for the total or differential ZZ production cross sections could be indicative of the production of new resonances decaying to Z bosons or other non-SM contributions.

Non-resonant ZZ production proceeds at leading order (LO) via t- and u-channel quark-antiquark interactions, while about 6% of the production proceeds via gluon fusion. The ZZZ and $ZZ\gamma$ neutral triple gauge boson couplings (nTGCs) are absent in the SM, hence there is no contribution from s-channel $q\bar{q}$ annihilation at tree level. These different production processes are shown in figure 1. At the one-loop level, nTGCs generated by fermion triangles have a magnitude of the order of 10^{-4} [1]. Many models of physics beyond the Standard Model predict values of nTGCs at the level of 10^{-4} to 10^{-3} [2]. The primary signatures of non-zero nTGCs are an increase in the ZZ cross section at high ZZ invariant mass and high transverse momentum of the Z bosons [3]. ZZ production has been studied in $e^{+}e^{-}$ collisions at LEP [4–8], in $p\bar{p}$ collisions at the Tevatron [9–12] and recently in pp collisions at the LHC [13, 14]. No deviation of the measured total cross section from the SM expectation has been observed, and limits on anomalous nTGCs have been set [8, 9, 13, 14]. In searching for the SM Higgs boson, the ATLAS and CMS collaborations observed recently a neutral boson resonance with a mass around 126 GeV [15–17]. A SM Higgs boson with that mass can decay to two Z bosons only when at least one Z boson is off-shell, and even in this case, the contribution is less than 3%. Searches for high-mass non-SM ZZ resonances have not resulted in any excess above the SM expectations [18].

This paper presents a measurement of ZZ production[1] in proton-proton collisions at a centre-of-mass energy $\sqrt{s} = 7$ TeV using 4.6 fb^{-1} of integrated luminosity collected by the ATLAS detector at the LHC. ZZ events are selected in two channels:[2] $\ell^{+}\ell^{-}\ell'^{+}\ell'^{-}$ and $\ell^{+}\ell^{-}\nu\bar{\nu}$. Two selections are used in the four-charged-lepton channel: an on-shell ZZ selection denoted by $ZZ \to \ell^{+}\ell^{-}\ell'^{+}\ell'^{-}$ where both Z bosons are required to be within the mass range 66-116 GeV[3] and a selection which includes an off-shell Z boson denoted by $ZZ^{*} \to \ell^{+}\ell^{-}\ell'^{+}\ell'^{-}$ where one Z boson is required to be within this mass range and the other can be off-shell and have any mass above 20 GeV. In the $\ell^{+}\ell^{-}\nu\bar{\nu}$ channel, the $\nu\bar{\nu}$ system is expected to be produced by an off-shell Z boson in 2.6% of the events. Since this fraction is small and only one event selection is used for this channel, it is referred to as $ZZ \to \ell^{+}\ell^{-}\nu\bar{\nu}$ throughout the paper. The $ZZ^{(*)} \to \ell^{+}\ell^{-}\ell'^{+}\ell'^{-}$ channel has an excellent signal-to-background ratio, but it has a branching fraction six times lower than the $ZZ \to \ell^{+}\ell^{-}\nu\bar{\nu}$ channel; the latter has higher background contributions with an expected

---

[1]Throughout this paper Z should be taken to mean Z/γ^{*} when referring to decays to charged leptons, and just Z when referring to decays to neutrinos.

[2]ℓ represents either electrons or muons. ℓ and ℓ' are used to denote leptons from a different Z parent, but not necessarily of different flavour. Decay modes mentioned with the use of ℓ indicate the sum of the decay modes with specific lepton flavours.

[3]Throughout this paper, the 66-116 GeV mass range is referred to as the Z mass window.
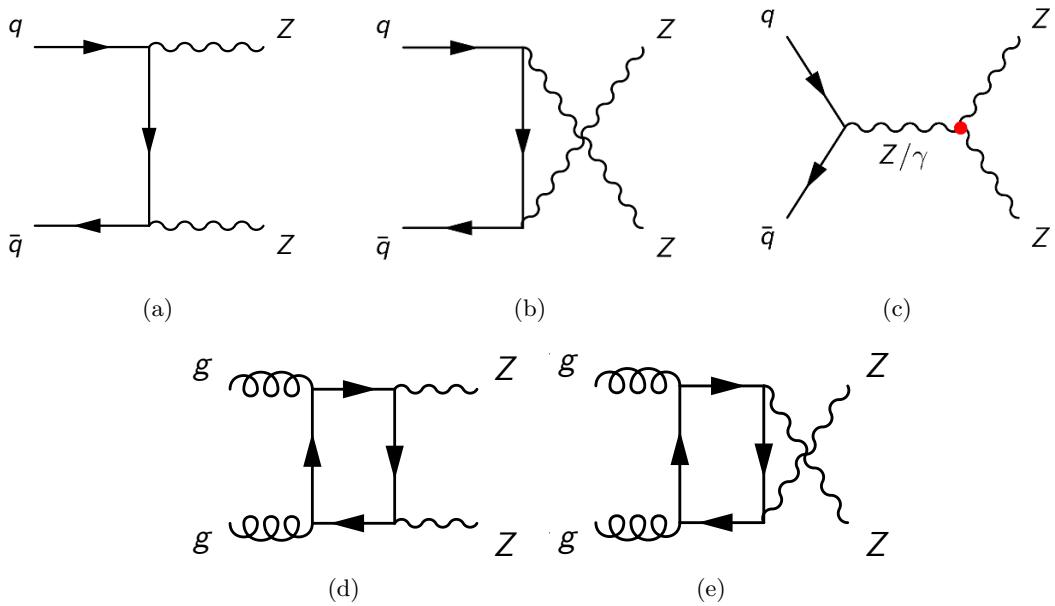
Figure 1. Leading order Feynman diagrams for ZZ production through the $q\bar{q}$ and gg initial state at hadron colliders. The s-channel diagram, (c), contains the ZZZ and $ZZ\gamma$ neutral TGC vertices which do not exist in the SM.

signal-to-background ratio around one (after applying the event selections described below). This paper presents the total ZZ production cross section, the fiducial cross section in a restricted phase space for each decay channel (integrated, and as a function of kinematic parameters for the ZZ selections) and limits on anomalous nTGCs using the observed ZZ event yields as a function of the transverse momentum of the leading Z boson.[4] The results presented in this paper supersede the previously published results [13] which were derived with the first 1.02 fb^{-1} of the dataset used here, only with the $ZZ \to \ell^+\ell^-\ell'^+\ell'^-$ decay channel and with the use of the total ZZ event count for the derivation of the limits on anomalous nTGCs.

The total cross section for non-resonant ZZ production is predicted at next-to-leading order (NLO) in QCD to be $6.18^{+0.25}_{-0.18}$ pb, where the quoted theoretical uncertainties result from varying the factorization and renormalization scales simultaneously by a factor of two whilst using the full CT10 parton distribution function (PDF) error set [19]. The cross section is calculated in the on-shell (zero-width) approximation using MCFM [20] with CT10; it includes a 5.8% contribution from gluon fusion. When the natural width of the Z boson is used and both Z bosons are required to be within the Z mass window, the NLO cross section is predicted to be $5.89^{+0.22}_{-0.18}$ pb. The cross sections given here are calculated at a renormalization and factorization scale equal to half the mass of the diboson system. The total cross section using the zero-width approximation was previously measured to be $8.5^{+2.7}_{-2.3}$ (stat.) $^{+0.4}_{-0.3}$ (syst.) ± 0.3 (lumi.) pb [13].

---

[4]Leading Z refers to the Z with the higher transverse momentum in $ZZ \to \ell^+\ell^-\ell'^+\ell'^-$ decays or to the Z boson decaying to a charged lepton pair in $ZZ \to \ell^+\ell^-\nu\bar{\nu}$ decays.

This paper is organized as follows: an overview of the ATLAS detector, data, signal and background Monte Carlo (MC) samples used for this analysis is given in section 2; section 3 describes the selection of the physics objects; section 4 describes the fiducial phase space of the measurement, the corresponding ZZ cross section definition and the acceptances of the event selection and fiducial phase space; section 5 explains how the backgrounds to the $\ell^+\ell^-\ell'^+\ell'^-$ and $\ell^+\ell^-\nu\bar{\nu}$ final states are estimated with a combination of simulation and data-driven techniques; section 6 presents the results: cross section, differential cross sections and nTGC limits; finally, a summary of the main results is given in section 7.

2 The ATLAS detector and data sample

The ATLAS detector [21] is a multipurpose particle detector with a cylindrical geometry. It consists of inner tracking devices surrounded by a superconducting solenoid, electromagnetic and hadronic calorimeters and a muon spectrometer with a toroidal magnetic field. The inner detector, in combination with the 2 T field from the solenoid, provides precision tracking of charged particles in the pseudorapidity range $|\eta| < 2.5$.[5] It consists of a silicon pixel detector, a silicon microstrip detector and a straw tube tracker that also provides transition radiation measurements for electron identification in the pseudorapidity range $|\eta| < 2.0$. The calorimeter system covers the pseudorapidity range $|\eta| < 4.9$. The electromagnetic calorimeter uses liquid argon (LAr) as the active material with lead as an absorber ($|\eta| < 3.2$). It identifies electromagnetic showers and measures their energy and position; in the region $|\eta| < 2.5$ it is finely segmented and provides electron identification in conjunction with the inner detector which covers the same η region. Hadronic showers are measured in the central rapidity range ($|\eta| < 1.7$) by scintillator tiles with iron absorber, while in the end-cap region ($1.5 < |\eta| < 3.2$) a LAr calorimeter with a copper absorber is used. In the forward region ($3.2 < |\eta| < 4.9$) a LAr calorimeter with a copper absorber for the first layer and tungsten for the last two layers is used for both electromagnetic and hadronic showers. All calorimeters are used to measure jets. The muon spectrometer surrounds the calorimeters; it consists of superconducting air-core toroid magnets, high-precision tracking chambers which provide muon identification and tracking measurement in the pseudorapidity range $|\eta| < 2.7$, and separate trigger chambers covering $|\eta| < 2.4$.

A three-level trigger system selects events to be recorded for offline analysis. The events used in this analysis were selected with single-lepton triggers with nominal transverse momentum (p_T) thresholds of 20 or 22 GeV (depending on the instantaneous luminosity of the LHC) for electrons and 18 GeV for muons. The efficiencies of the single-lepton triggers have been determined as a function of lepton pseudorapidity and transverse momentum using large samples of $Z \to \ell^+\ell^-$ events. The trigger efficiencies for events passing the offline selection described below are all greater than 98%.

---

[5]ATLAS uses a right-handed coordinate system with its origin at the nominal interaction point in the centre of the detector and the z-axis along the beam direction. The x-axis points from the interaction point to the centre of the LHC ring, and the y-axis points upwards. Cylindrical coordinates (r,ϕ) are used in the transverse plane, ϕ being the azimuthal angle around the beam direction. The pseudorapidity η is defined in terms of the polar angle θ as $\eta = -\ln\tan(\theta/2)$.

The measurements presented here uses the full data sample of proton-proton collisions at $\sqrt{s} = 7$ TeV recorded in 2011. After data quality requirements, the total integrated luminosity used in the analysis is 4.6 fb^{-1} with an uncertainty of 3.9% [22].

2.1 Simulated data samples

Monte Carlo simulated samples cross-checked with data are used to calculate several quantities used in this measurement, including acceptance, efficiency and some of the background to the $ZZ \to \ell^+\ell^-\nu\bar{\nu}$ decay channel. The NLO generator POWHEGBOX [23, 24] with the CT10 PDF set, interfaced to PYTHIA [25], is used to model the signal for both channels. The LO multi-leg generator SHERPA [26] with the CTEQ6L1 PDF set [27] in comparison with POWHEGBOX is used to evaluate systematic uncertainties. The contribution from $gg \to ZZ$ is modelled by the GG2ZZ generator [28] interfaced to HERWIG [29] to model parton showers and to JIMMY [30] for multiparton interactions. In each case, the simulation includes the interference terms between the Z and γ^* diagrams. For both the $\ell^+\ell^-\ell'^+\ell'^-$ and $\ell^+\ell^-\nu\bar{\nu}$ final states, MCFM is used to calculate theoretical uncertainties, and SHERPA is used for the generation of signal samples with neutral triple gauge couplings.

The LO generator ALPGEN [31] with CTEQ6L1 PDFs is used to simulate Z+jets, W+jets, $Z\gamma$ and $W\gamma$ background events with JIMMY used for multiparton interactions and HERWIG for parton showers. The NLO generator MC@NLO [32] with CT10 PDFs is used to model $t\bar{t}$ background processes as well as WW production. The single-top Wt process is modelled with ACERMC [33] with the MSTW2008 PDFs [34]. The LO generator HERWIG with MSTW2008 PDFs is used to model WZ production. The LO generator MADGRAPH [35] with CTEQ6L1 PDFs is also used to model $Z\gamma$ and $W\gamma^*$ events, where PYTHIA is used for hadronization and showering.

The detector response is simulated [36] with a program based on GEANT4 [37]. Additional inelastic pp events are included in the simulation, distributed so as to reproduce the number of collisions per bunch-crossing in the data. The detector response to interactions in the out-of-time bunches from pile-up is also modelled in the simulation. The results of the simulation are corrected with scale factors determined by comparing efficiencies observed in data to those in the simulated events, and the lepton momentum scale and resolution are finely adjusted to match the observed dilepton spectra in $Z \to \ell\ell$ events using a sample of Z bosons.

3 Event reconstruction and selection

Events are required to contain a primary vertex formed from at least three associated tracks with $p_{\mathrm{T}} > 400$ MeV.

3.1 Leptons, jets and missing energy

3.1.1 Common lepton selection

Muons are identified by matching tracks (or track segments) reconstructed in the muon spectrometer to tracks reconstructed in the inner detector [38]. The momenta of these

combined muons are calculated by combining the information from the two systems and correcting for the energy deposited in the calorimeters. The analyses of both decay channels use muons which have full tracks reconstructed in the muon spectrometer with $p_T > 20$ GeV and $|\eta| < 2.5$. The $ZZ^{(*)} \to \ell^+\ell^-\ell'^+\ell'^-$ channel recovers additional ZZ acceptance with minimal additional background using a lower threshold of $p_T > 7$ GeV and by accepting muons with segments reconstructed in the muon spectrometer (in this latter case, the muon spectrometer is used to identify the track as a muon, but its momentum is measured using the inner detector; for the purposes of the discussion below, these muons are also referred to as *combined* muons).

Electrons are reconstructed from an energy cluster in the electromagnetic calorimeter matched to a track in the inner detector [38]; the transverse momentum is computed from the calorimeter energy and the direction from the track parameters measured in the inner detector. The electron track parameters are corrected for bremsstrahlung energy loss using the Gaussian-sum filter algorithm [39]. Electron candidates in the $ZZ^{(*)} \to \ell^+\ell^-\ell'^+\ell'^-$ ($ZZ \to \ell^+\ell^-\nu\bar{\nu}$) channel are required to have longitudinal and transverse shower profiles consistent with those expected from electromagnetic showers, by satisfying the loose (medium) identification criteria described in ref. [40] reoptimized for the 2011 data-taking conditions. They are also required to have a transverse momentum of at least 7 (20) GeV and a pseudorapidity of $|\eta| < 2.47$.

In order to reject non-prompt leptons from the decay of heavy quarks and fake electrons from misidentified jets (charged hadrons or photon conversions), all selected leptons must satisfy isolation requirements based on calorimetric and tracking information and must be consistent with originating from the primary vertex. For the calorimetric isolation the scalar sum of the transverse energies, ΣE_T, of calorimeter deposits inside a cone around the lepton, corrected to remove the energy from the lepton and from additional interactions (pile-up), is formed. In the $ZZ^{(*)} \to \ell^+\ell^-\ell'^+\ell'^-$ ($ZZ \to \ell^+\ell^-\nu\bar{\nu}$) channel, the ΣE_T inside a cone of size $\Delta R = \sqrt{(\Delta\phi)^2 + (\Delta\eta)^2} = 0.2$ (0.3) around the lepton is required to be no more than 30% (15%) of the lepton p_T. For the track isolation, the scalar sum of the transverse momenta, Σp_T, of inner detector tracks inside a cone of size $\Delta R = 0.2$ (0.3) around the lepton is required to be no more than 15% of the lepton p_T. The wider cone size, in conjunction with the same or tighter requirements on the fraction of extra activity allowed in the cone, corresponds to more stringent isolation requirements applied to the $ZZ \to \ell^+\ell^-\nu\bar{\nu}$ channel compared to the $ZZ^{(*)} \to \ell^+\ell^-\ell'^+\ell'^-$ channel. This reflects the need to reduce the much higher reducible background (predominantly from Z+jets, $t\bar{t}$ and WW). To ensure that the lepton originates from the primary vertex, its longitudinal impact parameter $|z_0|$ is required to be less than 2 mm, and its transverse impact parameter significance (the transverse impact parameter divided by its error), $|d_0/\sigma_{d_0}|$, is required to be less than 3.5 (6) for muons (electrons). Electrons have a worse impact parameter resolution than muons due to bremsstrahlung.

Since muons can radiate photons which may then convert to electron-positron pairs, electron candidates within $\Delta R = 0.1$ of any selected muon are not considered. If two electron candidates are within $\Delta R = 0.1$ of each other, the one with the lower p_T is removed.

3.1.2 Extended-lepton selection

Two additional categories of muons are considered for the $ZZ^{(*)} \to \ell^+\ell^-\ell'^+\ell'^-$ channel: forward spectrometer muons with $2.5 < |\eta| < 2.7$ (in a region outside the nominal coverage of the inner detector) and calorimeter-tagged muons with $|\eta| < 0.1$ (where there is a limited geometric coverage in the muon spectrometer). Forward spectrometer muons are required to have a full track that is reconstructed in the muon spectrometer; if these muons are also measured in the inner detector, their momentum is measured using the combined information; otherwise, only the muon spectrometer information is used. In either case, such muons are required to have $p_{\mathrm{T}} > 10$ GeV and the ΣE_{T} of calorimeter deposits inside a cone of size $\Delta R = 0.2$ around the muon is required to be no more than 15% of the muon p_{T}, while no requirement is made on Σp_{T}. The same impact parameter requirements as for the combined muons are imposed for the forward muons measured in the inner detector; no such requirement is imposed on those measured in the muon spectrometer only. Calorimeter-tagged muons are reconstructed from calorimeter energy deposits consistent with a muon which are matched to an inner detector track with $p_{\mathrm{T}} > 20$ GeV and are required to satisfy the same impact parameter and isolation criteria as for the combined muons.

The $ZZ^{(*)} \to \ell^+\ell^-\ell'^+\ell'^-$ channel also uses calorimeter-only electrons with $2.5 < |\eta| < 3.16$ and $p_{\mathrm{T}} > 20$ GeV passing the tight identification requirements [40] for this forward η region, where only the longitudinal and transverse shower profiles in the calorimeters are used for their identification. Their transverse momentum is computed from the calorimeter energy and the electron direction, where the electron direction is computed using the primary vertex position and the shower barycentre position in the calorimeter. Being identified outside the acceptance of the inner detector, no impact parameter requirements can be applied to these calorimeter-only electron candidates, and their charge is not measured. Since only one such electron is allowed in the event, and since all other leptons have their charge measured, the calorimeter-only electron is assigned the charge needed to have two pairs of same-flavour opposite-sign leptons in the event. The requirements described above constrain the additional background introduced by the inclusion of calorimeter-only electrons, and no isolation requirements are imposed on such electrons.

The use of the extended-lepton selection increases the $ZZ \to \ell^+\ell^-\ell'^+\ell'^-$ and $ZZ^* \to \ell^+\ell^-\ell'^+\ell'^-$ acceptance by about 6% from the forward spectrometer muons, 4% from the calorimeter-tagged muons and 6% from the forward electrons. The expected background is kept small by requiring each event to have at most one lepton from each extended-lepton category, and each such lepton to be paired with a non-extended lepton.

3.1.3 Jets and missing transverse momentum

For the $ZZ \to \ell^+\ell^-\nu\bar{\nu}$ selection, events which contain at least one well-reconstructed jet are vetoed to reduce background from top-quark production. Jets are reconstructed from topological clusters of energy in the calorimeter [41] using the anti-k_t algorithm [42] with radius parameter $R = 0.4$. The measured jet energy is corrected for detector inhomogeneities and for the non-compensating nature of the calorimeter using p_{T}- and η-dependent correction factors based on Monte Carlo simulations with adjustments from in-situ measure-

ments [43, 44]. Jets are required to have $p_T > 25$ GeV and $|\eta| < 4.5$. In order to minimize the impact of jets from pile-up at high luminosity, the jet vertex fraction is required to be at least 0.75; the jet vertex fraction is defined as the sum of the p_T of tracks associated to the jet and originating from the primary vertex, divided by the sum of the p_T of all the tracks associated to the jet. If a reconstructed jet and a lepton lie within $\Delta R = 0.3$ of each other, the jet is not considered in the analysis.

The missing transverse momentum E_T^{miss} is the imbalance of transverse momentum in the event. A large imbalance in the transverse momentum is a signature of the $ZZ \rightarrow \ell^+\ell^-\nu\bar{\nu}$ decay channel. The two-dimensional E_T^{miss} vector is determined from the negative vectorial sum of reconstructed electron, muon and jet momenta together with calorimeter cells not associated to any object [45]. Calorimeter cells are calibrated to the jet energy scale if they are associated with a jet and to the electromagnetic energy scale otherwise. Using calorimeter timing and shower shape information, events that contain jets with $p_T > 20$ GeV and not originating from proton-proton collisions but from e.g. calorimeter signals due to noisy cells are rejected.

3.2 $ZZ^{(*)} \rightarrow \ell^+\ell^-\ell'^+\ell'^-$ selection

$ZZ^{(*)} \rightarrow \ell^+\ell^-\ell'^+\ell'^-$ events are characterized by four high-p_T, isolated electrons or muons, in three channels: $e^+e^-e^+e^-$, $\mu^+\mu^-\mu^+\mu^-$ and $e^+e^-\mu^+\mu^-$. Selected events are required to have exactly four leptons and to have passed at least a single-muon or single-electron trigger. Each combination of lepton pairs is required to satisfy $\Delta R(\ell_1, \ell_2) > 0.2$, where ℓ_1 and ℓ_2 are used hereafter to denote a pair of distinct leptons, independent of their Z parent assignment, flavour and charge. To ensure high and well-measured trigger efficiency, at least one lepton must have $p_T > 20$ GeV (25 GeV) for the offline muon (electron) and be matched to a muon (electron) reconstructed online by the trigger system within $\Delta R = 0.1$ (0.15).

Same-flavour, oppositely-charged lepton pairs are combined to form Z candidates. An event must contain two such pairs. In the $e^+e^-e^+e^-$ and $\mu^+\mu^-\mu^+\mu^-$ channels, ambiguities are resolved by choosing the combination which results in the smaller value of the sum of $|m_{\ell^+\ell^-} - m_Z|$ for the two pairs, where $m_{\ell^+\ell^-}$ is the mass of the dilepton system and m_Z is the mass of the Z boson [46]. Figure 2 shows the correlation between the invariant mass of the leading (higher p_T) and the sub-leading (lower p_T) lepton pair. The events cluster in the region where both masses are around m_Z. At least one lepton pair is required to have invariant mass within the Z mass window, $66 < m_{\ell^+\ell^-} < 116$ GeV. If the second lepton pair satisfies this as well, the event is classified as a ZZ event; if the second pair satisfies $m_{\ell^+\ell^-} > 20$ GeV, the event is classified as a ZZ^* event.

With the selection described here, 84 $ZZ^* \rightarrow \ell^+\ell^-\ell'^+\ell'^-$ candidates are observed, out of which 66 are classified as $ZZ \rightarrow \ell^+\ell^-\ell'^+\ell'^-$ candidates. From the 84 (66) $ZZ^* \rightarrow \ell^+\ell^-\ell'^+\ell'^-$ ($ZZ \rightarrow \ell^+\ell^-\ell'^+\ell'^-$) candidates, 8 (7) candidates contain extended leptons.

3.3 $ZZ \rightarrow \ell^+\ell^-\nu\bar{\nu}$ selection

$ZZ \rightarrow \ell^+\ell^-\nu\bar{\nu}$ events are characterized by large missing transverse momentum and two high-p_T, isolated electrons or muons. Selected events are required to have exactly two
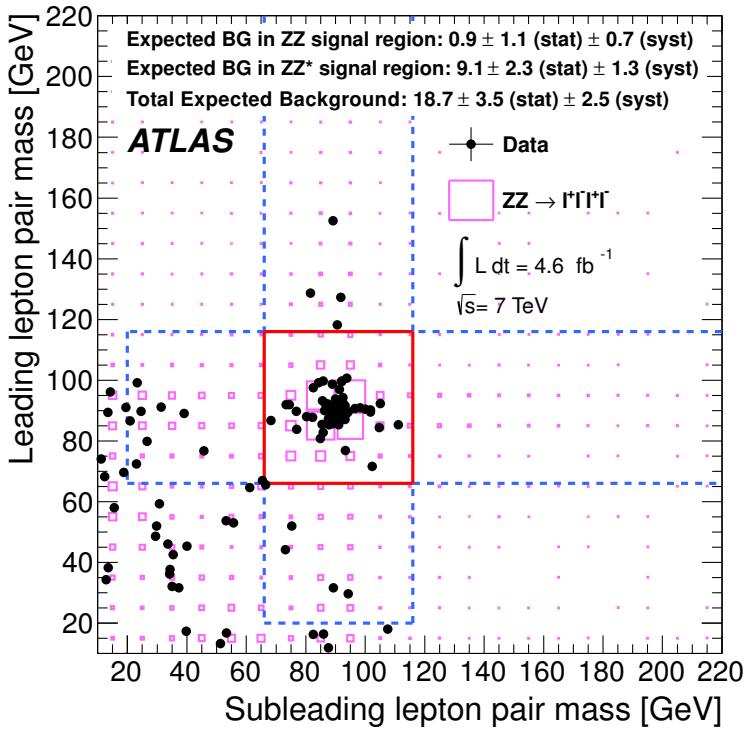
Figure 2. The mass of the leading lepton pair versus the mass of the sub-leading lepton pair. The events observed in the data are shown as solid circles and the $ZZ^{(*)} \rightarrow \ell^+\ell^-\ell'^+\ell'^-$ signal prediction from simulation as boxes. The size of each box is proportional to the number of events in each bin. The region enclosed by the solid (dashed) lines indicates the signal region defined by the requirements on the lepton-pair masses for ZZ (ZZ^*) events, as defined in the text.

leptons of the same flavour with $76 < m_{\ell^+\ell^-} < 106$ GeV and to have passed at least a single-muon or a single-electron trigger. The mass window is chosen to be tighter than the mass window used for the $ZZ^{(*)} \rightarrow \ell^+\ell^-\ell'^+\ell'^-$ channel in order to reduce the background from $t\bar{t}$ and WW. The lepton pair is required to have $\Delta R(\ell^+, \ell^-) > 0.3$. This requirement reflects the choice of the isolation cone for the leptons. The same trigger matching requirement as in the $ZZ^{(*)} \rightarrow \ell^+\ell^-\ell'^+\ell'^-$ channel is used.

The $ZZ \rightarrow \ell^+\ell^-\nu\bar{\nu}$ decay channel analysis makes use of several selections to reduce background. The largest background after the mass window requirement consists of Z+jets events, which are associated with non-zero missing transverse momentum when the E_T^{miss} is mismeasured or when a b-quark decays to leptons and neutrinos inside of a jet. Since the Z bosons tend to be produced back-to-back, the axial-E_T^{miss} (defined as the projection of the E_T^{miss} along the direction opposite to the $Z \rightarrow \ell^+\ell^-$ candidate in the transverse plane) is a powerful variable to distinguish $ZZ \rightarrow \ell^+\ell^-\nu\bar{\nu}$ decays from Z+jets. The axial-E_T^{miss} is given by $-\vec{E}_T^{\text{miss}} \cdot \vec{p}^{\,Z}/p_T^Z$, where p_T^Z is the magnitude of the transverse momentum of the Z candidate. Similarly, the fractional p_T difference, $|E_T^{\text{miss}} - p_T^Z|/p_T^Z$ is a good variable to distinguish the two. The axial-E_T^{miss} and fractional p_T difference are shown in figure 3. In order to reduce Z+jets background, the axial-E_T^{miss} must be greater than 75 GeV, and
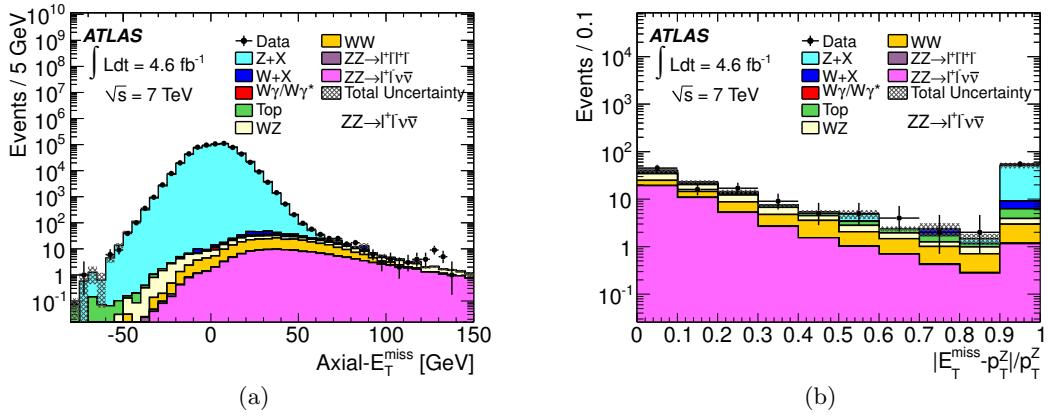
Figure 3. For $\ell^+\ell^-\nu\bar{\nu}$ candidates in all channels figure (a) shows the axial-$E_{\mathrm{T}}^{\mathrm{miss}}$ after all selection requirements, except for the axial-$E_{\mathrm{T}}^{\mathrm{miss}}$, and figure (b) shows the fractional p_{T} difference between $E_{\mathrm{T}}^{\mathrm{miss}}$ and p_{T}^Z after all selection requirements, except for the fractional p_{T} difference (the last bin also contains events with fractional p_{T} difference greater than 1). In all plots, the points are data and the stacked histograms show the signal prediction from simulation. The shaded band shows the combined statistical and systematic uncertainties.

the fractional p_{T} difference must be less than 0.4. To reduce background from top-quark production, events which contain at least one reconstructed jet with $p_{\mathrm{T}} > 25\,\mathrm{GeV}$ and $|\eta| < 4.5$ are rejected.

To reduce background from WZ production, events with a third lepton (electron or muon) with p_{T} greater than $10\,\mathrm{GeV}$ are rejected. The shape of the jet multiplicity distribution is well modelled in Monte Carlo simulation as shown in figure 4 for the $ZZ \to \ell^+\ell^-\ell'^+\ell'^-$ and $ZZ \to \ell^+\ell^-\nu\bar{\nu}$ selections, however, there is an overall excess of about 20% in the $ZZ \to \ell^+\ell^-\ell'^+\ell'^-$ selection. With this selection, 87 $ZZ \to \ell^+\ell^-\nu\bar{\nu}$ candidates are observed in data.

4 Signal acceptance

The Z boson decays to hadrons, neutrinos and charged leptons with branching fractions of 69.9%, 20.0% and 10.1%, respectively [46]. The two ZZ decay channels considered in this paper, $ZZ \to \ell^+\ell^-\ell'^+\ell'^-$ and $ZZ \to \ell^+\ell^-\nu\bar{\nu}$, have branching fractions of 0.45% and 2.69%, respectively,[6] where decays involving τ leptons are not included in these branching fractions. Some of the ZZ decays produce one or more charged leptons which pass through the uninstrumented regions of the detector, and as such cannot be reconstructed. In order to measure the total ZZ cross section, the measured decays are extrapolated to non-measured parts of the phase-space; this results in the measurement being more dependent on theory predictions. Consequently, two types of cross sections are measured: fiducial and total. The fiducial cross section is the cross section measured within a restricted phase space, and the total cross section is the cross section extrapolated to the total phase space.

---

[6]The quoted branching fraction to four charged leptons is for the case where both Z bosons are within the mass window, so that the γ^* contribution can be neglected.
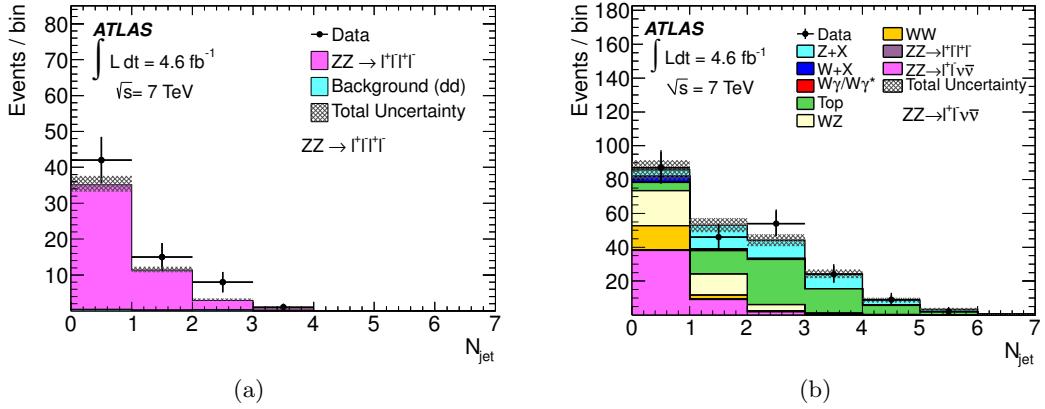
Figure 4. (a) Jet multiplicity for the $ZZ \to \ell^+\ell^-\ell'^+\ell'^-$ selection and (b) jet multiplicity for the $ZZ \to \ell^+\ell^-\nu\bar{\nu}$ selection (with all selections applied but the jet veto). The points represent the observed data. In (a) the $ZZ \to \ell^+\ell^-\ell'^+\ell'^-$ background is normalized to the data-driven (dd) estimate, while in (b) the histograms show the prediction from simulation. The shaded band shows the combined statistical and systematic uncertainty on the prediction.

The total cross section calculation depends on the choice of Z mass range. The cross section is calculated using the Z boson natural width rather than the zero-width approximation, and includes the mass window requirement (66 to 116 GeV) to remove most of the γ^* contamination. The ratio of the total cross section calculated with both Z bosons within the mass window to the total cross section calculated using the zero-width approximation is 0.953, as the mass window requirement removes some of the Z bosons in the tails of the mass distribution.

4.1 Fiducial region definitions

The fiducial cross section is restricted to a region which is constructed to closely match the instrumented region and the event selection; for simplicity, only the most inclusive requirements on the lepton η and p_T are used for the definition of the fiducial phase space. The fiducial cross section σ_{ZZ}^{fid} is calculated as:

$$\sigma_{ZZ}^{\text{fid}} = \frac{N_{\text{obs}} - N_{\text{bkg}}}{C_{ZZ} \times \mathcal{L}} \tag{4.1}$$

which depends on a correction factor given by the number of simulated $ZZ^{(*)}$ events which satisfy the full event selection divided by the number of $ZZ^{(*)}$ events generated in the fiducial region, C_{ZZ}; the integrated luminosity, $\mathcal{L}$; the number of selected events, N_{obs}; and the amount of estimated background, N_{bkg}. For the calculation of C_{ZZ}, final states including pairs of oppositely-charged leptons produced from decays of $Z \to \tau^+\tau^- \to \ell^+\ell^-\nu\bar{\nu}\nu\bar{\nu}$ are included in the number of selected events (numerator) since those decays have an identical final state to the signal and are not subtracted as background but are excluded from the fiducial region (denominator) because the fiducial regions are defined only with $ZZ^{(*)}$ decays directly to electrons, muons or neutrinos, depending on the channel. The contribution from such τ decays is estimated from Monte Carlo simulation to be < 0.1 % for the

Selection	C_{ZZ}
$ZZ \to \ell^+\ell^-\ell'^+\ell'^-$	$0.552 \pm 0.002 \pm 0.021$
$ZZ^* \to \ell^+\ell^-\ell'^+\ell'^-$	$0.542 \pm 0.002 \pm 0.022$
$ZZ \to \ell^+\ell^-\nu\bar{\nu}$	$0.679 \pm 0.004 \pm 0.014$

Table 1. Correction factors C_{ZZ} for each production and decay channel. The first uncertainty is statistical while the second is systematic.

$ZZ \to \ell^+\ell^-\nu\bar{\nu}$ selection, 0.24±0.01% for the $ZZ \to \ell^+\ell^-\ell'^+\ell'^-$ selection and 1.73±0.04% for the $ZZ^* \to \ell^+\ell^-\ell'^+\ell'^-$ selection. Fiducial requirements are applied at generator level. To reduce the dependence on QED radiation, the four-momentum assigned to each lepton includes the four-momentum of any neighbouring photon within $\Delta R \leq 0.1$.

The $ZZ \to \ell^+\ell^-\ell'^+\ell'^-$ fiducial region is defined using the following requirements: (i) two pairs of same-flavour opposite-sign electrons or muons, with each lepton satisfying $p_T^\ell > 7\,\text{GeV}$, $|\eta^\ell| < 3.16$ and at least a distance $\Delta R = 0.2$ from any other selected lepton, i.e., $\Delta R(\ell_1, \ell_2) > 0.2$, and (ii) both dilepton invariant masses within the Z mass window. A $ZZ^* \to \ell^+\ell^-\ell'^+\ell'^-$ fiducial region is defined with the same criteria as in the $ZZ \to \ell^+\ell^-\ell'^+\ell'^-$ case, except that one dilepton invariant mass requirement is relaxed to be greater than 20 GeV.

The $ZZ \to \ell^+\ell^-\nu\bar{\nu}$ fiducial region is defined by requiring: (i) two same-flavour opposite-sign electrons or muons, each with $p_T^\ell > 20\,\text{GeV}$, $|\eta^\ell| < 2.5$, with $\Delta R(\ell^+, \ell^-) > 0.3$, (ii) dilepton invariant mass close to the Z boson mass: $76 < m_{\ell^+\ell^-} < 106\,\text{GeV}$, (iii) dineutrino invariant mass close to the Z boson mass: $66 < m_{\nu\bar{\nu}} < 116\,\text{GeV}$, (iv) no jet with $p_T^j > 25\,\text{GeV}$ and $|\eta^j| < 4.5$, and (v) $(|p_T^{\nu\bar{\nu}} - p_T^Z|)/p_T^Z < 0.4$ and $-\vec{p}_T^{\,\nu\bar{\nu}} \cdot \vec{p}^{\,Z}/p_T^Z > 75\,\text{GeV}$. Jets are defined at generator level using the same jet algorithm as used in reconstructed events and including all final state particles after parton showering and hadronization.

Fiducial cross sections are calculated using the $ZZ \to \ell^+\ell^-\ell'^+\ell'^-$, $ZZ^* \to \ell^+\ell^-\ell'^+\ell'^-$ and $ZZ \to \ell^+\ell^-\nu\bar{\nu}$ selections, integrated over the corresponding full fiducial phase space volumes. For the $ZZ \to \ell^+\ell^-\ell'^+\ell'^-$ and $ZZ \to \ell^+\ell^-\nu\bar{\nu}$ selections the differential fiducial cross sections are derived in bins of the leading p_T^Z, $\Delta\phi(\ell^+, \ell^-)$ and the mass of the $ZZ \to \ell^+\ell^-\ell'^+\ell'^-$ system or the transverse mass of the $ZZ \to \ell^+\ell^-\nu\bar{\nu}$ system.

The correction factor, C_{ZZ}, is determined from Monte Carlo simulations (PowhegBox for the $ZZ \to \ell^+\ell^-\nu\bar{\nu}$ channel and PowhegBox and gg2zz for the $ZZ^{(*)} \to \ell^+\ell^-\ell'^+\ell'^-$ channel), after applying data-driven corrections as described in section 2.1. For the $ZZ \to \ell^+\ell^-\ell'^+\ell'^-$ ($ZZ^* \to \ell^+\ell^-\ell'^+\ell'^-$) selection it is 0.43 (0.41) for $e^+e^-e^+e^-$, 0.68 (0.69) for $\mu^+\mu^-\mu^+\mu^-$ and 0.55 (0.53) for $e^+e^-\mu^+\mu^-$ events. For the $ZZ \to \ell^+\ell^-\nu\bar{\nu}$ selection the correction factor is 0.63 for $e^+e^-\nu\bar{\nu}$ and 0.76 for $\mu^+\mu^-\nu\bar{\nu}$ events. The correction factors combining all lepton categories within the fiducial region are given in table 1 for the three event selections in both decay channels.

Selection	A_{ZZ}
$ZZ \to \ell^+\ell^-\ell'^+\ell'^-$	$0.804 \pm 0.001 \pm 0.010$
$ZZ \to \ell^+\ell^-\nu\bar{\nu}$	$0.081 \pm 0.001 \pm 0.004$

Table 2. Acceptance A_{ZZ} for the two decay channels used for the measurement of the total ZZ production cross section. The first uncertainty is statistical while the second is systematic.

4.2 Extrapolation to the total phase space

The total ZZ cross section is measured using the $ZZ \to \ell^+\ell^-\ell'^+\ell'^-$ and $ZZ \to \ell^+\ell^-\nu\bar{\nu}$ selections. The total cross section is calculated using the fiducial acceptance, A_{ZZ} (the fraction of ZZ events with Z bosons in the Z mass window that fall into the fiducial region) and the branching fraction, BF:

$$\sigma_{ZZ}^{\text{total}} = \frac{N_{\text{obs}} - N_{\text{bkg}}}{A_{ZZ} \times C_{ZZ} \times \mathcal{L} \times \text{BF}} \qquad (4.2)$$

The fiducial acceptances A_{ZZ} are estimated from Monte Carlo simulation, using POWHEG-BOX for the $ZZ \to \ell^+\ell^-\nu\bar{\nu}$ channel and POWHEGBOX and GG2ZZ for the $ZZ \to \ell^+\ell^-\ell'^+\ell'^-$ channel. The fiducial acceptance of the $ZZ \to \ell^+\ell^-\nu\bar{\nu}$ channel is much more constrained than the $ZZ \to \ell^+\ell^-\ell'^+\ell'^-$ channel in order to reduce background. Values are given in table 2.

4.3 Systematic uncertainties

Table 3 summarizes the systematic uncertainties on C_{ZZ} and A_{ZZ}. For C_{ZZ} in the $ZZ^{(*)} \to \ell^+\ell^-\ell'^+\ell'^-$ selections, the dominant systematic uncertainties arise from the lepton reconstruction efficiency, the efficiency of the isolation and impact parameter requirements, and the differences in C_{ZZ} estimated by SHERPA and POWHEGBOX; uncertainties on the trigger efficiency and the lepton energy scale and resolution are small. In the $ZZ \to \ell^+\ell^-\nu\bar{\nu}$ channel the dominant C_{ZZ} uncertainties are from uncertainties on the lepton reconstruction efficiency, the lepton energy scale and resolution, and the missing transverse momentum modelling and jet veto uncertainty; uncertainties on the trigger efficiency and due to differences in C_{ZZ} estimated by SHERPA and POWHEGBOX also contribute.

The uncertainties on C_{ZZ} from the reconstruction efficiency, energy scale and resolution, isolation and impact parameter requirements and trigger efficiency are estimated by varying the data-driven correction factors applied to simulation by their systematic and statistical uncertainties. The systematic uncertainties on events with extended leptons used in the $ZZ^{(*)} \to \ell^+\ell^-\ell'^+\ell'^-$ channel are slightly higher than in events without them; nevertheless, since their relative contribution is small, the effect on the uncertainty of the combined channels is negligible. The generator systematic uncertainty for C_{ZZ} accounts for the effect of choosing a different renormalization and factorization scale and PDF set.

For A_{ZZ}, the systematic uncertainties are due to theoretical uncertainties which come from the PDFs, the choice of the renormalization and factorization scales, the modelling of the contribution from gg initial states and the parton shower model, as given in table 3. For the $ZZ \to \ell^+\ell^-\nu\bar{\nu}$ channel, uncertainties in the efficiency of the jet veto are also taken into

Source	$ZZ \to \ell^+\ell^-\ell'^+\ell'^-$	$ZZ^* \to \ell^+\ell^-\ell'^+\ell'^-$	$ZZ \to \ell^+\ell^-\nu\bar{\nu}$
C_{ZZ}			
Lepton efficiency	3.0%	3.1%	1.3%
Lepton energy/momentum	0.2%	0.3%	1.1%
Lepton isolation and impact parameter	1.9%	2.0%	0.6%
Jet+$E_{\mathrm{T}}^{\mathrm{miss}}$ modelling	—	—	0.8%
Jet veto	—	—	0.9%
Trigger efficiency	0.2%	0.2%	0.4%
PDF and scale	1.6%	1.5%	0.4%
A_{ZZ}			
Jet veto	—	—	2.3%
PDF and scale	0.6%	—	1.9%
Generator modelling and parton shower	1.1%	—	4.6%

Table 3. Summary of systematic uncertainties, as relative percentages of the correction factor C_{ZZ} or the acceptance of the fiducial region A_{ZZ}. Dashes indicate uncertainties which are not relevant.

account through the calculation of a scale factor; the ratio of the jet veto efficiency in data to that in MC simulation is taken from a sample of single Z events and then applied to ZZ events [47]. The systematic uncertainties due to the PDFs and scales are evaluated with MCFM by taking the difference between the A_{ZZ} obtained using the CT10 and MSTW2008 PDF sets, as well as using the 44 CT10 error sets, and by shifting the factorization and renormalization scales up and down by a factor of two from the nominal value (half the mass of the diboson system). An additional uncertainty is assigned to account for the effect of different modelling at the generator level. Since the $ZZ^* \to \ell^+\ell^-\ell'^+\ell'^-$ measurement is not used for the total cross section, its A_{ZZ} acceptance is irrelevant and only uncertainty values related to C_{ZZ} are given.

The uncertainty on the integrated luminosity is 3.9% [22]. The uncertainty on the background estimates is discussed in the following sections.

5 Background estimation

5.1 $ZZ^{(*)} \to \ell^+\ell^-\ell'^+\ell'^-$ background

Background to the $ZZ^{(*)} \to \ell^+\ell^-\ell'^+\ell'^-$ signal originates from events with a Z (or W) boson decaying to leptons accompanied by additional jets or photons ($W/Z + X$), from top-quark production and from other diboson final states. Such events may contain electrons or muons from the decay of heavy-flavoured hadrons, muons from in-flight decay of pions and kaons, or jets and photons misidentified as electrons. The majority of these background leptons are rejected by the isolation requirements.

The background estimate follows a data-driven method in which a sample of events containing three leptons satisfying all selection criteria plus one 'lepton-like jet' is identified; such events are denoted as $\ell\ell\ell j$. For muons, the lepton-like jets are muon candidates that fail the isolation requirement or fail the impact parameter requirement but not both. For electrons with $|\eta| < 2.47$, the lepton-like jets are clusters in the electromagnetic

calorimeter matched to inner detector tracks that fail either the full electron selection or the isolation requirement but not both. For electrons with $|\eta| > 2.5$, the lepton-like jets are electromagnetic clusters that are reconstructed as electrons but fail the tight identification requirements. The events are otherwise required to satisfy the full event selection, treating the lepton-like jet as if it were a fully identified lepton. The background is then estimated by weighting the $\ell\ell\ell j$ events by a measured factor f, which is the ratio of the probability for a non-lepton to satisfy the full lepton selection criteria to the probability of a non-lepton satisfying the lepton-like jet criteria. The background in which two selected leptons originate from jets is treated similarly, by identifying a data sample with two leptons and two lepton-like jets; such events are denoted as $\ell\ell jj$. The total number of expected background $\ell^+\ell^-\ell'^+\ell'^-$ events, $N(\mathrm{BG})$, is calculated as:

$$N(\mathrm{BG}) = [N(\ell\ell\ell j) - N(ZZ)] \times f - N(\ell\ell jj) \times f^2 \qquad (5.1)$$

where double counting from $\ell\ell\ell j$ and $\ell\ell jj$ events is accounted for, and the term $N(ZZ)$ is a Monte Carlo estimate correcting for contributions from signal $ZZ^{(*)} \to \ell^+\ell^-\ell'^+\ell'^-$ events having a real lepton that is classified as a lepton-like jet (the equivalent correction to the term $N(\ell\ell jj)$ is negligible).

The factor f is measured in a sample of data selected with single-lepton triggers which contain a Z boson candidate: a pair of isolated same-flavour opposite-sign electrons or muons. In these selected events, f is measured, using the lepton and lepton-like jet candidates not assigned to the Z boson, as the ratio of the number of selected leptons to the number of lepton-like jets, after correcting for expected true lepton contributions from WZ and ZZ events using simulation. Independent values as a function of the η and p_{T} of the lepton-like jet are measured, which are then combined assuming they are uncorrelated. The factor f is found to vary from 0.33 ± 0.01 (0.26 ± 0.02) below $p_{\mathrm{T}} = 10$ GeV to 0.09 ± 0.02 (0.46 ± 0.20) above $p_{\mathrm{T}} = 50$ GeV for electrons (muons). The quoted uncertainties are statistical. Then, with the same procedure, a value for f is also derived using the simulated samples of background processes. The difference between the value of f derived in data and in simulation is assigned as a systematic uncertainty on f. The statistical and systematic uncertainties are then added in quadrature to derive a combined uncertainty on f, which varies as a function of p_{T} from 14% (19%) below 10 GeV to 22% (51%) above 50 GeV for electrons (muons). For the muons, the total uncertainty on f is dominated by its statistical uncertainty. The background estimates for the $ZZ \to \ell^+\ell^-\ell'^+\ell'^-$ and $ZZ^* \to \ell^+\ell^-\ell'^+\ell'^-$ selections are $0.9^{+1.1}_{-0.9}(\mathrm{stat.}) \pm 0.7(\mathrm{syst.})$ and $9.1 \pm 2.3(\mathrm{stat.}) \pm 1.3(\mathrm{syst.})$ events, respectively, as shown in tables 4 and 5. The statistical uncertainty on the background estimate comes from the statistical uncertainty on the numbers of $\ell\ell\ell j$, $\ell\ell jj$ and $ZZ^{(*)} \to \ell^+\ell^-\ell'^+\ell'^-$ events used in eq. 5.1. The systematic uncertainty results from the combined uncertainty on f. In cases where the overall estimate is negative, the background estimate is described using a truncated Gaussian with mean at zero and standard deviation equal to the estimated statistical and systematic uncertainties added in quadrature.

The extra background induced by the use of the extended leptons in the $ZZ^{(*)} \to \ell^+\ell^-\ell'^+\ell'^-$ channel is estimated to be negligible in the $ZZ \to \ell^+\ell^-\ell'^+\ell'^-$ selection, and about 20% (2 events out of the 9.1 estimated, compared to a signal gain of about 10.6 events out of the 64.4 expected) in the $ZZ^* \to \ell^+\ell^-\ell'^+\ell'^-$ selection.

	$e^+e^-e^+e^-$	$\mu^+\mu^-\mu^+\mu^-$	$e^+e^-\mu^+\mu^-$	$\ell^+\ell^-\ell'^+\ell'^-$
$(+)\ N(\ell\ell\ell j) \times f$	1.63 ± 0.34	0.21 ± 0.21	1.84 ± 0.40	3.67 ± 0.57
$(-)N(ZZ) \times f$	0.17 ± 0.13	$0.12^{+0.20}_{-0.12}$	0.34 ± 0.21	0.63 ± 0.32
$(-)N(\ell\ell jj) \times f^2$	0.96 ± 0.10	0.33 ± 0.16	0.83 ± 0.09	2.12 ± 0.21
Background estimate, $N(\text{BG})$	$0.5^{+0.6}_{-0.5}(\text{stat.})$	< 0.64	$0.7 \pm 0.7(\text{stat.})$	$0.9^{+1.1}_{-0.9}(\text{stat.})$
	$\pm 0.3(\text{syst.})$		$\pm 0.6\ (\text{syst.})$	$\pm 0.7(\text{syst.})$

Table 4. Expected number of background events for the $ZZ \to \ell^+\ell^-\ell'^+\ell'^-$ selection in 4.6 fb^{-1} of data, for the individual decay modes (columns 2, 3 and 4) and for their combination (last column). If the central value of the estimate is negative, the upper bound on the number of events in that channel is derived as detailed in section 5.1.

	$e^+e^-e^+e^-$	$\mu^+\mu^-\mu^+\mu^-$	$e^+e^-\mu^+\mu^-$	$\ell^+\ell^-\ell'^+\ell'^-$
$(+)\ N(\ell\ell\ell j) \times f$	8.85 ± 0.98	0.21 ± 0.21	10.63 ± 1.06	19.70 ± 1.46
$(-)N(ZZ) \times f$	0.29 ± 0.18	$0.20^{+0.25}_{-0.20}$	0.56 ± 0.28	1.05 ± 0.42
$(-)N(\ell\ell jj) \times f^2$	4.24 ± 0.23	1.10 ± 0.31	4.24 ± 0.23	9.58 ± 0.45
Background estimate, $N(\text{BG})$	$4.3 \pm 1.4(\text{stat.})$	< 0.91	$5.8 \pm 1.6(\text{stat.})$	$9.1 \pm 2.3(\text{stat.})$
	$\pm 0.6(\text{syst.})$		$\pm 0.9\ (\text{syst.})$	$\pm 1.3(\text{syst.})$

Table 5. Expected number of background events for the $ZZ^* \to \ell^+\ell^-\ell'^+\ell'^-$ selection in 4.6 fb^{-1} of data, for the individual decay modes (columns 2, 3 and 4) and for their combination (last column). If the central value of the estimate is negative, the upper bound on the number of events in that channel is derived as detailed in section 5.1.

The background is also estimated purely from the simulated samples of background processes, and is predicted to be 1.5 ± 0.4 events for the $ZZ \to \ell^+\ell^-\ell'^+\ell'^-$ selection and 8.3 ± 1.3 events for the $ZZ^* \to \ell^+\ell^-\ell'^+\ell'^-$ selection, with uncertainties being statistical only. These estimates compare well with the data-driven results given in tables 4 and 5. According to the estimate from simulation, the dominant source of background is Z+jets events, with only about a 10% to 20% contribution from other diboson channels (WZ and WW), and a negligible contribution from events with top quarks.

Differential background distributions are determined by first deriving the shape of the distributions from the background MC samples. This is achieved by selecting events where one Z candidate is required to satisfy the nominal lepton selection, while the other Z candidate is formed by leptons satisfying relaxed criteria for the isolation requirements and transverse impact parameter significance. The shape determined in this way is then scaled such that the total number of events in the distribution is equal to the data-driven background estimate shown in tables 4 and 5.

5.2 $ZZ \to \ell^+\ell^-\nu\bar{\nu}$ background

There are several sources of background to the $ZZ \to \ell^+\ell^-\nu\bar{\nu}$ channel. Processes such as $t\bar{t}$, WW, Wt or $Z \to \tau^+\tau^-$ production give two true isolated leptons with missing transverse momentum. Diboson WZ events in which both bosons decay leptonically have

Process	$e^+e^- E_{\mathrm{T}}^{\mathrm{miss}}$	$\mu^+\mu^- E_{\mathrm{T}}^{\mathrm{miss}}$	$\ell^+\ell^- E_{\mathrm{T}}^{\mathrm{miss}}$
$t\bar{t}, Wt, WW, Z \to \tau^+\tau^-$	$8.5 \pm 2.1 \pm 0.5$	$10.6 \pm 2.6 \pm 0.6$	$19.1 \pm 2.3 \pm 1.0$
WZ	$8.9 \pm 0.5 \pm 0.4$	$11.9 \pm 0.5 \pm 0.3$	$20.8 \pm 0.7 \pm 0.5$
$Z \to \mu^+\mu^-, e^+e^-$+jets	$2.6 \pm 0.7 \pm 1.0$	$2.7 \pm 0.8 \pm 1.2$	$5.3 \pm 1.1 \pm 1.6$
$W+$ jets	$0.7 \pm 0.3 \pm 0.3$	$0.7 \pm 0.2 \pm 0.2$	$1.5 \pm 0.4 \pm 0.4$
$W\gamma$	$0.1 \pm 0.1 \pm 0.0$	$0.2 \pm 0.1 \pm 0.0$	$0.3 \pm 0.1 \pm 0.0$
Total	$20.8 \pm 2.3 \pm 1.2$	$26.1 \pm 2.8 \pm 1.4$	$46.9 \pm 4.8 \pm 1.9$

Table 6. Expected number of background events to the $ZZ \to \ell^+\ell^-\nu\bar{\nu}$ channel in 4.6 fb^{-1} of data, for the individual decay modes (columns 2 and 3) and for their combination (last column). The first uncertainty is statistical while the second is systematic.

three charged leptons, but if one lepton from a W or Z boson decay is not identified, the event has the same signature as the signal. Production of a Z boson in association with jets gives two isolated leptons from the Z boson decay and may have missing transverse momentum if the jet momenta are mismeasured. Finally, production of a W boson in association with jets or photons may satisfy the selection requirements when one of the jets or photons is misidentified as an isolated lepton. All of the backgrounds are measured with data-driven techniques except for WZ and $W\gamma$. The total background is estimated to be $46.9 \pm 4.8 \pm 1.9$ events as summarized in table 6.

5.2.1 Backgrounds from $t\bar{t}$, Wt, WW and $Z \to \tau^+\tau^-$

The contributions from $t\bar{t}$, Wt, WW and $Z \to \tau^+\tau^-$ processes are measured by extrapolating from a control sample of events with one electron and one muon (instead of two electrons or two muons), which otherwise satisfy the full $ZZ \to \ell^+\ell^-\nu\bar{\nu}$ selection. This sample is free from signal events. The extrapolation from the $e\mu$ channel to the ee or $\mu\mu$ channel uses the relative branching fractions ($2:1:1$ for $e\mu : ee : \mu\mu$) as well as the ratio of the efficiencies ϵ_{ee} or $\epsilon_{\mu\mu}$ of the ee or $\mu\mu$ selections to the efficiency $\epsilon_{e\mu}$ of the $e\mu$ selection, which differs from unity due to differences in the electron and muon efficiencies.

For the electron channel, this is represented by the equation:

$$N_{ee}^{\mathrm{bkg}} = (N_{e\mu}^{\mathrm{data}} - N_{e\mu}^{\mathrm{sim}}) \times \frac{1}{2} \times \frac{\epsilon_{ee}}{\epsilon_{e\mu}} \tag{5.2}$$

where $N_{e\mu}^{\mathrm{data}}$ is the number of observed $e\mu$ events and $N_{e\mu}^{\mathrm{sim}}$ is the number expected events from processes other than $t\bar{t}$, Wt, WW and $Z \to \tau^+\tau^-$ (WZ, ZZ, W+jet, Z+jet and W/γ). Therefore, $(N_{e\mu}^{\mathrm{data}} - N_{e\mu}^{\mathrm{sim}})$ is the estimate of $t\bar{t}$, Wt, WW and $Z \to \tau^+\tau^-$ production in the control sample. The efficiency correction factor, $\epsilon_{ee}/\epsilon_{e\mu}$, corrects for the difference between electron and muon efficiency. The efficiency correction factor is measured in data using reconstructed $Z \to \ell^+\ell^-$ events, as

$$\frac{\epsilon_{ee}}{\epsilon_{e\mu}} = \frac{\epsilon_e^2}{\epsilon_e \epsilon_\mu} = \frac{\epsilon_e}{\epsilon_\mu} = \sqrt{\frac{N_{ee}^{\mathrm{data}}}{N_{\mu\mu}^{\mathrm{data}}}} \tag{5.3}$$

where N_{ee}^{data} and $N_{\mu\mu}^{\mathrm{data}}$ are the number of observed ee or $\mu\mu$ events in the Z boson mass window, respectively, after all lepton selection requirements and the Z boson mass window requirement are applied. A parallel argument gives $N_{\mu\mu}^{\mathrm{bkg}}$. This procedure is repeated in bins of p_{T}^{Z} in order to obtain the p_{T} distribution of the $t\bar{t}$, Wt, WW and $Z \to \tau^{+}\tau^{-}$ background.

The dominant uncertainty is statistical (25%), due to the limited number of events in the control samples. Additional uncertainties are due to systematic uncertainties in the normalization of the simulated samples used to correct the $e\mu$ contribution (5.5%) and the systematic uncertainty in the efficiency correction factor (4.5%).

5.2.2 Background from WZ production with leptonic decays

Events from leptonic WZ decays may result in an $\ell^{+}\ell^{-}E_{\mathrm{T}}^{\mathrm{miss}}$ signature when one lepton from the W or Z boson is not reconstructed. The contribution from this process is estimated using the simulated samples described in section 2.1. The estimate is checked using a control region with three high-p_{T} isolated leptons. The two dominant processes that contribute to this control region are WZ and Z+jets production, where the WZ boson pair decays to three leptons and a neutrino and the Z+jets contribution has two real leptons from the Z decay and a misidentified lepton from the jet. The technique used to estimate the background in the $ZZ^{(*)} \to \ell^{+}\ell^{-}\ell'^{+}\ell'^{-}$ channel is also used to normalize the contribution from Z+jets in the three-lepton control region. The WZ Monte Carlo expectation is consistent with the data. The systematic uncertainties are estimated in the same way as for signal Monte Carlo events.

5.2.3 Background from Z bosons with associated jets

Occasionally events with a Z boson produced in association with jets may have large amounts of missing transverse momentum due to mismeasurement of the momenta of the jets. This background is estimated using events with a high-p_{T} photon and jets as a template, since the mechanism for large missing transverse momentum is the same as in Z+jets events. The events are reweighted such that the photon E_{T} matches the observed Z boson p_{T} and are normalized to the observed Z + jets yield. The procedure is repeated in bins of p_{T}^{Z} in order to obtain the p_{T} distribution of the Z+jets backgrounds. The largest systematic uncertainty is due to the subtraction of $W\gamma$, $Z\gamma$, $t\bar{t}$ and $W \to e\nu$ contributions to the γ+jets sample, which is 33% in the ee channel and 37% in the $\mu\mu$ channel.

5.2.4 Background from events with a misidentified lepton

A small contribution to the selected sample is due to events in which one of the two leptons comes from the decay of a W or Z boson (called 'real' below) and the second is a 'fake', corresponding both non-prompt leptons and misidentified π^{0} mesons or conversions.

The dominant fake-muon mechanism is the decay of heavy-flavoured hadrons, in which a muon survives the isolation requirements. In the case of electrons, the three mechanisms are heavy-flavour hadron decay, light-flavour jets with a leading π^{0} overlapping with a charged particle, and conversion of photons. Processes that contribute are top-quark pair production, production of W bosons in association with jets and multi-jet production.

The 'matrix method' [48] is applied to estimate the fraction of events in the signal regions that contain at least one fake lepton. The method measures the number of fake leptons in background-dominated control regions and extrapolates to the ZZ selection region using factors measured in data. The shape of the background is provided by taking the background as uniformly distributed among the bins and treating each bin as statistically uncorrelated. The dominant systematic uncertainty is due to the uncertainty on the extrapolation factors and the limited numbers of events in the control samples, giving a total uncertainty of 63% and 44% in the ee and $\mu\mu$ channels, respectively.

6 Results

Three types of measurements are presented:

- integrated fiducial and total ZZ cross sections;

- differential cross sections normalized to the overall measured cross sections for the p_T^Z and $\Delta\phi(\ell^+, \ell^-)$ of the leading Z boson, and the mass (transverse mass[7]) of the ZZ system for the $ZZ \to \ell^+\ell^-\ell'^+\ell'^-$ ($ZZ \to \ell^+\ell^-\nu\bar{\nu}$) selection; and

- limits on the anomalous nTGCs.

6.1 Cross section measurements

The expected and observed event yields after applying all selection criteria are shown in table 7 for both channels. Figure 4 shows the jet multiplicity in selected $ZZ \to \ell^+\ell^-\ell'^+\ell'^-$ and $ZZ \to \ell^+\ell^-\nu\bar{\nu}$ events before the jet veto is applied. Figures 5 and 6 show the transverse momentum and mass of the ZZ system in selected $ZZ \to \ell^+\ell^-\ell'^+\ell'^-$ and $ZZ^* \to \ell^+\ell^-\ell'^+\ell'^-$ events respectively. Figure 7 shows the transverse momentum and mass of the two-charged-lepton system in selected $ZZ \to \ell^+\ell^-\nu\bar{\nu}$ events. The shapes of the distributions are consistent with the predictions from the simulation.

The $ZZ^{(*)} \to \ell^+\ell^-\ell'^+\ell'^-$ and $ZZ \to \ell^+\ell^-\nu\bar{\nu}$ fiducial cross sections are determined using a maximum likelihood fitting method, taking into account the integrated luminosity and the C_{ZZ} correction factors discussed in section 4. A Poisson probability function is used to model the number of expected events, multiplied by Gaussian distribution functions which model the nuisance parameters representing systematic uncertainties. The measured fiducial cross sections are:

$$\sigma_{ZZ \to \ell^+\ell^-\ell'^+\ell'^-}^{\mathrm{fid}} = 25.4_{-3.0}^{+3.3} \text{ (stat.) } _{-1.0}^{+1.2} \text{ (syst.) } \pm 1.0 \text{ (lumi.) fb,}$$
$$\sigma_{ZZ^* \to \ell^+\ell^-\ell'^+\ell'^-}^{\mathrm{fid}} = 29.8_{-3.5}^{+3.8} \text{ (stat.) } _{-1.5}^{+1.7} \text{ (syst.) } \pm 1.2 \text{ (lumi.) fb,}$$
$$\sigma_{ZZ \to \ell^+\ell^-\nu\bar{\nu}}^{\mathrm{fid}} = 12.7_{-2.9}^{+3.1} \text{ (stat.) } _{-1.7}^{+1.7} \text{ (syst.) } \pm 0.5 \text{ (lumi.) fb.}$$

where $\ell^+\ell^-\ell'^+\ell'^-$ refers to the sum of the $e^+e^-e^+e^-$, $e^+e^-\mu^+\mu^-$ and $\mu^+\mu^-\mu^+\mu^-$ final states and $\ell^+\ell^-\nu\bar{\nu}$ refers to the sum of the $e^+e^-E_\mathrm{T}^{\mathrm{miss}}$ and $\mu^+\mu^-E_\mathrm{T}^{\mathrm{miss}}$ final states.[8] The

---

[7]$m_\mathrm{T}^2 = \left(\sqrt{(m^Z)^2 + (p_\mathrm{T}^Z)^2} + \sqrt{(m^Z)^2 + (E_\mathrm{T}^{\mathrm{miss}})^2}\right)^2 - \left(\vec{p}_\mathrm{T}^Z + \vec{E}_\mathrm{T}^{\mathrm{miss}}\right)^2$.

[8]The $ZZ \to \ell^+\ell^-\nu\bar{\nu}$ fiducial region is more restricted compared to the $ZZ^{(*)} \to \ell^+\ell^-\ell'^+\ell'^-$ channel.

$ZZ^{(*)} \to \ell^+\ell^-\ell'^+\ell'^-$	$e^+e^-e^+e^-$	$\mu^+\mu^-\mu^+\mu^-$	$e^+e^-\mu^+\mu^-$	$\ell^+\ell^-\ell'^+\ell'^-$
Observed ZZ	16	23	27	66
Observed ZZ^*	21	30	33	84
Expected ZZ signal	$10.3 \pm 0.1 \pm 1.0$	$16.5 \pm 0.2 \pm 0.9$	$26.7 \pm 0.2 \pm 1.7$	$53.4 \pm 0.3 \pm 3.2$
Expected ZZ^* signal	$12.3 \pm 0.2 \pm 1.2$	$20.5 \pm 0.2 \pm 1.1$	$31.6 \pm 0.3 \pm 2.0$	$64.4 \pm 0.4 \pm 4.0$
Expected ZZ background	$0.5 \pm 0.6 \pm 0.3$	< 0.6	$0.7 \pm 0.7 \pm 0.6$	$0.9 \pm 1.1 \pm 0.7$
Expected ZZ^* background	$4.3 \pm 1.4 \pm 0.6$	< 0.9	$5.8 \pm 1.6 \pm 0.9$	$9.1 \pm 2.3 \pm 1.3$
$ZZ \to \ell^+\ell^-\nu\bar{\nu}$	$e^+e^- E_{\mathrm{T}}^{\mathrm{miss}}$	$\mu^+\mu^- E_{\mathrm{T}}^{\mathrm{miss}}$		$\ell^+\ell^- E_{\mathrm{T}}^{\mathrm{miss}}$
Observed ZZ	35	52		87
Expected ZZ signal	$17.8 \pm 0.3 \pm 1.7$	$21.6 \pm 0.3 \pm 2.0$		$39.3 \pm 0.4 \pm 3.7$
Expected ZZ background	$20.8 \pm 2.3 \pm 1.2$	$26.1 \pm 2.8 \pm 1.4$		$46.9 \pm 4.8 \pm 1.9$

Table 7. Summary of observed $ZZ \to \ell^+\ell^-\ell'^+\ell'^-$, $ZZ^* \to \ell^+\ell^-\ell'^+\ell'^-$ and $ZZ \to \ell^+\ell^-\nu\bar{\nu}$ candidates in the data, total background estimates and expected signal for the individual decay modes (columns 2 to 4) and for their combination (last column). The quoted uncertainties and limits represent 68% confidence intervals; the first uncertainty is statistical while the second is systematic. The uncertainty on the integrated luminosity (3.9%) is not included.

(a)

(b)
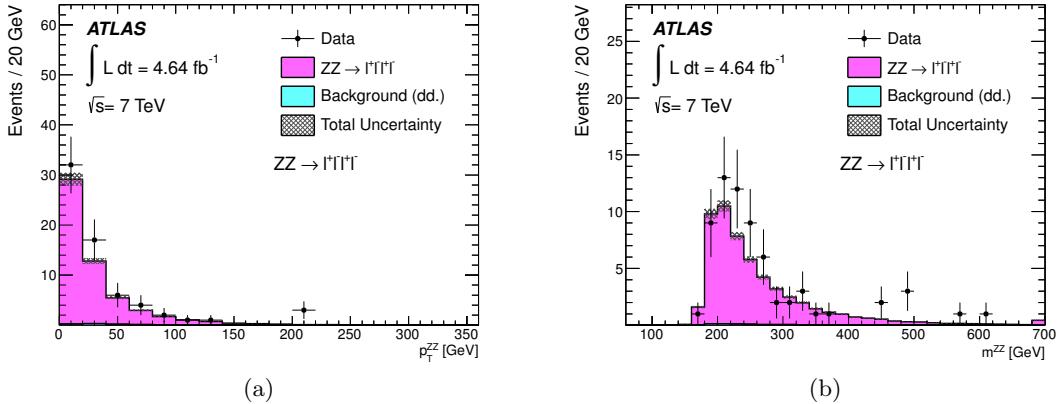
Figure 5. (a) Transverse momentum p_{T}^{ZZ} and (b) invariant mass m^{ZZ} of the four-lepton system for the ZZ selection. The points represent the observed data and the histograms show the prediction from simulation, where the background is normalized to the data-driven (dd) estimate as described in section 5.1. The shaded band shows the combined statistical and systematic uncertainty on the prediction.

expected SM fiducial cross sections, derived from PowhegBox and gg2zz, are:

$$\sigma_{ZZ \to \ell^+\ell^-\ell'^+\ell'^-}^{\mathrm{fid,SM}} = 20.9 \pm 0.1 \,\text{(stat.)} \, ^{+1.1}_{-0.9} \,\text{(theory)} \,\text{fb},$$

$$\sigma_{ZZ^* \to \ell^+\ell^-\ell'^+\ell'^-}^{\mathrm{fid,SM}} = 25.6 \pm 0.1 \,\text{(stat.)} \, ^{+1.3}_{-1.1} \,\text{(theory)} \,\text{fb},$$

$$\sigma_{ZZ \to \ell^+\ell^-\nu\bar{\nu}}^{\mathrm{fid,SM}} = 12.5 \pm 0.1 \,\text{(stat.)} \, ^{+1.0}_{-1.1} \,\text{(theory)} \,\text{fb}.$$

The measured cross sections are compatible with these theoretical values.
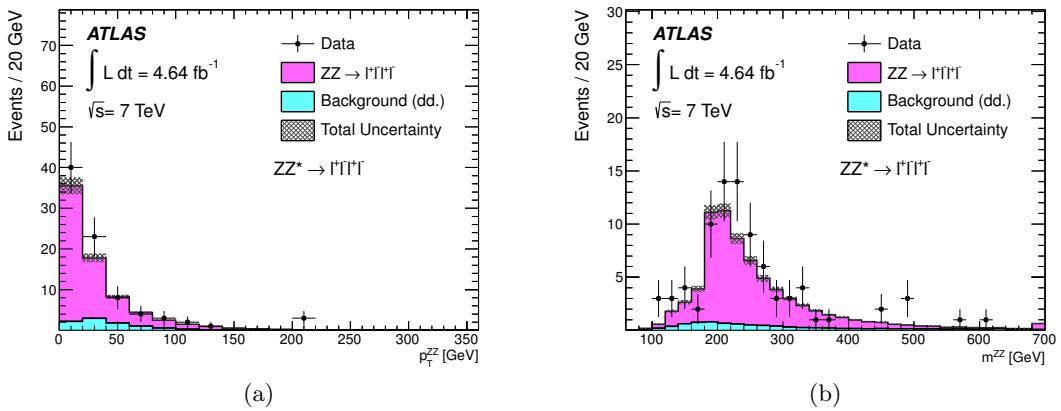
Figure 6. (a) Transverse momentum p_T^{ZZ} and (b) invariant mass m^{ZZ} of the four-lepton system for the ZZ^* selection. The points represent the observed data and the histograms show the prediction from simulation, where the background is normalized to the data-driven (dd) estimate. The shaded band shows the combined statistical and systematic uncertainty on the prediction.
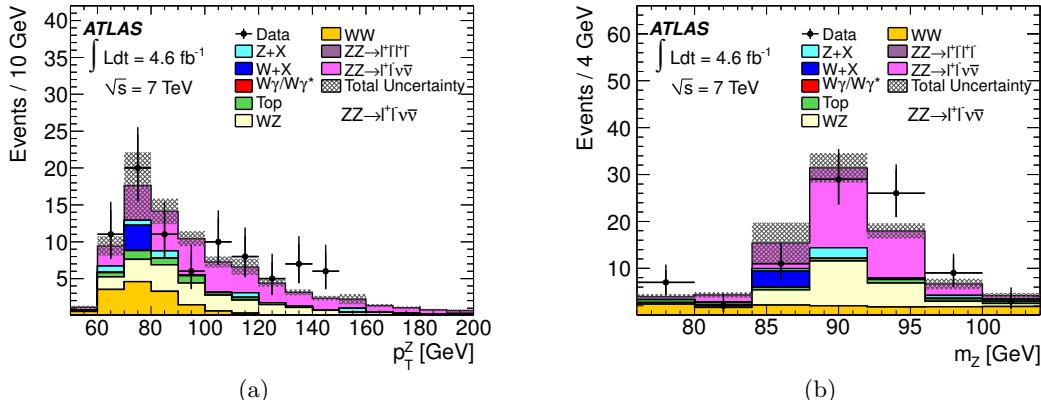
Figure 7. (a) Transverse momentum p_T^Z and (b) mass m_Z of the two-charged-lepton system for the $ZZ \to \ell^+\ell^-\nu\bar{\nu}$ selection. The points represent the observed data and the histograms show the prediction from simulation. The shaded band shows the combined statistical and systematic uncertainty on the prediction.

The total ZZ cross section is calculated by extrapolating to the full phase space while each Z boson is required to have a mass within the Z mass window. Both $ZZ \to \ell^+\ell^-\ell'^+\ell'^-$ and $ZZ \to \ell^+\ell^-\nu\bar{\nu}$ events are combined in the maximum likelihood fit, taking into account the known Z branching fractions [46] and the A_{ZZ} kinematic and geometrical acceptances (section 4). Correlated systematic uncertainties between the $ZZ \to \ell^+\ell^-\ell'^+\ell'^-$ and $ZZ \to \ell^+\ell^-\nu\bar{\nu}$ channels are taken into account in the fit using a single Gaussian for the nuisance parameter for each source of correlated uncertainty. The measured value of the total ZZ cross section is:

$$\sigma_{ZZ}^{\text{tot}} = 6.7 \pm 0.7 \text{ (stat.)} \ ^{+0.4}_{-0.3} \text{ (syst.)} \pm 0.3 \text{ (lumi.) pb.}$$

The result is consistent within errors with the NLO Standard Model total cross section for

this process of $5.89^{+0.22}_{-0.18}$ pb, where the quoted theoretical uncertainties result from varying the factorization and renormalization scales simultaneously by a factor of two and from using the full CT10 PDF error set.

6.2 Differential cross sections

The differential cross sections present a more detailed comparison of theory to measurement, allowing a generic comparison of the kinematic distributions to new theories. Variables which are sensitive to new phenomena, such as p_T^Z, m^{ZZ} and $\Delta\phi(\ell^+, \ell^-)$, are used with bin boundaries chosen to maximize sensitivity to nTGCs. At the same time, the bin widths were chosen to be commensurate with the resolution.

The measured distributions are unfolded back to the underlying distributions, accounting for the effect of detector resolution, efficiency and acceptance, within the fiducial region of each measurement. The unfolding procedure is based on a Bayesian iterative algorithm [49]. The algorithm takes as input a prior for the kinematic distribution and iterates using the posterior distribution as prior for the next iteration. The initial prior is taken from the signal Monte Carlo expectation calculated using the POWHEGBOX generator and three iterations are performed. The uncertainty on the unfolded distributions is dominated by the statistical uncertainty, which is about 30% in most bins. The systematic uncertainty is no more than 5% in any bin. The dependence of the unfolded cross sections on the choice of the initial prior is tested by unfolding the measured distributions using a different generator (SHERPA). The difference between the two is taken as a systematic uncertainty to account for differences in generator modelling (e.g. QCD radiation). The difference in unfolded distributions between three iterations and four iterations is much lower than the statistical uncertainty and it is taken as a further uncertainty on the unfolding procedure. Systematic uncertainties related to detector effects (e.g. lepton reconstruction efficiency) are evaluated using pseudo-experiments.

Figures 8 to 10 show the differential cross sections normalized to the fiducial cross sections for the p_T^Z and $\Delta\phi(\ell^+, \ell^-)$ of the leading Z boson, and for the mass (transverse mass) of the ZZ system for the $ZZ \to \ell^+\ell^-\ell'^+\ell'^-$ ($ZZ \to \ell^+\ell^-\nu\bar{\nu}$) selection. The Standard Model prediction is consistent with the measurement in each case.

6.3 Anomalous neutral triple gauge couplings

Anomalous nTGCs for on-shell ZZ production can be parameterized by two CP-violating (f_4^V) and two CP-conserving (f_5^V) complex parameters (where $V = Z, \gamma$) which are zero in the Standard Model [3]. A form-factor parameterization is introduced leading to couplings which vanish at high parton centre-of-mass energy $\sqrt{\hat{s}}$: $f_i^V = f_{i0}^V/(1 + \hat{s}/\Lambda^2)^n$, ensuring partial-wave unitarity. Here, Λ is the energy scale at which physics beyond the Standard Model would be directly observable, f_{i0}^V are the low-energy approximations of the couplings, and n is the form-factor power. Values of $n = 3$ and $\Lambda = 3$ TeV are chosen, so that expected limits are within the values allowed by requiring that unitarity is not violated at LHC energies [3]. The results with an energy cutoff $\Lambda = \infty$ (i.e. without a form factor) are also presented as a comparison in the unitarity violating scheme.
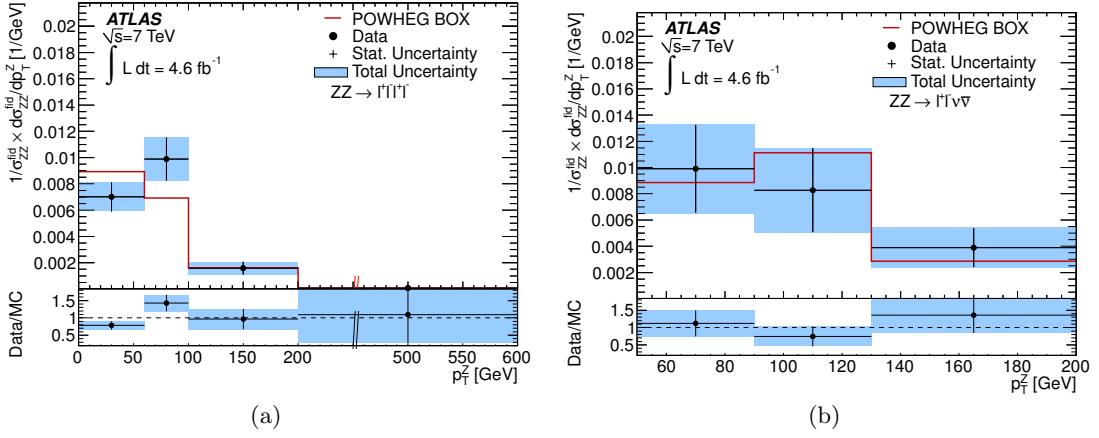
Figure 8. Unfolded ZZ fiducial cross sections in bins of the p_{T} of the leading Z boson for (a) the $ZZ \to \ell^+\ell^-\ell'^+\ell'^-$ selection, where a discontinuity is indicated by the parallel pairs of lines, and (b) the $ZZ \to \ell^+\ell^-\nu\bar{\nu}$ selection.
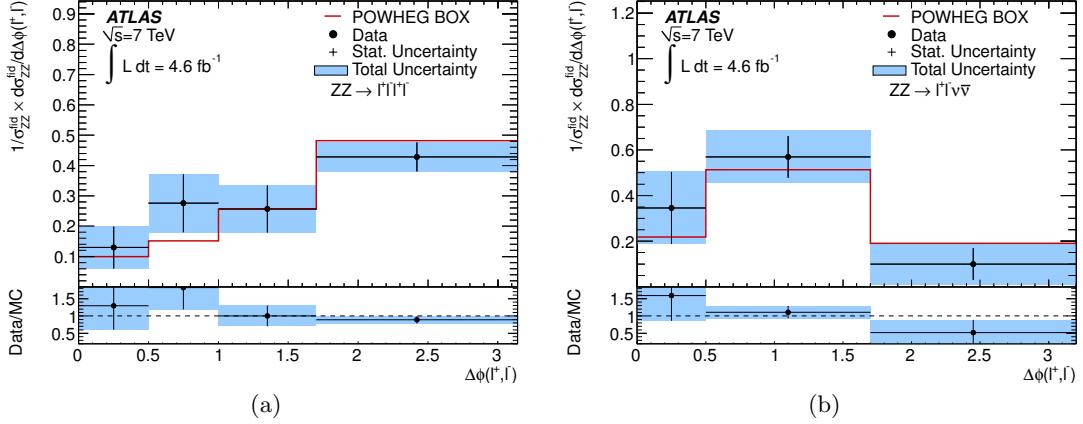
Figure 9. Unfolded ZZ fiducial cross sections in bins of the $\Delta\phi(\ell^+, \ell^-)$ of the leading Z boson for (a) the $ZZ \to \ell^+\ell^-\ell'^+\ell'^-$ selection and (b) the $ZZ \to \ell^+\ell^-\nu\bar{\nu}$ selection.

Limits on anomalous nTGCs are determined using the observed and expected numbers of $ZZ \to \ell^+\ell^-\ell'^+\ell'^-$ and $ZZ \to \ell^+\ell^-\nu\bar{\nu}$ events binned[9] in p_{T}^Z, as seen in table 8. Figure 11 shows the observed p_{T}^Z distributions, together with the SM expectation and the predicted distributions for nTGC values close to the previous limits obtained by ATLAS [13]. Using an increased data sample compared with our previous measurement, including the $ZZ \to \ell^+\ell^-\nu\bar{\nu}$ channel, and exploiting the differential event yields, the precision is expected to improve by about a factor of five. The dependency of the couplings on the expected number of events in each p_{T}^Z bin is parameterized using fully simulated events, generated with SHERPA [26], subsequently reweighted using the Baur-Rainwater [3, 50] and BHO [51] MC generators. The next-to-leading-order matrix elements with their nTGC dependence have been extracted from the BHO MC generator for $2 \to 5$ events and the Baur-Rainwater MC

---

[9]The raw (i.e. not unfolded) differential event yields are used, to avoid introducing theory dependence.

- 23 -
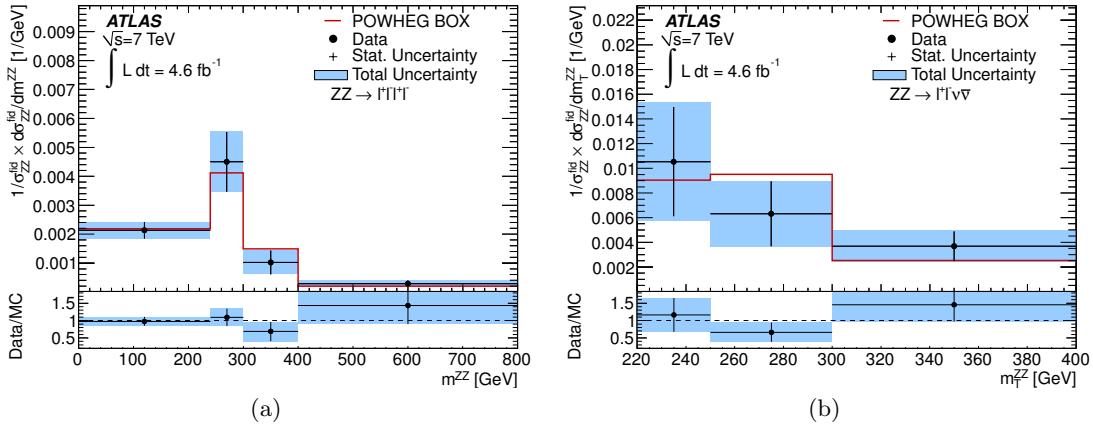
Figure 10. Unfolded ZZ fiducial cross sections in bins of (a) m^{ZZ} for the $ZZ \to \ell^+\ell^-\ell'^+\ell'^-$ selection and (b) m_{T}^{ZZ} for the $ZZ \to \ell^+\ell^-\nu\bar{\nu}$ selection.

	Expected background	Expected ZZ signal	Observed events
$ZZ \to \ell^+\ell^-\ell'^+\ell'^-$			
$0 < p_{\mathrm{T}}^Z < 60\,\mathrm{GeV}$	$0.6 \pm 0.8 \pm 0.5$	$27.9 \pm 0.2 \pm 2.0$	28
$60 < p_{\mathrm{T}}^Z < 100\,\mathrm{GeV}$	$0.2 \pm 0.2 \pm 0.2$	$14.6 \pm 0.2 \pm 1.2$	25
$100 < p_{\mathrm{T}}^Z < 200\,\mathrm{GeV}$	$0.1 \pm 0.1 \pm 0.1$	$9.3 \pm 0.1 \pm 0.9$	11
$p_{\mathrm{T}}^Z > 200\,\mathrm{GeV}$	$0.01 \pm 0.01 \pm 0.01$	$1.6 \pm 0.1 \pm 0.3$	2
$ZZ \to \ell^+\ell^-\nu\bar{\nu}$			
$50 < p_{\mathrm{T}}^Z < 90\,\mathrm{GeV}$	$26.0 \pm 4.5 \pm 1.1$	$13.6 \pm 0.2 \pm 1.3$	42
$90 < p_{\mathrm{T}}^Z < 130\,\mathrm{GeV}$	$16.0 \pm 2.8 \pm 0.7$	$15.7 \pm 0.3 \pm 1.7$	29
$p_{\mathrm{T}}^Z > 130\,\mathrm{GeV}$	$4.9 \pm 1.8 \pm 0.2$	$10.1 \pm 0.1 \pm 1.5$	16

Table 8. Total background, expected signal and observed events as a function of the p_{T} of the leading Z for the $ZZ \to \ell^+\ell^-\ell'^+\ell'^-$ and $ZZ \to \ell^+\ell^-\nu\bar{\nu}$ selections. For the expected signal and background events, the first uncertainty is statistical and the second is systematic.

generator for $2 \to 4$ events and introduced into a framework [52] that enables a calculation of the amplitude given the four vectors and the identity of the incoming and outgoing particles from the hard process.

Confidence intervals for the anomalous triple gauge couplings are determined using the maximum profile likelihood ratio. Limits are set on each coupling, assuming all of the other couplings are zero (as in the Standard Model), and on pairs of couplings assuming the remaining two couplings are zero. The profile likelihood ratio is calculated for the data, and also for 10000 pseudo-experiments generated using the expected number of events at each point in the one- or two-dimensional nTGC parameter space. A point is rejected if more than 95% of the pseudo-experiments have a larger profile likelihood ratio value than the one observed in data. The systematic errors are included as nuisance parameters.
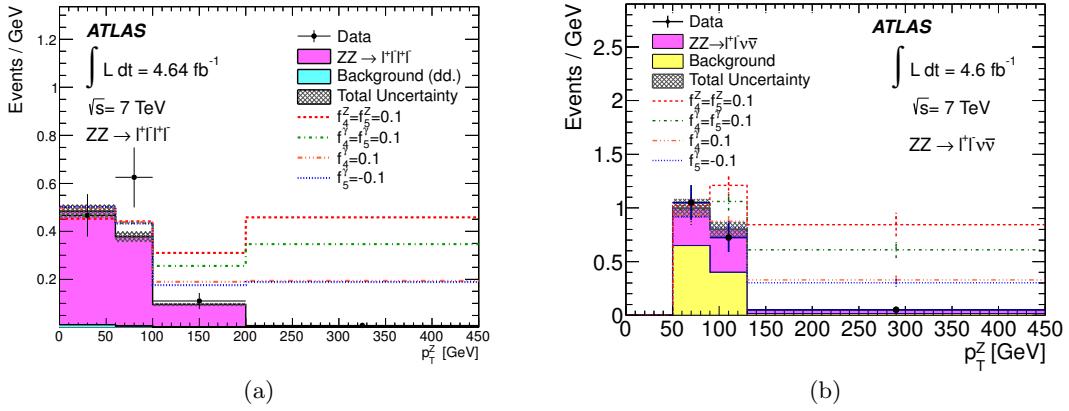
Figure 11. The leading Z boson transverse momentum distributions for (a) the $ZZ \to \ell^+\ell^-\ell'^+\ell'^-$ selection and (b) the $ZZ \to \ell^+\ell^-\nu\bar{\nu}$ selection. The observed distributions are shown as filled circles, the SM expected signal and background are shown as filled histograms, and the predicted distributions for four different nTGC samples with form factor scales of $\Lambda = 3\,\mathrm{TeV}$ and nTGC coupling values set near the edge of the exclusion set in the $1\,\mathrm{fb}^{-1}$ analysis [13] are shown as dashed lines.

Λ	f_{40}^{γ}	f_{40}^{Z}	f_{50}^{γ}	f_{50}^{Z}
3 TeV	$[-0.022, 0.023]$	$[-0.019, 0.019]$	$[-0.023, 0.023]$	$[-0.020, 0.019]$
∞	$[-0.015, 0.015]$	$[-0.013, 0.013]$	$[-0.016, 0.015]$	$[-0.013, 0.013]$

Table 9. One-dimensional 95% confidence intervals for anomalous neutral gauge boson couplings, where the limit for each coupling assumes the other couplings are fixed at zero, their SM value. Limits are presented for form factor scales of $\Lambda = 3$ TeV and $\Lambda = \infty$ and include both statistical and systematic uncertainties; the statistical uncertainties are dominant.

The resulting limits for each coupling are listed in table 9. Two-dimensional 95% confidence intervals[10] are shown in figure 12. The one-dimensional limits are more stringent than those derived from measurements at LEP [8] and the Tevatron [9] and previously by ATLAS [13]; it should be noted that the limits from LEP do not use a form factor, and those from the Tevatron use $\Lambda = 1.2$ TeV. A comparison of the LHC limits with those derived from LEP and Tevatron is shown in figure 13.

7 Conclusions

A measurement of the $ZZ^{(*)}$ production cross section in LHC proton-proton collisions at $\sqrt{s} = 7\,\mathrm{TeV}$ is presented with data collected by the ATLAS detector, using the $ZZ^{(*)} \to \ell^+\ell^-\ell'^+\ell'^-$ and $ZZ \to \ell^+\ell^-\nu\bar{\nu}$ decay channels. Fiducial cross sections are measured for three production and decay selections, and the results are compatible with the SM expected cross sections. Using the $ZZ \to \ell^+\ell^-\ell'^+\ell'^-$ and $ZZ \to \ell^+\ell^-\nu\bar{\nu}$ selections, the total ZZ

---

[10]Since most of the sensitivity of the measurement is contained in a single bin, the likelihood ratio used to obtain the two-dimensional limits has one effective degree of freedom.
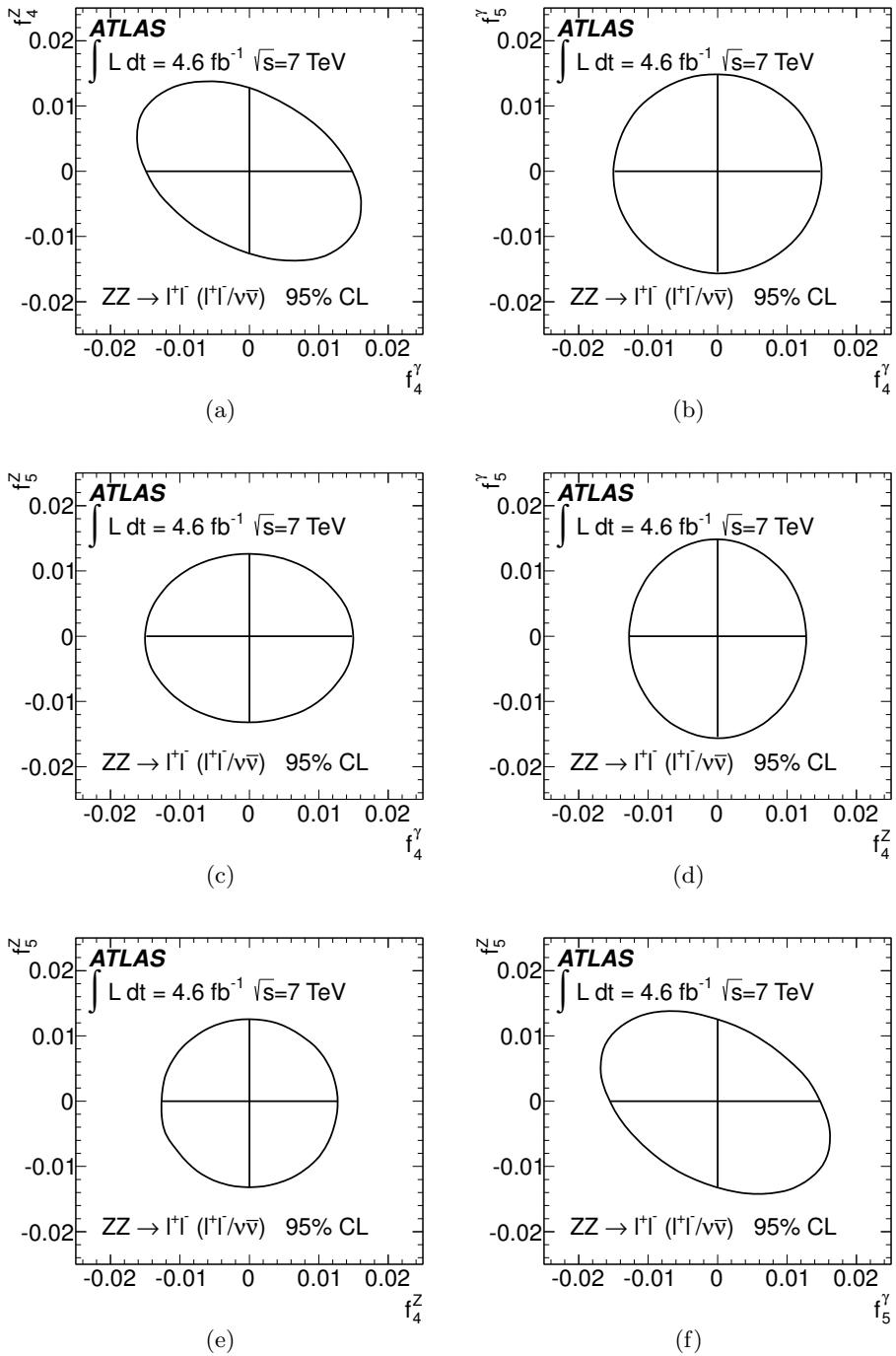
Figure 12. Two-dimensional triple gauge coupling limits for form factor scale $\Lambda = \infty$. The one-dimensional triple gauge coupling limits are shown as vertical and horizontal lines inside the two-dimensional ellipses, whose shape is determined by the theoretical correlations. For each two-dimensional limit the other TGC parameters are assumed to be zero. Since most of the sensitivity of the measurement is contained in a single bin, the likelihood ratio used to obtain the two-dimensional limits has one effective degree of freedom.
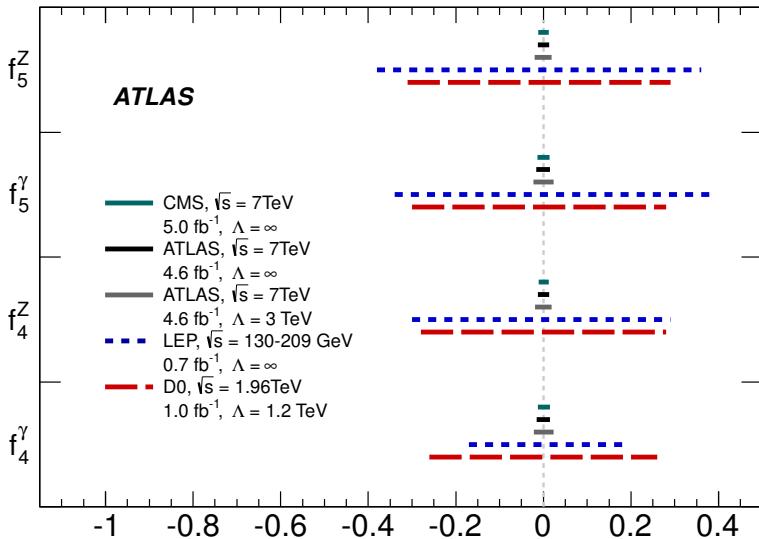
Figure 13. Anomalous nTGC 95% confidence intervals from ATLAS, LEP [8] and Tevatron [9] experiments. Luminosities, centre-of-mass energies and cut-offs Λ for each experiment are shown.

production cross section is determined to be:

$$\sigma_{ZZ}^{\rm tot} = 6.7 \pm 0.7 \ \text{(stat.)} \ ^{+0.4}_{-0.3} \ \text{(syst.)} \pm 0.3 \ \text{(lumi.)} \ \text{pb}.$$

The result is statistically consistent with the NLO Standard Model prediction of $5.89^{+0.22}_{-0.18}$ pb, calculated with Z bosons with a mass between 66 and 116 GeV, and supersedes the previous measurements made with part of the same dataset [13]. Unfolded distributions of the fiducial cross sections are derived for the $p_{\rm T}^Z$ and $\Delta\phi(\ell^+, \ell^-)$ of the leading Z boson and for m^{ZZ} in the $ZZ \to \ell^+\ell^-\ell'^+\ell'^-$ selection and the $m_{\rm T}$ in the $ZZ \to \ell^+\ell^-\nu\bar{\nu}$ selection.

The event yields as a function of the $p_{\rm T}$ of the leading Z boson for the $ZZ \to \ell^+\ell^-\ell'^+\ell'^-$ and $ZZ \to \ell^+\ell^-\nu\bar{\nu}$ selections are used to derive 95% confidence intervals for anomalous neutral triple gauge boson couplings. These limits are more stringent than those derived from measurements at LEP [8] and the Tevatron [9]. They improve the previous published results from ATLAS [13] by approximately a factor of five and supersede them.

Acknowledgments

References

[1] G. Gounaris, J. Layssac and F. Renard, *New and standard physics contributions to anomalous Z and gamma selfcouplings*, *Phys. Rev.* **D 62** (2000) 073013 [`hep-ph/0003143`] [INSPIRE].

[2] J. Ellison and J. Wudka, *Study of trilinear gauge boson couplings at the Tevatron collider*, *Ann. Rev. Nucl. Part. Sci.* **48** (1998) 33 [`hep-ph/9804322`] [INSPIRE].

[3] U. Baur and D.L. Rainwater, *Probing neutral gauge boson selfinteractions in ZZ production at the Tevatron*, *Int. J. Mod. Phys.* **A 16S1A** (2001) 315 [`hep-ph/0011016`] [INSPIRE].

[4] ALEPH collaboration, R. Barate et al., *Measurement of the $e^+e^- \to ZZ$ production cross-section at center-of-mass energies of* 183 GeV *and* 189 GeV, *Phys. Lett.* **B 469** (1999) 287 [`hep-ex/9911003`] [INSPIRE].

[5] DELPHI collaboration, J. Abdallah et al., *ZZ production in e^+e^- interactions at $\sqrt{s} = 183$ GeV to* 209 GeV, *Eur. Phys. J.* **C 30** (2003) 447 [`hep-ex/0307050`] [INSPIRE].

[6] L3 collaboration, M. Acciarri et al., *Study of Z boson pair production in e^+e^- collisions at LEP at $\sqrt{s} = 189$ GeV*, *Phys. Lett.* **B 465** (1999) 363 [`hep-ex/9909043`] [INSPIRE].

[7] OPAL collaboration, G. Abbiendi et al., *Study of Z pair production and anomalous couplings in e^+e^- collisions at $\sqrt{s}$ between* 190 GeV *and* 209 GeV, *Eur. Phys. J.* **C 32** (2003) 303 [`hep-ex/0310013`] [INSPIRE].

[8] ALEPH, DELPHI, L3, OPAL, LEP ELECTROWEAK WORKING GROUP collaboration, J. Alcaraz et al., *A combination of preliminary electroweak measurements and constraints on the standard model*, `hep-ex/0612034` [INSPIRE].

[9] D0 collaboration, V. Abazov et al., *Search for ZZ and $Z\gamma^*$ production in $p\bar{p}$ collisions at $\sqrt{s} = 1.96$ TeV and limits on anomalous ZZZ and $ZZ\gamma^*$ couplings*, *Phys. Rev. Lett.* **100** (2008) 131801 [`arXiv:0712.0599`] [INSPIRE].

[10] CDF collaboration, T. Aaltonen et al., *First measurement of ZZ production in $p\bar{p}$ collisions at $\sqrt{s} = 1.96\,TeV$*, *Phys. Rev. Lett.* **100** (2008) 201801 [arXiv:0801.4806] [INSPIRE].

[11] D0 collaboration, V. Abazov et al., *Observation of ZZ production in $p\bar{p}$ collisions at $\sqrt{s} = 1.96\,TeV$*, *Phys. Rev. Lett.* **101** (2008) 171803 [arXiv:0808.0703] [INSPIRE].

[12] D0 collaboration, V.M. Abazov et al., *Measurement of the ZZ production cross section in $p\bar{p}$ collisions at $\sqrt{s} = 1.96\,TeV$*, *Phys. Rev.* **D 84** (2011) 011103 [arXiv:1104.3078] [INSPIRE].

[13] ATLAS collaboration, *Measurement of the ZZ production cross section and limits on anomalous neutral triple gauge couplings in proton-proton collisions at $\sqrt{s} = 7\,TeV$ with the ATLAS detector*, *Phys. Rev. Lett.* **108** (2012) 041804 [arXiv:1110.5016] [INSPIRE].

[14] CMS collaboration, *Measurement of the ZZ production cross section and search for anomalous couplings in $2l2l'$ final states in pp collisions at $\sqrt{s} = 7\,TeV$*, *JHEP* **01** (2013) 063 [arXiv:1211.4890] [INSPIRE].

[15] ATLAS collaboration, *Observation of a new particle in the search for the standard model Higgs boson with the ATLAS detector at the LHC*, *Phys. Lett.* **B 716** (2012) 1 [arXiv:1207.7214] [INSPIRE].

[16] CMS collaboration, *Observation of a new boson at a mass of $125\,GeV$ with the CMS experiment at the LHC*, *Phys. Lett.* **B 716** (2012) 30 [arXiv:1207.7235] [INSPIRE].

[17] ATLAS collaboration, *Search for the Standard Model Higgs boson in the decay channel $H \to ZZ^{(*)} \to 4\ell$ with $4.8\,fb^{-1}$ of pp collision data at $\sqrt{s} = 7\,TeV$ with ATLAS*, *Phys. Lett.* **B 710** (2012) 383 [arXiv:1202.1415] [INSPIRE].

[18] ATLAS collaboration, *Search for new particles decaying to ZZ using final states with leptons and jets with the ATLAS detector in $\sqrt{s} = 7\,TeV$ proton-proton collisions*, *Phys. Lett.* **B 712** (2012) 331 [arXiv:1203.0718] [INSPIRE].

[19] H.-L. Lai et al., *New parton distributions for collider physics*, *Phys. Rev.* **D 82** (2010) 074024 [arXiv:1007.2241] [INSPIRE].

[20] J.M. Campbell, R.K. Ellis and C. Williams, *Vector boson pair production at the LHC*, *JHEP* **07** (2011) 018 [arXiv:1105.0020] [INSPIRE].

[21] ATLAS collaboration, *The ATLAS experiment at the CERN Large Hadron Collider*, 2008 *JINST* **3** S08003 [INSPIRE].

[22] ATLAS collaboration, *Luminosity determination in pp collisions at $\sqrt{s} = 7\,TeV$ using the ATLAS detector at the LHC*, *Eur. Phys. J.* **C 71** (2011) 1630 [arXiv:1101.2185] [INSPIRE].

[23] S. Alioli, P. Nason, C. Oleari and E. Re, *A general framework for implementing NLO calculations in shower Monte Carlo programs: the POWHEG BOX*, *JHEP* **06** (2010) 043 [arXiv:1002.2581] [INSPIRE].

[24] T. Melia, P. Nason, R. Rontsch and G. Zanderighi, *W^+W^-, WZ and ZZ production in the POWHEG BOX*, *JHEP* **11** (2011) 078 [arXiv:1107.5051] [INSPIRE].

[25] T. Sjöstrand, S. Mrenna and P.Z. Skands, *PYTHIA 6.4 physics and manual*, *JHEP* **05** (2006) 026 [hep-ph/0603175] [INSPIRE].

[26] T. Gleisberg et al., *Event generation with SHERPA 1.1*, *JHEP* **02** (2009) 007 [arXiv:0811.4622] [INSPIRE].

[27] J. Pumplin et al., *New generation of parton distributions with uncertainties from global QCD analysis*, *JHEP* **07** (2002) 012 [hep-ph/0201195] [INSPIRE].

[28] T. Binoth, N. Kauer and P. Mertsch, *Gluon-induced QCD corrections to* $pp \to ZZ \to \ell^+\ell^-\ell'^+\ell'^-$, arXiv:0807.0024 [INSPIRE].

[29] G. Corcella et al., *HERWIG 6: an event generator for hadron emission reactions with interfering gluons (including supersymmetric processes)*, *JHEP* **01** (2001) 010 [hep-ph/0011363] [INSPIRE].

[30] J. Butterworth, J.R. Forshaw and M. Seymour, *Multiparton interactions in photoproduction at HERA*, *Z. Phys.* **C 72** (1996) 637 [hep-ph/9601371] [INSPIRE].

[31] M.L. Mangano, M. Moretti, F. Piccinini, R. Pittau and A.D. Polosa, *ALPGEN, a generator for hard multiparton processes in hadronic collisions*, *JHEP* **07** (2003) 001 [hep-ph/0206293] [INSPIRE].

[32] S. Frixione and B.R. Webber, *Matching NLO QCD computations and parton shower simulations*, *JHEP* **06** (2002) 029 [hep-ph/0204244] [INSPIRE].

[33] B.P. Kersevan and E. Richter-Was, *The Monte Carlo event generator AcerMC version 1.0 with interfaces to PYTHIA 6.2 and HERWIG 6.3*, *Comput. Phys. Commun.* **149** (2003) 142 [hep-ph/0201302] [INSPIRE].

[34] A. Martin, W. Stirling, R. Thorne and G. Watt, *Parton distributions for the LHC*, *Eur. Phys. J.* **C 63** (2009) 189 [arXiv:0901.0002] [INSPIRE].

[35] J. Alwall et al., *MadGraph/MadEvent v4: the new web generation*, *JHEP* **09** (2007) 028 [arXiv:0706.2334] [INSPIRE].

[36] ATLAS collaboration, *The ATLAS simulation infrastructure*, *Eur. Phys. J.* **C 70** (2010) 823 [arXiv:1005.4568] [INSPIRE].

[37] GEANT4 collaboration, S. Agostinelli et al., *GEANT4: a simulation toolkit*, *Nucl. Instrum. Meth.* **A 506** (2003) 250 [INSPIRE].

[38] ATLAS collaboration, *Measurement of the* $W \to \ell\nu$ *and* $Z/\gamma^* \to \ell\ell$ *production cross sections in proton-proton collisions at* $\sqrt{s} = 7$ *TeV with the ATLAS detector*, *JHEP* **12** (2010) 060 [arXiv:1010.2130] [INSPIRE].

[39] R. Fruhwirth, *Track fitting with non-gaussian noise*, *Comput. Phys. Commun.* **100** (1997) 1 [INSPIRE].

[40] ATLAS collaboration, *Electron performance measurements with the ATLAS detector using the* 2010 *LHC proton-proton collision data*, *Eur. Phys. J.* **C 72** (2012) 1909 [arXiv:1110.3174] [INSPIRE].

[41] ATLAS collaboration, *Calorimeter clustering algorithms: description and performance*, ATL-LARG-PUB-2008-002 (2008).

[42] M. Cacciari, G.P. Salam and G. Soyez, *The Anti-k(t) jet clustering algorithm*, *JHEP* **04** (2008) 063 [arXiv:0802.1189] [INSPIRE].

[43] ATLAS collaboration, *Probing the measurement of jet energies with the ATLAS detector using photon+jet events in proton-proton collisions at* $\sqrt{s} = 7$ *TeV*, ATLAS-CONF-2012-063 (2012).

[44] ATLAS collaboration, *Probing the measurement of jet energies with the ATLAS detector using Z+jet events from proton-proton collisions at* $\sqrt{s} = 7$ *TeV*, ATLAS-CONF-2012-053 (2012).

[45] ATLAS collaboration, *Performance of missing transverse momentum reconstruction in proton-proton collisions at 7 TeV with ATLAS*, *Eur. Phys. J.* **C 72** (2012) 1844 [arXiv:1108.5602] [inSPIRE].

[46] PARTICLE DATA GROUP collaboration, J. Beringer et al., *Review of particle physics*, *Phys. Rev.* **D 86** (2012) 010001 [inSPIRE].

[47] ATLAS collaboration, *Measurement of W^+W^- production in pp collisions at $\sqrt{s} = 7$ TeV with the ATLAS detector and limits on anomalous WWZ and $WW\gamma$ couplings*, arXiv:1210.2979 [inSPIRE].

[48] ATLAS collaboration, *Measurement of the top quark pair cross section with ATLAS in pp collisions at $\sqrt{s} = 7$ TeV using final states with an electron or a muon and a hadronically decaying τ lepton*, *Phys. Lett.* **B 717** (2012) 89 [arXiv:1205.2067] [inSPIRE].

[49] G. D'Agostini, *Improved iterative Bayesian unfolding*, arXiv:1010.0632.

[50] U. Baur, T. Han and J. Ohnemus, *WZ production at hadron colliders: effects of nonstandard WWZ couplings and QCD corrections*, *Phys. Rev.* **D 51** (1995) 3381 [hep-ph/9410266] [inSPIRE].

[51] U. Baur, T. Han and J. Ohnemus, *QCD corrections and anomalous couplings in $Z\gamma$ production at hadron colliders*, *Phys. Rev.* **D 57** (1998) 2823 [hep-ph/9710416] [inSPIRE].

[52] G. Bella, *Weighting di-boson Monte Carlo events in hadron colliders*, arXiv:0803.3307 [inSPIRE].

The ATLAS collaboration

G. Aad[48], T. Abajyan[21], B. Abbott[111], J. Abdallah[12], S. Abdel Khalek[115], A.A. Abdelalim[49],
O. Abdinov[11], R. Aben[105], B. Abi[112], M. Abolins[88], O.S. AbouZeid[158], H. Abramowicz[153],
H. Abreu[136], B.S. Acharya[164a,164b,a], L. Adamczyk[38], D.L. Adams[25], T.N. Addy[56],
J. Adelman[176], S. Adomeit[98], P. Adragna[75], T. Adye[129], S. Aefsky[23], J.A. Aguilar-Saavedra[124b,b],
M. Agustoni[17], M. Aharrouche[81], S.P. Ahlen[22], F. Ahles[48], A. Ahmad[148], M. Ahsan[41],
G. Aielli[133a,133b], T.P.A. Åkesson[79], G. Akimoto[155], A.V. Akimov[94], M.S. Alam[2], M.A. Alam[76],
J. Albert[169], S. Albrand[55], M. Aleksa[30], I.N. Aleksandrov[64], F. Alessandria[89a], C. Alexa[26a],
G. Alexander[153], G. Alexandre[49], T. Alexopoulos[10], M. Alhroob[164a,164c], M. Aliev[16],
G. Alimonti[89a], J. Alison[120], B.M.M. Allbrooke[18], P.P. Allport[73], S.E. Allwood-Spiers[53],
J. Almond[82], A. Aloisio[102a,102b], R. Alon[172], A. Alonso[79], F. Alonso[70], A. Altheimer[35],
B. Alvarez Gonzalez[88], M.G. Alviggi[102a,102b], K. Amako[65], C. Amelung[23], V.V. Ammosov[128,*],
S.P. Amor Dos Santos[124a], A. Amorim[124a,c], N. Amram[153], C. Anastopoulos[30], L.S. Ancu[17],
N. Andari[115], T. Andeen[35], C.F. Anders[58b], G. Anders[58a], K.J. Anderson[31], A. Andreazza[89a,89b],
V. Andrei[58a], M-L. Andrieux[55], X.S. Anduaga[70], S. Angelidakis[9], P. Anger[44], A. Angerami[35],
F. Anghinolfi[30], A. Anisenkov[107], N. Anjos[124a], A. Annovi[47], A. Antonaki[9], M. Antonelli[47],
A. Antonov[96], J. Antos[144b], F. Anulli[132a], M. Aoki[101], S. Aoun[83], L. Aperio Bella[5], R. Apolle[118,d],
G. Arabidze[88], I. Aracena[143], Y. Arai[65], A.T.H. Arce[45], S. Arfaoui[148], J-F. Arguin[93],
S. Argyropoulos[42], E. Arik[19a,*], M. Arik[19a], A.J. Armbruster[87], O. Arnaez[81], V. Arnal[80],
A. Artamonov[95], G. Artoni[132a,132b], D. Arutinov[21], S. Asai[155], S. Ask[28], B. Åsman[146a,146b],
L. Asquith[6], K. Assamagan[25,e], A. Astbury[169], M. Atkinson[165], B. Aubert[5], E. Auge[115],
K. Augsten[126], M. Aurousseau[145a], G. Avolio[30], D. Axen[168], G. Azuelos[93,f], Y. Azuma[155],
M.A. Baak[30], G. Baccaglioni[89a], C. Bacci[134a,134b], A.M. Bach[15], H. Bachacou[136], K. Bachas[154],
M. Backes[49], M. Backhaus[21], J. Backus Mayes[143], E. Badescu[26a], P. Bagnaia[132a,132b],
S. Bahinipati[3], Y. Bai[33a], D.C. Bailey[158], T. Bain[35], J.T. Baines[129], O.K. Baker[176], M.D. Baker[25],
S. Baker[77], P. Balek[127], E. Banas[39], P. Banerjee[93], Sw. Banerjee[173], D. Banfi[30], A. Bangert[150],
V. Bansal[169], H.S. Bansil[18], L. Barak[172], S.P. Baranov[94], A. Barbaro Galtieri[15], T. Barber[48],
E.L. Barberio[86], D. Barberis[50a,50b], M. Barbero[21], D.Y. Bardin[64], T. Barillari[99], M. Barisonzi[175],
T. Barklow[143], N. Barlow[28], B.M. Barnett[129], R.M. Barnett[15], A. Baroncelli[134a], G. Barone[49],
A.J. Barr[118], F. Barreiro[80], J. Barreiro Guimarães da Costa[57], R. Bartoldus[143], A.E. Barton[71],
V. Bartsch[149], A. Basye[165], R.L. Bates[53], L. Batkova[144a], J.R. Batley[28], A. Battaglia[17],
M. Battistin[30], F. Bauer[136], H.S. Bawa[143,g], S. Beale[98], T. Beau[78], P.H. Beauchemin[161],
R. Beccherle[50a], P. Bechtle[21], H.P. Beck[17], K. Becker[175], S. Becker[98], M. Beckingham[138],
K.H. Becks[175], A.J. Beddall[19c], A. Beddall[19c], S. Bedikian[176], V.A. Bednyakov[64], C.P. Bee[83],
L.J. Beemster[105], M. Begel[25], S. Behar Harpaz[152], P.K. Behera[62], M. Beimforde[99],
C. Belanger-Champagne[85], P.J. Bell[49], W.H. Bell[49], G. Bella[153], L. Bellagamba[20a], M. Bellomo[30],
A. Belloni[57], O. Beloborodova[107,h], K. Belotskiy[96], O. Beltramello[30], O. Benary[153],
D. Benchekroun[135a], K. Bendtz[146a,146b], N. Benekos[165], Y. Benhammou[153], E. Benhar Noccioli[49],
J.A. Benitez Garcia[159b], D.P. Benjamin[45], M. Benoit[115], J.R. Bensinger[23], K. Benslama[130],
S. Bentvelsen[105], D. Berge[30], E. Bergeaas Kuutmann[42], N. Berger[5], F. Berghaus[169],
E. Berglund[105], J. Beringer[15], P. Bernat[77], R. Bernhard[48], C. Bernius[25], T. Berry[76], C. Bertella[83],
A. Bertin[20a,20b], F. Bertolucci[122a,122b], M.I. Besana[89a,89b], G.J. Besjes[104], N. Besson[136],
S. Bethke[99], W. Bhimji[46], R.M. Bianchi[30], L. Bianchini[23], M. Bianco[72a,72b], O. Biebel[98],
S.P. Bieniek[77], K. Bierwagen[54], J. Biesiada[15], M. Biglietti[134a], H. Bilokon[47], M. Bindi[20a,20b],
S. Binet[115], A. Bingul[19c], C. Bini[132a,132b], C. Biscarat[178], B. Bittner[99], C.W. Black[150],
K.M. Black[22], R.E. Blair[6], J.-B. Blanchard[136], G. Blanchot[30], T. Blazek[144a], I. Bloch[42],
C. Blocker[23], J. Blocki[39], A. Blondel[49], W. Blum[81], U. Blumenschein[54], G.J. Bobbink[105],
V.S. Bobrovnikov[107], S.S. Bocchetta[79], A. Bocci[45], C.R. Boddy[118], M. Boehler[48], J. Boek[175],
T.T. Boek[175], N. Boelaert[36], J.A. Bogaerts[30], A. Bogdanchikov[107], A. Bogouch[90,*], C. Bohm[146a],
J. Bohm[125], V. Boisvert[76], T. Bold[38], V. Boldea[26a], N.M. Bolnet[136], M. Bomben[78], M. Bona[75],
M. Boonekamp[136], S. Bordoni[78], C. Borer[17], A. Borisov[128], G. Borissov[71], I. Borjanovic[13a],
M. Borri[82], S. Borroni[87], J. Bortfeldt[98], V. Bortolotto[134a,134b], K. Bos[105], D. Boscherini[20a],

M. Bosman[12], H. Boterenbrood[105], J. Bouchami[93], J. Boudreau[123], E.V. Bouhova-Thacker[71],
D. Boumediene[34], C. Bourdarios[115], N. Bousson[83], A. Boveia[31], J. Boyd[30], I.R. Boyko[64],
I. Bozovic-Jelisavcic[13b], J. Bracinik[18], P. Branchini[134a], A. Brandt[8], G. Brandt[118], O. Brandt[54],
U. Bratzler[156], B. Brau[84], J.E. Brau[114], H.M. Braun[175,*], S.F. Brazzale[164a,164c], B. Brelier[158],
J. Bremer[30], K. Brendlinger[120], R. Brenner[166], S. Bressler[172], D. Britton[53], F.M. Brochu[28],
I. Brock[21], R. Brock[88], F. Broggi[89a], C. Bromberg[88], J. Bronner[99], G. Brooijmans[35], T. Brooks[76],
W.K. Brooks[32b], G. Brown[82], P.A. Bruckman de Renstrom[39], D. Bruncko[144b], R. Bruneliere[48],
S. Brunet[60], A. Bruni[20a], G. Bruni[20a], M. Bruschi[20a], L. Bryngemark[79], T. Buanes[14], Q. Buat[55],
F. Bucci[49], J. Buchanan[118], P. Buchholz[141], R.M. Buckingham[118], A.G. Buckley[46], S.I. Buda[26a],
I.A. Budagov[64], B. Budick[108], V. Büscher[81], L. Bugge[117], O. Bulekov[96], A.C. Bundock[73],
M. Bunse[43], T. Buran[117], H. Burckhart[30], S. Burdin[73], T. Burgess[14], S. Burke[129], E. Busato[34],
P. Bussey[53], C.P. Buszello[166], B. Butler[143], J.M. Butler[22], C.M. Buttar[53], J.M. Butterworth[77],
W. Buttinger[28], M. Byszewski[30], S. Cabrera Urbán[167], D. Caforio[20a,20b], O. Cakir[4a],
P. Calafiura[15], G. Calderini[78], P. Calfayan[98], R. Calkins[106], L.P. Caloba[24a], R. Caloi[132a,132b],
D. Calvet[34], S. Calvet[34], R. Camacho Toro[34], P. Camarri[133a,133b], D. Cameron[117],
L.M. Caminada[15], R. Caminal Armadans[12], S. Campana[30], M. Campanelli[77], V. Canale[102a,102b],
F. Canelli[31], A. Canepa[159a], J. Cantero[80], R. Cantrill[76], L. Capasso[102a,102b],
M.D.M. Capeans Garrido[30], I. Caprini[26a], M. Caprini[26a], D. Capriotti[99], M. Capua[37a,37b],
R. Caputo[81], R. Cardarelli[133a], T. Carli[30], G. Carlino[102a], L. Carminati[89a,89b], B. Caron[85],
S. Caron[104], E. Carquin[32b], G.D. Carrillo-Montoya[145b], A.A. Carter[75], J.R. Carter[28],
J. Carvalho[124a,i], D. Casadei[108], M.P. Casado[12], M. Cascella[122a,122b], C. Caso[50a,50b,*],
A.M. Castaneda Hernandez[173,j], E. Castaneda-Miranda[173], V. Castillo Gimenez[167],
N.F. Castro[124a], G. Cataldi[72a], P. Catastini[57], A. Catinaccio[30], J.R. Catmore[30], A. Cattai[30],
G. Cattani[133a,133b], S. Caughron[88], V. Cavaliere[165], P. Cavalleri[78], D. Cavalli[89a],
M. Cavalli-Sforza[12], V. Cavasinni[122a,122b], F. Ceradini[134a,134b], A.S. Cerqueira[24b], A. Cerri[15],
L. Cerrito[75], F. Cerutti[15], S.A. Cetin[19b], A. Chafaq[135a], D. Chakraborty[106], I. Chalupkova[127],
K. Chan[3], P. Chang[165], B. Chapleau[85], J.D. Chapman[28], J.W. Chapman[87], D.G. Charlton[18],
V. Chavda[82], C.A. Chavez Barajas[30], S. Cheatham[85], S. Chekanov[6], S.V. Chekulaev[159a],
G.A. Chelkov[64], M.A. Chelstowska[104], C. Chen[63], H. Chen[25], S. Chen[33c], X. Chen[173], Y. Chen[35],
Y. Cheng[31], A. Cheplakov[64], R. Cherkaoui El Moursli[135e], V. Chernyatin[25], E. Cheu[7],
S.L. Cheung[158], L. Chevalier[136], G. Chiefari[102a,102b], L. Chikovani[51a,*], J.T. Childers[30],
A. Chilingarov[71], G. Chiodini[72a], A.S. Chisholm[18], R.T. Chislett[77], A. Chitan[26a],
M.V. Chizhov[64], G. Choudalakis[31], S. Chouridou[137], I.A. Christidi[77], A. Christov[48],
D. Chromek-Burckhart[30], M.L. Chu[151], J. Chudoba[125], G. Ciapetti[132a,132b], A.K. Ciftci[4a],
R. Ciftci[4a], D. Cinca[34], V. Cindro[74], A. Ciocio[15], M. Cirilli[87], P. Cirkovic[13b], Z.H. Citron[172],
M. Citterio[89a], M. Ciubancan[26a], A. Clark[49], P.J. Clark[46], R.N. Clarke[15], W. Cleland[123],
J.C. Clemens[83], B. Clement[55], C. Clement[146a,146b], Y. Coadou[83], M. Cobal[164a,164c],
A. Coccaro[138], J. Cochran[63], L. Coffey[23], J.G. Cogan[143], J. Coggeshall[165], J. Colas[5], S. Cole[106],
A.P. Colijn[105], N.J. Collins[18], C. Collins-Tooth[53], J. Collot[55], T. Colombo[119a,119b], G. Colon[84],
G. Compostella[99], P. Conde Muiño[124a], E. Coniavitis[166], M.C. Conidi[12], S.M. Consonni[89a,89b],
V. Consorti[48], S. Constantinescu[26a], C. Conta[119a,119b], G. Conti[57], F. Conventi[102a,k], M. Cooke[15],
B.D. Cooper[77], A.M. Cooper-Sarkar[118], K. Copic[15], T. Cornelissen[175], M. Corradi[20a],
F. Corriveau[85,l], A. Cortes-Gonzalez[165], G. Cortiana[99], G. Costa[89a], M.J. Costa[167],
D. Costanzo[139], D. Côté[30], L. Courneyea[169], G. Cowan[76], B.E. Cox[82], K. Cranmer[108],
F. Crescioli[78], M. Cristinziani[21], G. Crosetti[37a,37b], S. Crépé-Renaudin[55], C.-M. Cuciuc[26a],
C. Cuenca Almenar[176], T. Cuhadar Donszelmann[139], J. Cummings[176], M. Curatolo[47],
C.J. Curtis[18], C. Cuthbert[150], P. Cwetanski[60], H. Czirr[141], P. Czodrowski[44], Z. Czyczula[176],
S. D'Auria[53], M. D'Onofrio[73], A. D'Orazio[132a,132b], M.J. Da Cunha Sargedas De Sousa[124a],
C. Da Via[82], W. Dabrowski[38], A. Dafinca[118], T. Dai[87], F. Dallaire[93], C. Dallapiccola[84],
M. Dam[36], M. Dameri[50a,50b], D.S. Damiani[137], H.O. Danielsson[30], V. Dao[49], G. Darbo[50a],
G.L. Darlea[26b], J.A. Dassoulas[42], W. Davey[21], T. Davidek[127], N. Davidson[86], R. Davidson[71],
E. Davies[118,d], M. Davies[93], O. Davignon[78], A.R. Davison[77], Y. Davygora[58a], E. Dawe[142],

I. Dawson[139], R.K. Daya-Ishmukhametova[23], K. De[8], R. de Asmundis[102a], S. De Castro[20a,20b],
S. De Cecco[78], J. de Graat[98], N. De Groot[104], P. de Jong[105], C. De La Taille[115], H. De la Torre[80],
F. De Lorenzi[63], L. de Mora[71], L. De Nooij[105], D. De Pedis[132a], A. De Salvo[132a],
U. De Sanctis[164a,164c], A. De Santo[149], J.B. De Vivie De Regie[115], G. De Zorzi[132a,132b],
W.J. Dearnaley[71], R. Debbe[25], C. Debenedetti[46], B. Dechenaux[55], D.V. Dedovich[64],
J. Degenhardt[120], J. Del Peso[80], T. Del Prete[122a,122b], T. Delemontex[55], M. Deliyergiyev[74],
A. Dell'Acqua[30], L. Dell'Asta[22], M. Della Pietra[102a,k], D. della Volpe[102a,102b], M. Delmastro[5],
P.A. Delsart[55], C. Deluca[105], S. Demers[176], M. Demichev[64], B. Demirkoz[12,m], S.P. Denisov[128],
D. Derendarz[39], J.E. Derkaoui[135d], F. Derue[78], P. Dervan[73], K. Desch[21], E. Devetak[148],
P.O. Deviveiros[105], A. Dewhurst[129], B. DeWilde[148], S. Dhaliwal[158], R. Dhullipudi[25,n],
A. Di Ciaccio[133a,133b], L. Di Ciaccio[5], C. Di Donato[102a,102b], A. Di Girolamo[30], B. Di Girolamo[30],
S. Di Luise[134a,134b], A. Di Mattia[152], B. Di Micco[30], R. Di Nardo[47], A. Di Simone[133a,133b],
R. Di Sipio[20a,20b], M.A. Diaz[32a], E.B. Diehl[87], J. Dietrich[42], T.A. Dietzsch[58a], S. Diglio[86],
K. Dindar Yagci[40], J. Dingfelder[21], F. Dinut[26a], C. Dionisi[132a,132b], P. Dita[26a], S. Dita[26a],
F. Dittus[30], F. Djama[83], T. Djobava[51b], M.A.B. do Vale[24c], A. Do Valle Wemans[124a,o],
T.K.O. Doan[5], M. Dobbs[85], D. Dobos[30], E. Dobson[30,p], J. Dodd[35], C. Doglioni[49], T. Doherty[53],
Y. Doi[65,*], J. Dolejsi[127], Z. Dolezal[127], B.A. Dolgoshein[96,*], T. Dohmae[155], M. Donadelli[24d],
J. Donini[34], J. Dopke[30], A. Doria[102a], A. Dos Anjos[173], A. Dotti[122a,122b], M.T. Dova[70],
A.D. Doxiadis[105], A.T. Doyle[53], N. Dressnandt[120], M. Dris[10], J. Dubbert[99], S. Dube[15],
E. Duchovni[172], G. Duckeck[98], D. Duda[175], A. Dudarev[30], F. Dudziak[63], M. Dührssen[30],
I.P. Duerdoth[82], L. Duflot[115], M-A. Dufour[85], L. Duguid[76], M. Dunford[58a], H. Duran Yildiz[4a],
R. Duxfield[139], M. Dwuznik[38], M. Düren[52], W.L. Ebenstein[45], J. Ebke[98], S. Eckweiler[81],
K. Edmonds[81], W. Edson[2], C.A. Edwards[76], N.C. Edwards[53], W. Ehrenfeld[42], T. Eifert[143],
G. Eigen[14], K. Einsweiler[15], E. Eisenhandler[75], T. Ekelof[166], M. El Kacimi[135c], M. Ellert[166],
S. Elles[5], F. Ellinghaus[81], K. Ellis[75], N. Ellis[30], J. Elmsheuser[98], M. Elsing[30], D. Emeliyanov[129],
R. Engelmann[148], A. Engl[98], B. Epp[61], J. Erdmann[176], A. Ereditato[17], D. Eriksson[146a], J. Ernst[2],
M. Ernst[25], J. Ernwein[136], D. Errede[165], S. Errede[165], E. Ertel[81], M. Escalier[115], H. Esch[43],
C. Escobar[123], X. Espinal Curull[12], B. Esposito[47], F. Etienne[83], A.I. Etienvre[136], E. Etzion[153],
D. Evangelakou[54], H. Evans[60], L. Fabbri[20a,20b], C. Fabre[30], R.M. Fakhrutdinov[128],
S. Falciano[132a], Y. Fang[33a], M. Fanti[89a,89b], A. Farbin[8], A. Farilla[134a], J. Farley[148],
T. Farooque[158], S. Farrell[163], S.M. Farrington[170], P. Farthouat[30], F. Fassi[167], P. Fassnacht[30],
D. Fassouliotis[9], B. Fatholahzadeh[158], A. Favareto[89a,89b], L. Fayard[115], S. Fazio[37a,37b],
P. Federic[144a], O.L. Fedin[121], W. Fedorko[88], M. Fehling-Kaschek[48], L. Feligioni[83], C. Feng[33d],
E.J. Feng[6], A.B. Fenyuk[128], J. Ferencei[144b], W. Fernando[6], S. Ferrag[53], J. Ferrando[53],
V. Ferrara[42], A. Ferrari[166], P. Ferrari[105], R. Ferrari[119a], D.E. Ferreira de Lima[53], A. Ferrer[167],
D. Ferrere[49], C. Ferretti[87], A. Ferretto Parodi[50a,50b], M. Fiascaris[31], F. Fiedler[81], A. Filipčič[74],
F. Filthaut[104], M. Fincke-Keeler[169], M.C.N. Fiolhais[124a,i], L. Fiorini[167], A. Firan[40], G. Fischer[42],
M.J. Fisher[109], M. Flechl[48], I. Fleck[141], J. Fleckner[81], P. Fleischmann[174], S. Fleischmann[175],
T. Flick[175], A. Floderus[79], L.R. Flores Castillo[173], A.C. Florez Bustos[159b], M.J. Flowerdew[99],
T. Fonseca Martin[17], A. Formica[136], A. Forti[82], D. Fortin[159a], D. Fournier[115], A.J. Fowler[45],
H. Fox[71], P. Francavilla[12], M. Franchini[20a,20b], S. Franchino[119a,119b], D. Francis[30], T. Frank[172],
M. Franklin[57], S. Franz[30], M. Fraternali[119a,119b], S. Fratina[120], S.T. French[28], C. Friedrich[42],
F. Friedrich[44], D. Froidevaux[30], J.A. Frost[28], C. Fukunaga[156], E. Fullana Torregrosa[127],
B.G. Fulsom[143], J. Fuster[167], C. Gabaldon[30], O. Gabizon[172], T. Gadfort[25], S. Gadomski[49],
G. Gagliardi[50a,50b], P. Gagnon[60], C. Galea[98], B. Galhardo[124a], E.J. Gallas[118], V. Gallo[17],
B.J. Gallop[129], P. Gallus[125], K.K. Gan[109], Y.S. Gao[143,g], A. Gaponenko[15], F. Garberson[176],
M. Garcia-Sciveres[15], C. García[167], J.E. García Navarro[167], R.W. Gardner[31], N. Garelli[30],
V. Garonne[30], C. Gatti[47], G. Gaudio[119a], B. Gaur[141], L. Gauthier[136], P. Gauzzi[132a,132b],
I.L. Gavrilenko[94], C. Gay[168], G. Gaycken[21], E.N. Gazis[10], P. Ge[33d], Z. Gecse[168], C.N.P. Gee[129],
D.A.A. Geerts[105], Ch. Geich-Gimbel[21], K. Gellerstedt[146a,146b], C. Gemme[50a], A. Gemmell[53],
M.H. Genest[55], S. Gentile[132a,132b], M. George[54], S. George[76], D. Gerbaudo[12], P. Gerlach[175],
A. Gershon[153], C. Geweniger[58a], H. Ghazlane[135b], N. Ghodbane[34], B. Giacobbe[20a],

S. Giagu[132a,132b], V. Giangiobbe[12], F. Gianotti[30], B. Gibbard[25], A. Gibson[158], S.M. Gibson[30], M. Gilchriese[15], D. Gillberg[29], A.R. Gillman[129], D.M. Gingrich[3,f], J. Ginzburg[153], N. Giokaris[9], M.P. Giordani[164c], R. Giordano[102a,102b], F.M. Giorgi[16], P. Giovannini[99], P.F. Giraud[136], D. Giugni[89a], M. Giunta[93], B.K. Gjelsten[117], L.K. Gladilin[97], C. Glasman[80], J. Glatzer[21], A. Glazov[42], K.W. Glitza[175], G.L. Glonti[64], J.R. Goddard[75], J. Godfrey[142], J. Godlewski[30], M. Goebel[42], T. Göpfert[44], C. Goeringer[81], C. Gössling[43], S. Goldfarb[87], T. Golling[176], D. Golubkov[128], A. Gomes[124a,c], L.S. Gomez Fajardo[42], R. Gonçalo[76], J. Goncalves Pinto Firmino Da Costa[42], L. Gonella[21], S. González de la Hoz[167], G. Gonzalez Parra[12], M.L. Gonzalez Silva[27], S. Gonzalez-Sevilla[49], J.J. Goodson[148], L. Goossens[30], P.A. Gorbounov[95], H.A. Gordon[25], I. Gorelov[103], G. Gorfine[175], B. Gorini[30], E. Gorini[72a,72b], A. Gorišek[74], E. Gornicki[39], A.T. Goshaw[6], M. Gosselink[105], M.I. Gostkin[64], I. Gough Eschrich[163], M. Gouighri[135a], D. Goujdami[135c], M.P. Goulette[49], A.G. Goussiou[138], C. Goy[5], S. Gozpinar[23], I. Grabowska-Bold[38], P. Grafström[20a,20b], K-J. Grahn[42], E. Gramstad[117], F. Grancagnolo[72a], S. Grancagnolo[16], V. Grassi[148], V. Gratchev[121], N. Grau[35], H.M. Gray[30], J.A. Gray[148], E. Graziani[134a], O.G. Grebenyuk[121], T. Greenshaw[73], Z.D. Greenwood[25,n], K. Gregersen[36], I.M. Gregor[42], P. Grenier[143], J. Griffiths[8], N. Grigalashvili[64], A.A. Grillo[137], S. Grinstein[12], Ph. Gris[34], Y.V. Grishkevich[97], J.-F. Grivaz[115], E. Gross[172], J. Grosse-Knetter[54], J. Groth-Jensen[172], K. Grybel[141], D. Guest[176], C. Guicheney[34], E. Guido[50a,50b], S. Guindon[54], U. Gul[53], J. Gunther[125], B. Guo[158], J. Guo[35], P. Gutierrez[111], N. Guttman[153], O. Gutzwiller[173], C. Guyot[136], C. Gwenlan[118], C.B. Gwilliam[73], A. Haas[108], S. Haas[30], C. Haber[15], H.K. Hadavand[8], D.R. Hadley[18], P. Haefner[21], F. Hahn[30], Z. Hajduk[39], H. Hakobyan[177], D. Hall[118], K. Hamacher[175], P. Hamal[113], K. Hamano[86], M. Hamer[54], A. Hamilton[145b,q], S. Hamilton[161], L. Han[33b], K. Hanagaki[116], K. Hanawa[160], M. Hance[15], C. Handel[81], P. Hanke[58a], J.R. Hansen[36], J.B. Hansen[36], J.D. Hansen[36], P.H. Hansen[36], P. Hansson[143], K. Hara[160], T. Harenberg[175], S. Harkusha[90], D. Harper[87], R.D. Harrington[46], O.M. Harris[138], J. Hartert[48], F. Hartjes[105], T. Haruyama[65], A. Harvey[56], S. Hasegawa[101], Y. Hasegawa[140], S. Hassani[136], S. Haug[17], M. Hauschild[30], R. Hauser[88], M. Havranek[21], C.M. Hawkes[18], R.J. Hawkings[30], A.D. Hawkins[79], T. Hayakawa[66], T. Hayashi[160], D. Hayden[76], C.P. Hays[118], H.S. Hayward[73], S.J. Haywood[129], S.J. Head[18], V. Hedberg[79], L. Heelan[8], S. Heim[120], B. Heinemann[15], S. Heisterkamp[36], L. Helary[22], C. Heller[98], M. Heller[30], S. Hellman[146a,146b], D. Hellmich[21], C. Helsens[12], R.C.W. Henderson[71], M. Henke[58a], A. Henrichs[176], A.M. Henriques Correia[30], S. Henrot-Versille[115], C. Hensel[54], C.M. Hernandez[8], Y. Hernández Jiménez[167], R. Herrberg[16], G. Herten[48], R. Hertenberger[98], L. Hervas[30], G.G. Hesketh[77], N.P. Hessey[105], E. Higón-Rodriguez[167], J.C. Hill[28], K.H. Hiller[42], S. Hillert[21], S.J. Hillier[18], I. Hinchliffe[15], E. Hines[120], M. Hirose[116], F. Hirsch[43], D. Hirschbuehl[175], J. Hobbs[148], N. Hod[153], M.C. Hodgkinson[139], P. Hodgson[139], A. Hoecker[30], M.R. Hoeferkamp[103], J. Hoffman[40], D. Hoffmann[83], M. Hohlfeld[81], M. Holder[141], S.O. Holmgren[146a], T. Holy[126], J.L. Holzbauer[88], T.M. Hong[120], L. Hooft van Huysduynen[108], S. Horner[48], J-Y. Hostachy[55], S. Hou[151], A. Hoummada[135a], J. Howard[118], J. Howarth[82], I. Hristova[16], J. Hrivnac[115], T. Hryn'ova[5], P.J. Hsu[81], S.-C. Hsu[138], D. Hu[35], Z. Hubacek[30], F. Hubaut[83], F. Huegging[21], A. Huettmann[42], T.B. Huffman[118], E.W. Hughes[35], G. Hughes[71], M. Huhtinen[30], M. Hurwitz[15], N. Huseynov[64,r], J. Huston[88], J. Huth[57], G. Iacobucci[49], G. Iakovidis[10], M. Ibbotson[82], I. Ibragimov[141], L. Iconomidou-Fayard[115], J. Idarraga[115], P. Iengo[102a], O. Igonkina[105], Y. Ikegami[65], M. Ikeno[65], D. Iliadis[154], N. Ilic[158], T. Ince[99], P. Ioannou[9], M. Iodice[134a], K. Iordanidou[9], V. Ippolito[132a,132b], A. Irles Quiles[167], C. Isaksson[166], M. Ishino[67], M. Ishitsuka[157], R. Ishmukhametov[109], C. Issever[118], S. Istin[19a], A.V. Ivashin[128], W. Iwanski[39], H. Iwasaki[65], J.M. Izen[41], V. Izzo[102a], B. Jackson[120], J.N. Jackson[73], P. Jackson[1], M.R. Jaekel[30], V. Jain[2], K. Jakobs[48], S. Jakobsen[36], T. Jakoubek[125], J. Jakubek[126], D.O. Jamin[151], D.K. Jana[111], E. Jansen[77], H. Jansen[30], J. Janssen[21], A. Jantsch[99], M. Janus[48], R.C. Jared[173], G. Jarlskog[79], L. Jeanty[57], I. Jen-La Plante[31], G.-Y. Jeng[150], D. Jennens[86], P. Jenni[30], A.E. Loevschall-Jensen[36], P. Jež[36], S. Jézéquel[5], M.K. Jha[20a], H. Ji[173], W. Ji[81], J. Jia[148], Y. Jiang[33b], M. Jimenez Belenguer[42], S. Jin[33a], O. Jinnouchi[157], M.D. Joergensen[36], D. Joffe[40], M. Johansen[146a,146b],

K.E. Johansson[146a], P. Johansson[139], S. Johnert[42], K.A. Johns[7], K. Jon-And[146a,146b], G. Jones[170],
R.W.L. Jones[71], T.J. Jones[73], C. Joram[30], P.M. Jorge[124a], K.D. Joshi[82], J. Jovicevic[147],
T. Jovin[13b], X. Ju[173], C.A. Jung[43], R.M. Jungst[30], V. Juranek[125], P. Jussel[61], A. Juste Rozas[12],
S. Kabana[17], M. Kaci[167], A. Kaczmarska[39], P. Kadlecik[36], M. Kado[115], H. Kagan[109], M. Kagan[57],
E. Kajomovitz[152], S. Kalinin[175], L.V. Kalinovskaya[64], S. Kama[40], N. Kanaya[155], M. Kaneda[30],
S. Kaneti[28], T. Kanno[157], V.A. Kantserov[96], J. Kanzaki[65], B. Kaplan[108], A. Kapliy[31],
J. Kaplon[30], D. Kar[53], M. Karagounis[21], K. Karakostas[10], M. Karnevskiy[58b], V. Kartvelishvili[71],
A.N. Karyukhin[128], L. Kashif[173], G. Kasieczka[58b], R.D. Kass[109], A. Kastanas[14], M. Kataoka[5],
Y. Kataoka[155], J. Katzy[42], V. Kaushik[7], K. Kawagoe[69], T. Kawamoto[155], G. Kawamura[81],
M.S. Kayl[105], S. Kazama[155], V.F. Kazanin[107], M.Y. Kazarinov[64], R. Keeler[169], P.T. Keener[120],
R. Kehoe[40], M. Keil[54], G.D. Kekelidze[64], J.S. Keller[138], M. Kenyon[53], O. Kepka[125],
N. Kerschen[30], B.P. Kerševan[74], S. Kersten[175], K. Kessoku[155], J. Keung[158], F. Khalil-zada[11],
H. Khandanyan[146a,146b], A. Khanov[112], D. Kharchenko[64], A. Khodinov[96], A. Khomich[58a],
T.J. Khoo[28], G. Khoriauli[21], A. Khoroshilov[175], V. Khovanskiy[95], E. Khramov[64], J. Khubua[51b],
H. Kim[146a,146b], S.H. Kim[160], N. Kimura[171], O. Kind[16], B.T. King[73], M. King[66], R.S.B. King[118],
J. Kirk[129], A.E. Kiryunin[99], T. Kishimoto[66], D. Kisielewska[38], T. Kitamura[66], T. Kittelmann[123],
K. Kiuchi[160], E. Kladiva[144b], M. Klein[73], U. Klein[73], K. Kleinknecht[81], M. Klemetti[85],
A. Klier[172], P. Klimek[146a,146b], A. Klimentov[25], R. Klingenberg[43], J.A. Klinger[82], E.B. Klinkby[36],
T. Klioutchnikova[30], P.F. Klok[104], S. Klous[105], E.-E. Kluge[58a], T. Kluge[73], P. Kluit[105],
S. Kluth[99], E. Kneringer[61], E.B.F.G. Knoops[83], A. Knue[54], B.R. Ko[45], T. Kobayashi[155],
M. Kobel[44], M. Kocian[143], P. Kodys[127], K. Köneke[30], A.C. König[104], S. Koenig[81], L. Köpke[81],
F. Koetsveld[104], P. Koevesarki[21], T. Koffas[29], E. Koffeman[105], L.A. Kogan[118], S. Kohlmann[175],
F. Kohn[54], Z. Kohout[126], T. Kohriki[65], T. Koi[143], G.M. Kolachev[107,*], H. Kolanoski[16],
V. Kolesnikov[64], I. Koletsou[89a], J. Koll[88], A.A. Komar[94], Y. Komori[155], T. Kondo[65], T. Kono[42,s],
A.I. Kononov[48], R. Konoplich[108,t], N. Konstantinidis[77], R. Kopeliansky[152], S. Koperny[38],
K. Korcyl[39], K. Kordas[154], A. Korn[118], A. Korol[107], I. Korolkov[12], E.V. Korolkova[139],
V.A. Korotkov[128], O. Kortner[99], S. Kortner[99], V.V. Kostyukhin[21], S. Kotov[99], V.M. Kotov[64],
A. Kotwal[45], C. Kourkoumelis[9], V. Kouskoura[154], A. Koutsman[159a], R. Kowalewski[169],
T.Z. Kowalski[38], W. Kozanecki[136], A.S. Kozhin[128], V. Kral[126], V.A. Kramarenko[97],
G. Kramberger[74], M.W. Krasny[78], A. Krasznahorkay[108], J.K. Kraus[21], A. Kravchenko[25],
S. Kreiss[108], F. Krejci[126], J. Kretzschmar[73], K. Kreutzfeldt[52], N. Krieger[54], P. Krieger[158],
K. Kroeninger[54], H. Kroha[99], J. Kroll[120], J. Kroseberg[21], J. Krstic[13a], U. Kruchonak[64],
H. Krüger[21], T. Kruker[17], N. Krumnack[63], Z.V. Krumshteyn[64], M.K. Kruse[45], T. Kubota[86],
S. Kuday[4a], S. Kuehn[48], A. Kugel[58c], T. Kuhl[42], D. Kuhn[61], V. Kukhtin[64], Y. Kulchitsky[90],
S. Kuleshov[32b], C. Kummer[98], M. Kuna[78], J. Kunkle[120], A. Kupco[125], H. Kurashige[66],
M. Kurata[160], Y.A. Kurochkin[90], V. Kus[125], E.S. Kuwertz[147], M. Kuze[157], J. Kvita[142],
R. Kwee[16], A. La Rosa[49], L. La Rotonda[37a,37b], L. Labarga[80], S. Lablak[135a], C. Lacasta[167],
F. Lacava[132a,132b], J. Lacey[29], H. Lacker[16], D. Lacour[78], V.R. Lacuesta[167], E. Ladygin[64],
R. Lafaye[5], B. Laforge[78], T. Lagouri[176], S. Lai[48], E. Laisne[55], L. Lambourne[77], C.L. Lampen[7],
W. Lampl[7], E. Lancon[136], U. Landgraf[48], M.P.J. Landon[75], V.S. Lang[58a], C. Lange[42],
A.J. Lankford[163], F. Lanni[25], K. Lantzsch[30], A. Lanza[119a], S. Laplace[78], C. Lapoire[21],
J.F. Laporte[136], T. Lari[89a], A. Larner[118], M. Lassnig[30], P. Laurelli[47], V. Lavorini[37a,37b],
W. Lavrijsen[15], P. Laycock[73], O. Le Dortz[78], E. Le Guirriec[83], E. Le Menedeu[12], T. LeCompte[6],
F. Ledroit-Guillon[55], H. Lee[105], J.S.H. Lee[116], S.C. Lee[151], L. Lee[176], M. Lefebvre[169],
M. Legendre[136], F. Legger[98], C. Leggett[15], M. Lehmacher[21], G. Lehmann Miotto[30],
A.G. Leister[176], M.A.L. Leite[24d], R. Leitner[127], D. Lellouch[172], B. Lemmer[54], V. Lendermann[58a],
K.J.C. Leney[145b], T. Lenz[105], G. Lenzen[175], B. Lenzi[30], K. Leonhardt[44], S. Leontsinis[10],
F. Lepold[58a], C. Leroy[93], J-R. Lessard[169], C.G. Lester[28], C.M. Lester[120], J. Levêque[5], D. Levin[87],
L.J. Levinson[172], A. Lewis[118], G.H. Lewis[108], A.M. Leyko[21], M. Leyton[16], B. Li[33b], B. Li[83],
H. Li[148], H.L. Li[31], S. Li[33b,u], X. Li[87], Z. Liang[118,v], H. Liao[34], B. Liberti[133a], P. Lichard[30],
M. Lichtnecker[98], K. Lie[165], W. Liebig[14], C. Limbach[21], A. Limosani[86], M. Limper[62],
S.C. Lin[151,w], F. Linde[105], J.T. Linnemann[88], E. Lipeles[120], A. Lipniacka[14], T.M. Liss[165],

D. Lissauer[25], A. Lister[49], A.M. Litke[137], C. Liu[29], D. Liu[151], J.B. Liu[87], L. Liu[87], M. Liu[33b],
Y. Liu[33b], M. Livan[119a,119b], S.S.A. Livermore[118], A. Lleres[55], J. Llorente Merino[80], S.L. Lloyd[75],
E. Lobodzinska[42], P. Loch[7], W.S. Lockman[137], T. Loddenkoetter[21], F.K. Loebinger[82],
A. Loginov[176], C.W. Loh[168], T. Lohse[16], K. Lohwasser[48], M. Lokajicek[125], V.P. Lombardo[5],
R.E. Long[71], L. Lopes[124a], D. Lopez Mateos[57], J. Lorenz[98], N. Lorenzo Martinez[115],
M. Losada[162], P. Loscutoff[15], F. Lo Sterzo[132a,132b], M.J. Losty[159a,*], X. Lou[41], A. Lounis[115],
K.F. Loureiro[162], J. Love[6], P.A. Love[71], A.J. Lowe[143,g], F. Lu[33a], H.J. Lubatti[138],
C. Luci[132a,132b], A. Lucotte[55], D. Ludwig[44], D. Ludwig[42], I. Ludwig[48], J. Ludwig[48],
F. Luehring[60], G. Luijckx[105], W. Lukas[61], L. Luminari[132a], E. Lund[117], B. Lund-Jensen[147],
B. Lundberg[79], J. Lundberg[146a,146b], O. Lundberg[146a,146b], J. Lundquist[36], M. Lungwitz[81],
D. Lynn[25], E. Lytken[79], H. Ma[25], L.L. Ma[173], G. Maccarrone[47], A. Macchiolo[99], B. Maček[74],
J. Machado Miguens[124a], D. Macina[30], R. Mackeprang[36], R.J. Madaras[15], H.J. Maddocks[71],
W.F. Mader[44], R. Maenner[58c], T. Maeno[25], P. Mättig[175], S. Mättig[42], L. Magnoni[163],
E. Magradze[54], K. Mahboubi[48], J. Mahlstedt[105], S. Mahmoud[73], G. Mahout[18], C. Maiani[136],
C. Maidantchik[24a], A. Maio[124a,c], S. Majewski[25], Y. Makida[65], N. Makovec[115], P. Mal[136],
B. Malaescu[30], Pa. Malecki[39], P. Malecki[39], V.P. Maleev[121], F. Malek[55], U. Mallik[62], D. Malon[6],
C. Malone[143], S. Maltezos[10], V. Malyshev[107], S. Malyukov[30], J. Mamuzic[13b], A. Manabe[65],
L. Mandelli[89a], I. Mandić[74], R. Mandrysch[62], J. Maneira[124a], A. Manfredini[99],
L. Manhaes de Andrade Filho[24b], J.A. Manjarres Ramos[136], A. Mann[98], P.M. Manning[137],
A. Manousakis-Katsikakis[9], B. Mansoulie[136], A. Mapelli[30], L. Mapelli[30], L. March[167],
J.F. Marchand[29], F. Marchese[133a,133b], G. Marchiori[78], M. Marcisovsky[125], C.P. Marino[169],
F. Marroquim[24a], Z. Marshall[30], L.F. Marti[17], S. Marti-Garcia[167], B. Martin[30], B. Martin[88],
J.P. Martin[93], T.A. Martin[18], V.J. Martin[46], B. Martin dit Latour[49], S. Martin-Haugh[149],
M. Martinez[12], V. Martinez Outschoorn[57], A.C. Martyniuk[169], M. Marx[82], F. Marzano[132a],
A. Marzin[111], L. Masetti[81], T. Mashimo[155], R. Mashinistov[94], J. Masik[82], A.L. Maslennikov[107],
I. Massa[20a,20b], G. Massaro[105], N. Massol[5], P. Mastrandrea[148], A. Mastroberardino[37a,37b],
T. Masubuchi[155], H. Matsunaga[155], T. Matsushita[66], C. Mattravers[118,d], J. Maurer[83],
S.J. Maxfield[73], D.A. Maximov[107,h], A. Mayne[139], R. Mazini[151], M. Mazur[21],
L. Mazzaferro[133a,133b], M. Mazzanti[89a], J. Mc Donald[85], S.P. Mc Kee[87], A. McCarn[165],
R.L. McCarthy[148], T.G. McCarthy[29], N.A. McCubbin[129], K.W. McFarlane[56,*], J.A. Mcfayden[139],
G. Mchedlidze[51b], T. Mclaughlan[18], S.J. McMahon[129], R.A. McPherson[169,l], A. Meade[84],
J. Mechnich[105], M. Mechtel[175], M. Medinnis[42], S. Meehan[31], R. Meera-Lebbai[111], T. Meguro[116],
S. Mehlhase[36], A. Mehta[73], K. Meier[58a], B. Meirose[79], C. Melachrinos[31], B.R. Mellado Garcia[173],
F. Meloni[89a,89b], L. Mendoza Navas[162], Z. Meng[151,x], A. Mengarelli[20a,20b], S. Menke[99],
E. Meoni[161], K.M. Mercurio[57], P. Mermod[49], L. Merola[102a,102b], C. Meroni[89a], F.S. Merritt[31],
H. Merritt[109], A. Messina[30,y], J. Metcalfe[25], A.S. Mete[163], C. Meyer[81], C. Meyer[31], J-P. Meyer[136],
J. Meyer[174], J. Meyer[54], S. Michal[30], L. Micu[26a], R.P. Middleton[129], S. Migas[73], L. Mijović[136],
G. Mikenberg[172], M. Mikestikova[125], M. Mikuž[74], D.W. Miller[31], R.J. Miller[88], W.J. Mills[168],
C. Mills[57], A. Milov[172], D.A. Milstead[146a,146b], D. Milstein[172], A.A. Minaenko[128],
M. Miñano Moya[167], I.A. Minashvili[64], A.I. Mincer[108], B. Mindur[38], M. Mineev[64], Y. Ming[173],
L.M. Mir[12], G. Mirabelli[132a], J. Mitrevski[137], V.A. Mitsou[167], S. Mitsui[65], P.S. Miyagawa[139],
J.U. Mjörnmark[79], T. Moa[146a,146b], V. Moeller[28], K. Mönig[42], N. Möser[21], S. Mohapatra[148],
W. Mohr[48], R. Moles-Valls[167], A. Molfetas[30], J. Monk[77], E. Monnier[83], J. Montejo Berlingen[12],
F. Monticelli[70], S. Monzani[20a,20b], R.W. Moore[3], G.F. Moorhead[86], C. Mora Herrera[49],
A. Moraes[53], N. Morange[136], J. Morel[54], G. Morello[37a,37b], D. Moreno[81], M. Moreno Llácer[167],
P. Morettini[50a], M. Morgenstern[44], M. Morii[57], A.K. Morley[30], G. Mornacchi[30], J.D. Morris[75],
L. Morvaj[101], H.G. Moser[99], M. Mosidze[51b], J. Moss[109], R. Mount[143], E. Mountricha[10,z],
S.V. Mouraviev[94,*], E.J.W. Moyse[84], F. Mueller[58a], J. Mueller[123], K. Mueller[21], T.A. Müller[98],
T. Mueller[81], D. Muenstermann[30], Y. Munwes[153], W.J. Murray[129], I. Mussche[105], E. Musto[152],
A.G. Myagkov[128], M. Myska[125], O. Nackenhorst[54], J. Nadal[12], K. Nagai[160], R. Nagai[157],
K. Nagano[65], A. Nagarkar[109], Y. Nagasaka[59], M. Nagel[99], A.M. Nairz[30], Y. Nakahama[30],
K. Nakamura[155], T. Nakamura[155], I. Nakano[110], G. Nanava[21], A. Napier[161], R. Narayan[58b],

M. Nash[77,d], T. Nattermann[21], T. Naumann[42], G. Navarro[162], H.A. Neal[87], P.Yu. Nechaeva[94],
T.J. Neep[82], A. Negri[119a,119b], G. Negri[30], M. Negrini[20a], S. Nektarijevic[49], A. Nelson[163],
T.K. Nelson[143], S. Nemecek[125], P. Nemethy[108], A.A. Nepomuceno[24a], M. Nessi[30,aa],
M.S. Neubauer[165], M. Neumann[175], A. Neusiedl[81], R.M. Neves[108], P. Nevski[25],
F.M. Newcomer[120], P.R. Newman[18], V. Nguyen Thi Hong[136], R.B. Nickerson[118], R. Nicolaidou[136],
B. Nicquevert[30], F. Niedercorn[115], J. Nielsen[137], N. Nikiforou[35], A. Nikiforov[16], V. Nikolaenko[128],
I. Nikolic-Audit[78], K. Nikolics[49], K. Nikolopoulos[18], H. Nilsen[48], P. Nilsson[8], Y. Ninomiya[155],
A. Nisati[132a], R. Nisius[99], T. Nobe[157], L. Nodulman[6], M. Nomachi[116], I. Nomidis[154],
S. Norberg[111], M. Nordberg[30], P.R. Norton[129], J. Novakova[127], M. Nozaki[65], L. Nozka[113],
I.M. Nugent[159a], A.-E. Nuncio-Quiroz[21], G. Nunes Hanninger[86], T. Nunnemann[98], E. Nurse[77],
B.J. O'Brien[46], D.C. O'Neil[142], V. O'Shea[53], L.B. Oakes[98], F.G. Oakham[29,f], H. Oberlack[99],
J. Ocariz[78], A. Ochi[66], S. Oda[69], S. Odaka[65], J. Odier[83], H. Ogren[60], A. Oh[82], S.H. Oh[45],
C.C. Ohm[30], T. Ohshima[101], W. Okamura[116], H. Okawa[25], Y. Okumura[31], T. Okuyama[155],
A. Olariu[26a], A.G. Olchevski[64], S.A. Olivares Pino[32a], M. Oliveira[124a,i], D. Oliveira Damazio[25],
E. Oliver Garcia[167], D. Olivito[120], A. Olszewski[39], J. Olszowska[39], A. Onofre[124a,ab],
P.U.E. Onyisi[31,ac], C.J. Oram[159a], M.J. Oreglia[31], Y. Oren[153], D. Orestano[134a,134b],
N. Orlando[72a,72b], I. Orlov[107], C. Oropeza Barrera[53], R.S. Orr[158], B. Osculati[50a,50b],
R. Ospanov[120], C. Osuna[12], G. Otero y Garzon[27], J.P. Ottersbach[105], M. Ouchrif[135d],
E.A. Ouellette[169], F. Ould-Saada[117], A. Ouraou[136], Q. Ouyang[33a], A. Ovcharova[15], M. Owen[82],
S. Owen[139], V.E. Ozcan[19a], N. Ozturk[8], A. Pacheco Pages[12], C. Padilla Aranda[12],
S. Pagan Griso[15], E. Paganis[139], C. Pahl[99], F. Paige[25], P. Pais[84], K. Pajchel[117], G. Palacino[159b],
C.P. Paleari[7], S. Palestini[30], D. Pallin[34], A. Palma[124a], J.D. Palmer[18], Y.B. Pan[173],
E. Panagiotopoulou[10], J.G. Panduro Vazquez[76], P. Pani[105], N. Panikashvili[87], S. Panitkin[25],
D. Pantea[26a], A. Papadelis[146a], Th.D. Papadopoulou[10], A. Paramonov[6], D. Paredes Hernandez[34],
W. Park[25,ad], M.A. Parker[28], F. Parodi[50a,50b], J.A. Parsons[35], U. Parzefall[48], S. Pashapour[54],
E. Pasqualucci[132a], S. Passaggio[50a], A. Passeri[134a], F. Pastore[134a,134b,*], Fr. Pastore[76],
G. Pásztor[49,ae], S. Pataraia[175], N. Patel[150], J.R. Pater[82], S. Patricelli[102a,102b], T. Pauly[30],
M. Pecsy[144a], S. Pedraza Lopez[167], M.I. Pedraza Morales[173], S.V. Peleganchuk[107], D. Pelikan[166],
H. Peng[33b], B. Penning[31], A. Penson[35], J. Penwell[60], M. Perantoni[24a], K. Perez[35,af],
T. Perez Cavalcanti[42], E. Perez Codina[159a], M.T. Pérez García-Estañ[167], V. Perez Reale[35],
L. Perini[89a,89b], H. Pernegger[30], R. Perrino[72a], P. Perrodo[5], V.D. Peshekhonov[64], K. Peters[30],
B.A. Petersen[30], J. Petersen[30], T.C. Petersen[36], E. Petit[5], A. Petridis[154], C. Petridou[154],
E. Petrolo[132a], F. Petrucci[134a,134b], D. Petschull[42], M. Petteni[142], R. Pezoa[32b], A. Phan[86],
P.W. Phillips[129], G. Piacquadio[30], A. Picazio[49], E. Piccaro[75], M. Piccinini[20a,20b], S.M. Piec[42],
R. Piegaia[27], D.T. Pignotti[109], J.E. Pilcher[31], A.D. Pilkington[82], J. Pina[124a,c],
M. Pinamonti[164a,164c], A. Pinder[118], J.L. Pinfold[3], A. Pingel[36], B. Pinto[124a], C. Pizio[89a,89b],
M.-A. Pleier[25], E. Plotnikova[64], A. Poblaguev[25], S. Poddar[58a], F. Podlyski[34], L. Poggioli[115],
D. Pohl[21], M. Pohl[49], G. Polesello[119a], A. Policicchio[37a,37b], A. Polini[20a], J. Poll[75],
V. Polychronakos[25], D. Pomeroy[23], K. Pommès[30], L. Pontecorvo[132a], B.G. Pope[88],
G.A. Popeneciu[26a], D.S. Popovic[13a], A. Poppleton[30], X. Portell Bueso[30], G.E. Pospelov[99],
S. Pospisil[126], I.N. Potrap[99], C.J. Potter[149], C.T. Potter[114], G. Poulard[30], J. Poveda[60],
V. Pozdnyakov[64], R. Prabhu[77], P. Pralavorio[83], A. Pranko[15], S. Prasad[30], R. Pravahan[25],
S. Prell[63], K. Pretzl[17], D. Price[60], J. Price[73], L.E. Price[6], D. Prieur[123], M. Primavera[72a],
K. Prokofiev[108], F. Prokoshin[32b], S. Protopopescu[25], J. Proudfoot[6], X. Prudent[44],
M. Przybycien[38], H. Przysiezniak[5], S. Psoroulas[21], E. Ptacek[114], E. Pueschel[84], D. Puldon[148],
J. Purdham[87], M. Purohit[25,ad], P. Puzo[115], Y. Pylypchenko[62], J. Qian[87], A. Quadt[54],
D.R. Quarrie[15], W.B. Quayle[173], M. Raas[104], V. Radeka[25], V. Radescu[42], P. Radloff[114],
F. Ragusa[89a,89b], G. Rahal[178], A.M. Rahimi[109], D. Rahm[25], S. Rajagopalan[25], M. Rammensee[48],
M. Rammes[141], A.S. Randle-Conde[40], K. Randrianarivony[29], K. Rao[163], F. Rauscher[98],
T.C. Rave[48], M. Raymond[30], A.L. Read[117], D.M. Rebuzzi[119a,119b], A. Redelbach[174],
G. Redlinger[25], R. Reece[120], K. Reeves[41], A. Reinsch[114], I. Reisinger[43], C. Rembser[30],
Z.L. Ren[151], A. Renaud[115], M. Rescigno[132a], S. Resconi[89a], B. Resende[136], P. Reznicek[98],

R. Rezvani[158], R. Richter[99], E. Richter-Was[5,ag], M. Ridel[78], M. Rijpstra[105], M. Rijssenbeek[148],
A. Rimoldi[119a,119b], L. Rinaldi[20a], R.R. Rios[40], I. Riu[12], G. Rivoltella[89a,89b], F. Rizatdinova[112],
E. Rizvi[75], S.H. Robertson[85,l], A. Robichaud-Veronneau[118], D. Robinson[28], J.E.M. Robinson[82],
A. Robson[53], J.G. Rocha de Lima[106], C. Roda[122a,122b], D. Roda Dos Santos[30], A. Roe[54],
S. Roe[30], O. Røhne[117], S. Rolli[161], A. Romaniouk[96], M. Romano[20a,20b], G. Romeo[27],
E. Romero Adam[167], N. Rompotis[138], L. Roos[78], E. Ros[167], S. Rosati[132a], K. Rosbach[49],
A. Rose[149], M. Rose[76], G.A. Rosenbaum[158], E.I. Rosenberg[63], P.L. Rosendahl[14], O. Rosenthal[141],
L. Rosselet[49], V. Rossetti[12], E. Rossi[132a,132b], L.P. Rossi[50a], M. Rotaru[26a], I. Roth[172],
J. Rothberg[138], D. Rousseau[115], C.R. Royon[136], A. Rozanov[83], Y. Rozen[152], X. Ruan[33a,ah],
F. Rubbo[12], I. Rubinskiy[42], N. Ruckstuhl[105], V.I. Rud[97], C. Rudolph[44], G. Rudolph[61], F. Rühr[7],
A. Ruiz-Martinez[63], L. Rumyantsev[64], Z. Rurikova[48], N.A. Rusakovich[64], A. Ruschke[98],
J.P. Rutherfoord[7], P. Ruzicka[125], Y.F. Ryabov[121], M. Rybar[127], G. Rybkin[115], N.C. Ryder[118],
A.F. Saavedra[150], I. Sadeh[153], H.F-W. Sadrozinski[137], R. Sadykov[64], F. Safai Tehrani[132a],
H. Sakamoto[155], G. Salamanna[75], A. Salamon[133a], M. Saleem[111], D. Salek[30], D. Salihagic[99],
A. Salnikov[143], J. Salt[167], B.M. Salvachua Ferrando[6], D. Salvatore[37a,37b], F. Salvatore[149],
A. Salvucci[104], A. Salzburger[30], D. Sampsonidis[154], B.H. Samset[117], A. Sanchez[102a,102b],
V. Sanchez Martinez[167], H. Sandaker[14], H.G. Sander[81], M.P. Sanders[98], M. Sandhoff[175],
T. Sandoval[28], C. Sandoval[162], R. Sandstroem[99], D.P.C. Sankey[129], A. Sansoni[47],
C. Santamarina Rios[85], C. Santoni[34], R. Santonico[133a,133b], H. Santos[124a], I. Santoyo Castillo[149],
J.G. Saraiva[124a], T. Sarangi[173], E. Sarkisyan-Grinbaum[8], B. Sarrazin[21], F. Sarri[122a,122b],
G. Sartisohn[175], O. Sasaki[65], Y. Sasaki[155], N. Sasao[67], I. Satsounkevitch[90], G. Sauvage[5,*],
E. Sauvan[5], J.B. Sauvan[115], P. Savard[158,f], V. Savinov[123], D.O. Savu[30], L. Sawyer[25,n],
D.H. Saxon[53], J. Saxon[120], C. Sbarra[20a], A. Sbrizzi[20a,20b], D.A. Scannicchio[163], M. Scarcella[150],
J. Schaarschmidt[115], P. Schacht[99], D. Schaefer[120], U. Schäfer[81], A. Schaelicke[46], S. Schaepe[21],
S. Schaetzel[58b], A.C. Schaffer[115], D. Schaile[98], R.D. Schamberger[148], A.G. Schamov[107],
V. Scharf[58a], V.A. Schegelsky[121], D. Scheirich[87], M. Schernau[163], M.I. Scherzer[35],
C. Schiavi[50a,50b], J. Schieck[98], M. Schioppa[37a,37b], S. Schlenker[30], E. Schmidt[48], K. Schmieden[21],
C. Schmitt[81], S. Schmitt[58b], B. Schneider[17], U. Schnoor[44], L. Schoeffel[136], A. Schoening[58b],
A.L.S. Schorlemmer[54], M. Schott[30], D. Schouten[159a], J. Schovancova[125], M. Schram[85],
C. Schroeder[81], N. Schroer[58c], M.J. Schultens[21], J. Schultes[175], H.-C. Schultz-Coulon[58a],
H. Schulz[16], M. Schumacher[48], B.A. Schumm[137], Ph. Schune[136], A. Schwartzman[143],
Ph. Schwegler[99], Ph. Schwemling[78], R. Schwienhorst[88], R. Schwierz[44], J. Schwindling[136],
T. Schwindt[21], M. Schwoerer[5], F.G. Sciacca[17], G. Sciolla[23], W.G. Scott[129], J. Searcy[114],
G. Sedov[42], E. Sedykh[121], S.C. Seidel[103], A. Seiden[137], F. Seifert[44], J.M. Seixas[24a],
G. Sekhniaidze[102a], S.J. Sekula[40], K.E. Selbach[46], D.M. Seliverstov[121], B. Sellden[146a], G. Sellers[73],
M. Seman[144b], N. Semprini-Cesari[20a,20b], C. Serfon[98], L. Serin[115], L. Serkin[54], R. Seuster[159a],
H. Severini[111], A. Sfyrla[30], E. Shabalina[54], M. Shamim[114], L.Y. Shan[33a], J.T. Shank[22],
Q.T. Shao[86], M. Shapiro[15], P.B. Shatalov[95], K. Shaw[164a,164c], D. Sherman[176], P. Sherwood[77],
S. Shimizu[101], M. Shimojima[100], T. Shin[56], M. Shiyakova[64], A. Shmeleva[94], M.J. Shochet[31],
D. Short[118], S. Shrestha[63], E. Shulga[96], M.A. Shupe[7], P. Sicho[125], A. Sidoti[132a], F. Siegert[48],
Dj. Sijacki[13a], O. Silbert[172], J. Silva[124a], Y. Silver[153], D. Silverstein[143], S.B. Silverstein[146a],
V. Simak[126], O. Simard[136], Lj. Simic[13a], S. Simion[115], E. Simioni[81], B. Simmons[77],
R. Simoniello[89a,89b], M. Simonyan[36], P. Sinervo[158], N.B. Sinev[114], V. Sipica[141], G. Siragusa[174],
A. Sircar[25], A.N. Sisakyan[64,*], S.Yu. Sivoklokov[97], J. Sjölin[146a,146b], T.B. Sjursen[14],
L.A. Skinnari[15], H.P. Skottowe[57], K. Skovpen[107], P. Skubic[111], M. Slater[18], T. Slavicek[126],
K. Sliwa[161], V. Smakhtin[172], B.H. Smart[46], L. Smestad[117], S.Yu. Smirnov[96], Y. Smirnov[96],
L.N. Smirnova[97], O. Smirnova[79], B.C. Smith[57], D. Smith[143], K.M. Smith[53], M. Smizanska[71],
K. Smolek[126], A.A. Snesarev[94], S.W. Snow[82], J. Snow[111], S. Snyder[25], R. Sobie[169,l],
J. Sodomka[126], A. Soffer[153], C.A. Solans[167], M. Solar[126], J. Solc[126], E.Yu. Soldatov[96],
U. Soldevila[167], E. Solfaroli Camillocci[132a,132b], A.A. Solodkov[128], O.V. Solovyanov[128],
V. Solovyev[121], N. Soni[1], A. Sood[15], V. Sopko[126], B. Sopko[126], M. Sosebee[8], R. Soualah[164a,164c],
P. Soueid[93], A. Soukharev[107], S. Spagnolo[72a,72b], F. Spanò[76], R. Spighi[20a], G. Spigo[30],

R. Spiwoks[30], M. Spousta[127,ai], T. Spreitzer[158], B. Spurlock[8], R.D. St. Denis[53], J. Stahlman[120],
R. Stamen[58a], E. Stanecka[39], R.W. Stanek[6], C. Stanescu[134a], M. Stanescu-Bellu[42],
M.M. Stanitzki[42], S. Stapnes[117], E.A. Starchenko[128], J. Stark[55], P. Staroba[125], P. Starovoitov[42],
R. Staszewski[39], A. Staude[98], P. Stavina[144a,*], G. Steele[53], P. Steinbach[44], P. Steinberg[25],
I. Stekl[126], B. Stelzer[142], H.J. Stelzer[88], O. Stelzer-Chilton[159a], H. Stenzel[52], S. Stern[99],
G.A. Stewart[30], J.A. Stillings[21], M.C. Stockton[85], K. Stoerig[48], G. Stoicea[26a], S. Stonjek[99],
P. Strachota[127], A.R. Stradling[8], A. Straessner[44], J. Strandberg[147], S. Strandberg[146a,146b],
A. Strandlie[117], M. Strang[109], E. Strauss[143], M. Strauss[111], P. Strizenec[144b], R. Ströhmer[174],
D.M. Strom[114], J.A. Strong[76,*], R. Stroynowski[40], B. Stugu[14], I. Stumer[25,*], J. Stupak[148],
P. Sturm[175], N.A. Styles[42], D.A. Soh[151,v], D. Su[143], HS. Subramania[3], R. Subramaniam[25],
A. Succurro[12], Y. Sugaya[116], C. Suhr[106], M. Suk[127], V.V. Sulin[94], S. Sultansoy[4d], T. Sumida[67],
X. Sun[55], J.E. Sundermann[48], K. Suruliz[139], G. Susinno[37a,37b], M.R. Sutton[149], Y. Suzuki[65],
Y. Suzuki[66], M. Svatos[125], S. Swedish[168], I. Sykora[144a], T. Sykora[127], J. Sánchez[167], D. Ta[105],
K. Tackmann[42], A. Taffard[163], R. Tafirout[159a], N. Taiblum[153], Y. Takahashi[101], H. Takai[25],
R. Takashima[68], H. Takeda[66], T. Takeshita[140], Y. Takubo[65], M. Talby[83], A. Talyshev[107,h],
M.C. Tamsett[25], K.G. Tan[86], J. Tanaka[155], R. Tanaka[115], S. Tanaka[131], S. Tanaka[65],
A.J. Tanasijczuk[142], K. Tani[66], N. Tannoury[83], S. Tapprogge[81], D. Tardif[158], S. Tarem[152],
F. Tarrade[29], G.F. Tartarelli[89a], P. Tas[127], M. Tasevsky[125], E. Tassi[37a,37b], Y. Tayalati[135d],
C. Taylor[77], F.E. Taylor[92], G.N. Taylor[86], W. Taylor[159b], M. Teinturier[115], F.A. Teischinger[30],
M. Teixeira Dias Castanheira[75], P. Teixeira-Dias[76], K.K. Temming[48], H. Ten Kate[30],
P.K. Teng[151], S. Terada[65], K. Terashi[155], J. Terron[80], M. Testa[47], R.J. Teuscher[158,l],
J. Therhaag[21], T. Theveneaux-Pelzer[78], S. Thoma[48], J.P. Thomas[18], E.N. Thompson[35],
P.D. Thompson[18], P.D. Thompson[158], A.S. Thompson[53], L.A. Thomsen[36], E. Thomson[120],
M. Thomson[28], W.M. Thong[86], R.P. Thun[87], F. Tian[35], M.J. Tibbetts[15], T. Tic[125],
V.O. Tikhomirov[94], Y.A. Tikhonov[107,h], S. Timoshenko[96], E. Tiouchichine[83], P. Tipton[176],
S. Tisserant[83], T. Todorov[5], S. Todorova-Nova[161], B. Toggerson[163], J. Tojo[69], S. Tokár[144a],
K. Tokushuku[65], K. Tollefson[88], M. Tomoto[101], L. Tompkins[31], K. Toms[103], A. Tonoyan[14],
C. Topfel[17], N.D. Topilin[64], E. Torrence[114], H. Torres[78], E. Torró Pastor[167], J. Toth[83,ae],
F. Touchard[83], D.R. Tovey[139], T. Trefzger[174], L. Tremblet[30], A. Tricoli[30], I.M. Trigger[159a],
S. Trincaz-Duvoid[78], M.F. Tripiana[70], N. Triplett[25], W. Trischuk[158], B. Trocmé[55], C. Troncon[89a],
M. Trottier-McDonald[142], P. True[88], M. Trzebinski[39], A. Trzupek[39], C. Tsarouchas[30],
J.C-L. Tseng[118], M. Tsiakiris[105], P.V. Tsiareshka[90], D. Tsionou[5,aj], G. Tsipolitis[10],
S. Tsiskaridze[12], V. Tsiskaridze[48], E.G. Tskhadadze[51a], I.I. Tsukerman[95], V. Tsulaia[15],
J.-W. Tsung[21], S. Tsuno[65], D. Tsybychev[148], A. Tua[139], A. Tudorache[26a], V. Tudorache[26a],
J.M. Tuggle[31], M. Turala[39], D. Turecek[126], I. Turk Cakir[4e], E. Turlay[105], R. Turra[89a,89b],
P.M. Tuts[35], A. Tykhonov[74], M. Tylmad[146a,146b], M. Tyndel[129], G. Tzanakos[9], K. Uchida[21],
I. Ueda[155], R. Ueno[29], M. Ughetto[83], M. Ugland[14], M. Uhlenbrock[21], M. Uhrmacher[54],
F. Ukegawa[160], G. Unal[30], A. Undrus[25], G. Unel[163], Y. Unno[65], D. Urbaniec[35], P. Urquijo[21],
G. Usai[8], M. Uslenghi[119a,119b], L. Vacavant[83], V. Vacek[126], B. Vachon[85], S. Vahsen[15],
J. Valenta[125], S. Valentinetti[20a,20b], A. Valero[167], S. Valkar[127], E. Valladolid Gallego[167],
S. Vallecorsa[152], J.A. Valls Ferrer[167], R. Van Berg[120], P.C. Van Der Deijl[105], R. van der Geer[105],
H. van der Graaf[105], R. Van Der Leeuw[105], E. van der Poel[105], D. van der Ster[30], N. van Eldik[30],
P. van Gemmeren[6], J. Van Nieuwkoop[142], I. van Vulpen[105], M. Vanadia[99], W. Vandelli[30],
A. Vaniachine[6], P. Vankov[42], F. Vannucci[78], R. Vari[132a], E.W. Varnes[7], T. Varol[84],
D. Varouchas[15], A. Vartapetian[8], K.E. Varvell[150], V.I. Vassilakopoulos[56], F. Vazeille[34],
T. Vazquez Schroeder[54], G. Vegni[89a,89b], J.J. Veillet[115], F. Veloso[124a], R. Veness[30],
S. Veneziano[132a], A. Ventura[72a,72b], D. Ventura[84], M. Venturi[48], N. Venturi[158], V. Vercesi[119a],
M. Verducci[138], W. Verkerke[105], J.C. Vermeulen[105], A. Vest[44], M.C. Vetterli[142,f], I. Vichou[165],
T. Vickey[145b,ak], O.E. Vickey Boeriu[145b], G.H.A. Viehhauser[118], S. Viel[168], M. Villa[20a,20b],
M. Villaplana Perez[167], E. Vilucchi[47], M.G. Vincter[29], E. Vinek[30], V.B. Vinogradov[64],
M. Virchaux[136,*], J. Virzi[15], O. Vitells[172], M. Viti[42], I. Vivarelli[48], F. Vives Vaque[3], S. Vlachos[10],
D. Vladoiu[98], M. Vlasak[126], A. Vogel[21], P. Vokac[126], G. Volpi[47], M. Volpi[86], G. Volpini[89a],

H. von der Schmitt[99], H. von Radziewski[48], E. von Toerne[21], V. Vorobel[127], V. Vorwerk[12],
M. Vos[167], R. Voss[30], J.H. Vossebeld[73], N. Vranjes[136], M. Vranjes Milosavljevic[105], V. Vrba[125],
M. Vreeswijk[105], T. Vu Anh[48], R. Vuillermet[30], I. Vukotic[31], W. Wagner[175], P. Wagner[120],
H. Wahlen[175], S. Wahrmund[44], J. Wakabayashi[101], S. Walch[87], J. Walder[71], R. Walker[98],
W. Walkowiak[141], R. Wall[176], P. Waller[73], B. Walsh[176], C. Wang[45], H. Wang[173], H. Wang[40],
J. Wang[151], J. Wang[33a], R. Wang[103], S.M. Wang[151], T. Wang[21], A. Warburton[85], C.P. Ward[28],
D.R. Wardrope[77], M. Warsinsky[48], A. Washbrook[46], C. Wasicki[42], I. Watanabe[66],
P.M. Watkins[18], A.T. Watson[18], I.J. Watson[150], M.F. Watson[18], G. Watts[138], S. Watts[82],
A.T. Waugh[150], B.M. Waugh[77], M.S. Weber[17], J.S. Webster[31], A.R. Weidberg[118], P. Weigell[99],
J. Weingarten[54], C. Weiser[48], P.S. Wells[30], T. Wenaus[25], D. Wendland[16], Z. Weng[151,v],
T. Wengler[30], S. Wenig[30], N. Wermes[21], M. Werner[48], P. Werner[30], M. Werth[163], M. Wessels[58a],
J. Wetter[161], C. Weydert[55], K. Whalen[29], A. White[8], M.J. White[86], S. White[122a,122b],
S.R. Whitehead[118], D. Whiteson[163], D. Whittington[60], D. Wicke[175], F.J. Wickens[129],
W. Wiedenmann[173], M. Wielers[129], P. Wienemann[21], C. Wiglesworth[75], L.A.M. Wiik-Fuchs[21],
P.A. Wijeratne[77], A. Wildauer[99], M.A. Wildt[42,s], I. Wilhelm[127], H.G. Wilkens[30], J.Z. Will[98],
E. Williams[35], H.H. Williams[120], S. Williams[28], W. Willis[35], S. Willocq[84], J.A. Wilson[18],
M.G. Wilson[143], A. Wilson[87], I. Wingerter-Seez[5], S. Winkelmann[48], F. Winklmeier[30],
M. Wittgen[143], S.J. Wollstadt[81], M.W. Wolter[39], H. Wolters[124a,i], W.C. Wong[41], G. Wooden[87],
B.K. Wosiek[39], J. Wotschack[30], M.J. Woudstra[82], K.W. Wozniak[39], K. Wraight[53], M. Wright[53],
B. Wrona[73], S.L. Wu[173], X. Wu[49], Y. Wu[33b,al], E. Wulf[35], B.M. Wynne[46], S. Xella[36], M. Xiao[136],
S. Xie[48], C. Xu[33b,z], D. Xu[33a], L. Xu[33b], B. Yabsley[150], S. Yacoob[145a,am], M. Yamada[65],
H. Yamaguchi[155], A. Yamamoto[65], K. Yamamoto[63], S. Yamamoto[155], T. Yamamura[155],
T. Yamanaka[155], T. Yamazaki[155], Y. Yamazaki[66], Z. Yan[22], H. Yang[87], U.K. Yang[82], Y. Yang[109],
Z. Yang[146a,146b], S. Yanush[91], L. Yao[33a], Y. Yasu[65], E. Yatsenko[42], J. Ye[40], S. Ye[25], A.L. Yen[57],
M. Yilmaz[4c], R. Yoosoofmiya[123], K. Yorita[171], R. Yoshida[6], K. Yoshihara[155], C. Young[143],
C.J. Young[118], S. Youssef[22], D. Yu[25], D.R. Yu[15], J. Yu[8], J. Yu[112], L. Yuan[66], A. Yurkewicz[106],
B. Zabinski[39], R. Zaidan[62], A.M. Zaitsev[128], L. Zanello[132a,132b], D. Zanzi[99], A. Zaytsev[25],
C. Zeitnitz[175], M. Zeman[126], A. Zemla[39], O. Zenin[128], T. Ženiš[144a], Z. Zinonos[122a,122b],
D. Zerwas[115], G. Zevi della Porta[57], D. Zhang[87], H. Zhang[88], J. Zhang[6], X. Zhang[33d],
Z. Zhang[115], L. Zhao[108], Z. Zhao[33b], A. Zhemchugov[64], J. Zhong[118], B. Zhou[87], N. Zhou[163],
Y. Zhou[151], C.G. Zhu[33d], H. Zhu[42], J. Zhu[87], Y. Zhu[33b], X. Zhuang[98], V. Zhuravlov[99],
A. Zibell[98], D. Zieminska[60], N.I. Zimin[64], R. Zimmermann[21], S. Zimmermann[21],
S. Zimmermann[48], M. Ziolkowski[141], R. Zitoun[5], L. Živković[35], V.V. Zmouchko[128,*],
G. Zobernig[173], A. Zoccoli[20a,20b], M. zur Nedden[16], V. Zutshi[106], L. Zwalinski[30]

1 School of Chemistry and Physics, University of Adelaide, Adelaide, Australia
2 Physics Department, SUNY Albany, Albany NY, United States of America
3 Department of Physics, University of Alberta, Edmonton AB, Canada
4 (a) Department of Physics, Ankara University, Ankara; (b) Department of Physics, Dumlupinar University, Kutahya; (c) Department of Physics, Gazi University, Ankara; (d) Division of Physics, TOBB University of Economics and Technology, Ankara; (e) Turkish Atomic Energy Authority, Ankara, Turkey
5 LAPP, CNRS/IN2P3 and Université de Savoie, Annecy-le-Vieux, France
6 High Energy Physics Division, Argonne National Laboratory, Argonne IL, United States of America
7 Department of Physics, University of Arizona, Tucson AZ, United States of America
8 Department of Physics, The University of Texas at Arlington, Arlington TX, United States of America
9 Physics Department, University of Athens, Athens, Greece
10 Physics Department, National Technical University of Athens, Zografou, Greece
11 Institute of Physics, Azerbaijan Academy of Sciences, Baku, Azerbaijan
12 Institut de Física d'Altes Energies and Departament de Física de la Universitat Autònoma de Barcelona and ICREA, Barcelona, Spain

13 [a] Institute of Physics, University of Belgrade, Belgrade; [b] Vinca Institute of Nuclear Sciences, University of Belgrade, Belgrade, Serbia

14 Department for Physics and Technology, University of Bergen, Bergen, Norway

15 Physics Division, Lawrence Berkeley National Laboratory and University of California, Berkeley CA, United States of America

16 Department of Physics, Humboldt University, Berlin, Germany

17 Albert Einstein Center for Fundamental Physics and Laboratory for High Energy Physics, University of Bern, Bern, Switzerland

18 School of Physics and Astronomy, University of Birmingham, Birmingham, United Kingdom

19 [a] Department of Physics, Bogazici University, Istanbul; [b] Division of Physics, Dogus University, Istanbul; [c] Department of Physics Engineering, Gaziantep University, Gaziantep; [d] Department of Physics, Istanbul Technical University, Istanbul, Turkey

20 [a] INFN Sezione di Bologna; [b] Dipartimento di Fisica, Università di Bologna, Bologna, Italy

21 Physikalisches Institut, University of Bonn, Bonn, Germany

22 Department of Physics, Boston University, Boston MA, United States of America

23 Department of Physics, Brandeis University, Waltham MA, United States of America

24 [a] Universidade Federal do Rio De Janeiro COPPE/EE/IF, Rio de Janeiro; [b] Federal University of Juiz de Fora (UFJF), Juiz de Fora; [c] Federal University of Sao Joao del Rei (UFSJ), Sao Joao del Rei; [d] Instituto de Fisica, Universidade de Sao Paulo, Sao Paulo, Brazil

25 Physics Department, Brookhaven National Laboratory, Upton NY, United States of America

26 [a] National Institute of Physics and Nuclear Engineering, Bucharest; [b] University Politehnica Bucharest, Bucharest; [c] West University in Timisoara, Timisoara, Romania

27 Departamento de Física, Universidad de Buenos Aires, Buenos Aires, Argentina

28 Cavendish Laboratory, University of Cambridge, Cambridge, United Kingdom

29 Department of Physics, Carleton University, Ottawa ON, Canada

30 CERN, Geneva, Switzerland

31 Enrico Fermi Institute, University of Chicago, Chicago IL, United States of America

32 [a] Departamento de Física, Pontificia Universidad Católica de Chile, Santiago; [b] Departamento de Física, Universidad Técnica Federico Santa María, Valparaíso, Chile

33 [a] Institute of High Energy Physics, Chinese Academy of Sciences, Beijing; [b] Department of Modern Physics, University of Science and Technology of China, Anhui; [c] Department of Physics, Nanjing University, Jiangsu; [d] School of Physics, Shandong University, Shandong; [e] Physics Department, Shanghai Jiao Tong University, Shanghai, China

34 Laboratoire de Physique Corpusculaire, Clermont Université and Université Blaise Pascal and CNRS/IN2P3, Clermont-Ferrand, France

35 Nevis Laboratory, Columbia University, Irvington NY, United States of America

36 Niels Bohr Institute, University of Copenhagen, Kobenhavn, Denmark

37 [a] INFN Gruppo Collegato di Cosenza; [b] Dipartimento di Fisica, Università della Calabria, Arcavata di Rende, Italy

38 AGH University of Science and Technology, Faculty of Physics and Applied Computer Science, Krakow, Poland

39 The Henryk Niewodniczanski Institute of Nuclear Physics, Polish Academy of Sciences, Krakow, Poland

40 Physics Department, Southern Methodist University, Dallas TX, United States of America

41 Physics Department, University of Texas at Dallas, Richardson TX, United States of America

42 DESY, Hamburg and Zeuthen, Germany

43 Institut für Experimentelle Physik IV, Technische Universität Dortmund, Dortmund, Germany

44 Institut für Kern- und Teilchenphysik, Technical University Dresden, Dresden, Germany

45 Department of Physics, Duke University, Durham NC, United States of America

46 SUPA - School of Physics and Astronomy, University of Edinburgh, Edinburgh, United Kingdom

47 INFN Laboratori Nazionali di Frascati, Frascati, Italy

48 Fakultät für Mathematik und Physik, Albert-Ludwigs-Universität, Freiburg, Germany

49 Section de Physique, Université de Genève, Geneva, Switzerland
50 (a) INFN Sezione di Genova; (b) Dipartimento di Fisica, Università di Genova, Genova, Italy
51 (a) E. Andronikashvili Institute of Physics, Iv. Javakhishvili Tbilisi State University, Tbilisi; (b) High Energy Physics Institute, Tbilisi State University, Tbilisi, Georgia
52 II Physikalisches Institut, Justus-Liebig-Universität Giessen, Giessen, Germany
53 SUPA - School of Physics and Astronomy, University of Glasgow, Glasgow, United Kingdom
54 II Physikalisches Institut, Georg-August-Universität, Göttingen, Germany
55 Laboratoire de Physique Subatomique et de Cosmologie, Université Joseph Fourier and CNRS/IN2P3 and Institut National Polytechnique de Grenoble, Grenoble, France
56 Department of Physics, Hampton University, Hampton VA, United States of America
57 Laboratory for Particle Physics and Cosmology, Harvard University, Cambridge MA, United States of America
58 (a) Kirchhoff-Institut für Physik, Ruprecht-Karls-Universität Heidelberg, Heidelberg; (b) Physikalisches Institut, Ruprecht-Karls-Universität Heidelberg, Heidelberg; (c) ZITI Institut für technische Informatik, Ruprecht-Karls-Universität Heidelberg, Mannheim, Germany
59 Faculty of Applied Information Science, Hiroshima Institute of Technology, Hiroshima, Japan
60 Department of Physics, Indiana University, Bloomington IN, United States of America
61 Institut für Astro- und Teilchenphysik, Leopold-Franzens-Universität, Innsbruck, Austria
62 University of Iowa, Iowa City IA, United States of America
63 Department of Physics and Astronomy, Iowa State University, Ames IA, United States of America
64 Joint Institute for Nuclear Research, JINR Dubna, Dubna, Russia
65 KEK, High Energy Accelerator Research Organization, Tsukuba, Japan
66 Graduate School of Science, Kobe University, Kobe, Japan
67 Faculty of Science, Kyoto University, Kyoto, Japan
68 Kyoto University of Education, Kyoto, Japan
69 Department of Physics, Kyushu University, Fukuoka, Japan
70 Instituto de Física La Plata, Universidad Nacional de La Plata and CONICET, La Plata, Argentina
71 Physics Department, Lancaster University, Lancaster, United Kingdom
72 (a) INFN Sezione di Lecce; (b) Dipartimento di Matematica e Fisica, Università del Salento, Lecce, Italy
73 Oliver Lodge Laboratory, University of Liverpool, Liverpool, United Kingdom
74 Department of Physics, Jožef Stefan Institute and University of Ljubljana, Ljubljana, Slovenia
75 School of Physics and Astronomy, Queen Mary University of London, London, United Kingdom
76 Department of Physics, Royal Holloway University of London, Surrey, United Kingdom
77 Department of Physics and Astronomy, University College London, London, United Kingdom
78 Laboratoire de Physique Nucléaire et de Hautes Energies, UPMC and Université Paris-Diderot and CNRS/IN2P3, Paris, France
79 Fysiska institutionen, Lunds universitet, Lund, Sweden
80 Departamento de Fisica Teorica C-15, Universidad Autonoma de Madrid, Madrid, Spain
81 Institut für Physik, Universität Mainz, Mainz, Germany
82 School of Physics and Astronomy, University of Manchester, Manchester, United Kingdom
83 CPPM, Aix-Marseille Université and CNRS/IN2P3, Marseille, France
84 Department of Physics, University of Massachusetts, Amherst MA, United States of America
85 Department of Physics, McGill University, Montreal QC, Canada
86 School of Physics, University of Melbourne, Victoria, Australia
87 Department of Physics, The University of Michigan, Ann Arbor MI, United States of America
88 Department of Physics and Astronomy, Michigan State University, East Lansing MI, United States of America
89 (a) INFN Sezione di Milano; (b) Dipartimento di Fisica, Università di Milano, Milano, Italy
90 B.I. Stepanov Institute of Physics, National Academy of Sciences of Belarus, Minsk, Republic of Belarus
91 National Scientific and Educational Centre for Particle and High Energy Physics, Minsk, Republic of Belarus

92 Department of Physics, Massachusetts Institute of Technology, Cambridge MA, United States of America

93 Group of Particle Physics, University of Montreal, Montreal QC, Canada

94 P.N. Lebedev Institute of Physics, Academy of Sciences, Moscow, Russia

95 Institute for Theoretical and Experimental Physics (ITEP), Moscow, Russia

96 Moscow Engineering and Physics Institute (MEPhI), Moscow, Russia

97 Skobeltsyn Institute of Nuclear Physics, Lomonosov Moscow State University, Moscow, Russia

98 Fakultät für Physik, Ludwig-Maximilians-Universität München, München, Germany

99 Max-Planck-Institut für Physik (Werner-Heisenberg-Institut), München, Germany

100 Nagasaki Institute of Applied Science, Nagasaki, Japan

101 Graduate School of Science and Kobayashi-Maskawa Institute, Nagoya University, Nagoya, Japan

102 [a] INFN Sezione di Napoli; [b] Dipartimento di Scienze Fisiche, Università di Napoli, Napoli, Italy

103 Department of Physics and Astronomy, University of New Mexico, Albuquerque NM, United States of America

104 Institute for Mathematics, Astrophysics and Particle Physics, Radboud University Nijmegen/Nikhef, Nijmegen, Netherlands

105 Nikhef National Institute for Subatomic Physics and University of Amsterdam, Amsterdam, Netherlands

106 Department of Physics, Northern Illinois University, DeKalb IL, United States of America

107 Budker Institute of Nuclear Physics, SB RAS, Novosibirsk, Russia

108 Department of Physics, New York University, New York NY, United States of America

109 Ohio State University, Columbus OH, United States of America

110 Faculty of Science, Okayama University, Okayama, Japan

111 Homer L. Dodge Department of Physics and Astronomy, University of Oklahoma, Norman OK, United States of America

112 Department of Physics, Oklahoma State University, Stillwater OK, United States of America

113 Palacký University, RCPTM, Olomouc, Czech Republic

114 Center for High Energy Physics, University of Oregon, Eugene OR, United States of America

115 LAL, Université Paris-Sud and CNRS/IN2P3, Orsay, France

116 Graduate School of Science, Osaka University, Osaka, Japan

117 Department of Physics, University of Oslo, Oslo, Norway

118 Department of Physics, Oxford University, Oxford, United Kingdom

119 [a] INFN Sezione di Pavia; [b] Dipartimento di Fisica, Università di Pavia, Pavia, Italy

120 Department of Physics, University of Pennsylvania, Philadelphia PA, United States of America

121 Petersburg Nuclear Physics Institute, Gatchina, Russia

122 [a] INFN Sezione di Pisa; [b] Dipartimento di Fisica E. Fermi, Università di Pisa, Pisa, Italy

123 Department of Physics and Astronomy, University of Pittsburgh, Pittsburgh PA, United States of America

124 [a] Laboratorio de Instrumentacao e Fisica Experimental de Particulas - LIP, Lisboa, Portugal; [b] Departamento de Fisica Teorica y del Cosmos and CAFPE, Universidad de Granada, Granada, Spain

125 Institute of Physics, Academy of Sciences of the Czech Republic, Praha, Czech Republic

126 Czech Technical University in Prague, Praha, Czech Republic

127 Faculty of Mathematics and Physics, Charles University in Prague, Praha, Czech Republic

128 State Research Center Institute for High Energy Physics, Protvino, Russia

129 Particle Physics Department, Rutherford Appleton Laboratory, Didcot, United Kingdom

130 Physics Department, University of Regina, Regina SK, Canada

131 Ritsumeikan University, Kusatsu, Shiga, Japan

132 [a] INFN Sezione di Roma I; [b] Dipartimento di Fisica, Università La Sapienza, Roma, Italy

133 [a] INFN Sezione di Roma Tor Vergata; [b] Dipartimento di Fisica, Università di Roma Tor Vergata, Roma, Italy

134 [a] INFN Sezione di Roma Tre; [b] Dipartimento di Fisica, Università Roma Tre, Roma, Italy

135 $^{(a)}$ Faculté des Sciences Ain Chock, Réseau Universitaire de Physique des Hautes Energies - Université Hassan II, Casablanca; $^{(b)}$ Centre National de l'Energie des Sciences Techniques Nucleaires, Rabat; $^{(c)}$ Faculté des Sciences Semlalia, Université Cadi Ayyad, LPHEA-Marrakech; $^{(d)}$ Faculté des Sciences, Université Mohamed Premier and LPTPM, Oujda; $^{(e)}$ Faculté des sciences, Université Mohammed V-Agdal, Rabat, Morocco

136 DSM/IRFU (Institut de Recherches sur les Lois Fondamentales de l'Univers), CEA Saclay (Commissariat à l'Energie Atomique et aux Energies Alternatives), Gif-sur-Yvette, France

137 Santa Cruz Institute for Particle Physics, University of California Santa Cruz, Santa Cruz CA, United States of America

138 Department of Physics, University of Washington, Seattle WA, United States of America

139 Department of Physics and Astronomy, University of Sheffield, Sheffield, United Kingdom

140 Department of Physics, Shinshu University, Nagano, Japan

141 Fachbereich Physik, Universität Siegen, Siegen, Germany

142 Department of Physics, Simon Fraser University, Burnaby BC, Canada

143 SLAC National Accelerator Laboratory, Stanford CA, United States of America

144 $^{(a)}$ Faculty of Mathematics, Physics & Informatics, Comenius University, Bratislava; $^{(b)}$ Department of Subnuclear Physics, Institute of Experimental Physics of the Slovak Academy of Sciences, Kosice, Slovak Republic

145 $^{(a)}$ Department of Physics, University of Johannesburg, Johannesburg; $^{(b)}$ School of Physics, University of the Witwatersrand, Johannesburg, South Africa

146 $^{(a)}$ Department of Physics, Stockholm University; $^{(b)}$ The Oskar Klein Centre, Stockholm, Sweden

147 Physics Department, Royal Institute of Technology, Stockholm, Sweden

148 Departments of Physics & Astronomy and Chemistry, Stony Brook University, Stony Brook NY, United States of America

149 Department of Physics and Astronomy, University of Sussex, Brighton, United Kingdom

150 School of Physics, University of Sydney, Sydney, Australia

151 Institute of Physics, Academia Sinica, Taipei, Taiwan

152 Department of Physics, Technion: Israel Institute of Technology, Haifa, Israel

153 Raymond and Beverly Sackler School of Physics and Astronomy, Tel Aviv University, Tel Aviv, Israel

154 Department of Physics, Aristotle University of Thessaloniki, Thessaloniki, Greece

155 International Center for Elementary Particle Physics and Department of Physics, The University of Tokyo, Tokyo, Japan

156 Graduate School of Science and Technology, Tokyo Metropolitan University, Tokyo, Japan

157 Department of Physics, Tokyo Institute of Technology, Tokyo, Japan

158 Department of Physics, University of Toronto, Toronto ON, Canada

159 $^{(a)}$ TRIUMF, Vancouver BC; $^{(b)}$ Department of Physics and Astronomy, York University, Toronto ON, Canada

160 Faculty of Pure and Applied Sciences, University of Tsukuba, Tsukuba, Japan

161 Department of Physics and Astronomy, Tufts University, Medford MA, United States of America

162 Centro de Investigaciones, Universidad Antonio Narino, Bogota, Colombia

163 Department of Physics and Astronomy, University of California Irvine, Irvine CA, United States of America

164 $^{(a)}$ INFN Gruppo Collegato di Udine; $^{(b)}$ ICTP, Trieste; $^{(c)}$ Dipartimento di Chimica, Fisica e Ambiente, Università di Udine, Udine, Italy

165 Department of Physics, University of Illinois, Urbana IL, United States of America

166 Department of Physics and Astronomy, University of Uppsala, Uppsala, Sweden

167 Instituto de Física Corpuscular (IFIC) and Departamento de Física Atómica, Molecular y Nuclear and Departamento de Ingeniería Electrónica and Instituto de Microelectrónica de Barcelona (IMB-CNM), University of Valencia and CSIC, Valencia, Spain

168 Department of Physics, University of British Columbia, Vancouver BC, Canada

169 Department of Physics and Astronomy, University of Victoria, Victoria BC, Canada

– 45 –

170 Department of Physics, University of Warwick, Coventry, United Kingdom
171 Waseda University, Tokyo, Japan
172 Department of Particle Physics, The Weizmann Institute of Science, Rehovot, Israel
173 Department of Physics, University of Wisconsin, Madison WI, United States of America
174 Fakultät für Physik und Astronomie, Julius-Maximilians-Universität, Würzburg, Germany
175 Fachbereich C Physik, Bergische Universität Wuppertal, Wuppertal, Germany
176 Department of Physics, Yale University, New Haven CT, United States of America
177 Yerevan Physics Institute, Yerevan, Armenia
178 Centre de Calcul de l'Institut National de Physique Nucléaire et de Physique des Particules (IN2P3), Villeurbanne, France

[a] Also at Department of Physics, King's College London, London, United Kingdom
[b] Also at Laboratorio de Instrumentacao e Fisica Experimental de Particulas - LIP, Lisboa, Portugal
[c] Also at Faculdade de Ciencias and CFNUL, Universidade de Lisboa, Lisboa, Portugal
[d] Also at Particle Physics Department, Rutherford Appleton Laboratory, Didcot, United Kingdom
[e] Also at Department of Physics, University of Johannesburg, Johannesburg, South Africa
[f] Also at TRIUMF, Vancouver BC, Canada
[g] Also at Department of Physics, California State University, Fresno CA, United States of America
[h] Also at Novosibirsk State University, Novosibirsk, Russia
[i] Also at Department of Physics, University of Coimbra, Coimbra, Portugal
[j] Also at Department of Physics, UASLP, San Luis Potosi, Mexico
[k] Also at Università di Napoli Parthenope, Napoli, Italy
[l] Also at Institute of Particle Physics (IPP), Canada
[m] Also at Department of Physics, Middle East Technical University, Ankara, Turkey
[n] Also at Louisiana Tech University, Ruston LA, United States of America
[o] Also at Dep Fisica and CEFITEC of Faculdade de Ciencias e Tecnologia, Universidade Nova de Lisboa, Caparica, Portugal
[p] Also at Department of Physics and Astronomy, University College London, London, United Kingdom
[q] Also at Department of Physics, University of Cape Town, Cape Town, South Africa
[r] Also at Institute of Physics, Azerbaijan Academy of Sciences, Baku, Azerbaijan
[s] Also at Institut für Experimentalphysik, Universität Hamburg, Hamburg, Germany
[t] Also at Manhattan College, New York NY, United States of America
[u] Also at CPPM, Aix-Marseille Université and CNRS/IN2P3, Marseille, France
[v] Also at School of Physics and Engineering, Sun Yat-sen University, Guanzhou, China
[w] Also at Academia Sinica Grid Computing, Institute of Physics, Academia Sinica, Taipei, Taiwan
[x] Also at School of Physics, Shandong University, Shandong, China
[y] Also at Dipartimento di Fisica, Università La Sapienza, Roma, Italy
[z] Also at DSM/IRFU (Institut de Recherches sur les Lois Fondamentales de l'Univers), CEA Saclay (Commissariat à l'Energie Atomique et aux Energies Alternatives), Gif-sur-Yvette, France
[aa] Also at Section de Physique, Université de Genève, Geneva, Switzerland
[ab] Also at Departamento de Fisica, Universidade de Minho, Braga, Portugal
[ac] Also at Department of Physics, The University of Texas at Austin, Austin TX, United States of America
[ad] Also at Department of Physics and Astronomy, University of South Carolina, Columbia SC, United States of America
[ae] Also at Institute for Particle and Nuclear Physics, Wigner Research Centre for Physics, Budapest, Hungary
[af] Also at California Institute of Technology, Pasadena CA, United States of America
[ag] Also at Institute of Physics, Jagiellonian University, Krakow, Poland
[ah] Also at LAL, Université Paris-Sud and CNRS/IN2P3, Orsay, France
[ai] Also at Nevis Laboratory, Columbia University, Irvington NY, United States of America

^{aj} Also at Department of Physics and Astronomy, University of Sheffield, Sheffield, United Kingdom

^{ak} Also at Department of Physics, Oxford University, Oxford, United Kingdom

^{al} Also at Department of Physics, The University of Michigan, Ann Arbor MI, United States of America

^{am} Also at Discipline of Physics, University of KwaZulu-Natal, Durban, South Africa

* Deceased